الجمهورية الجزائرية الديموقراطية الشعبية
REPUBLIQUE ALGERIENNE DEMOCRATIQUE ET POPULAIRE
وزارة التعليم العالي و البحث العلمي
MINISTERE DE L'ENSEIGNEMENT SUPERIEUR
ET DE LA RECHERCHE SCIENTIFIQUE
جامعة فرحات عباس سطيف 1
UNIVERSITE FERHAT ABBES - SETIF 1
UFAS (ALGERIE)

**THESE**

Présentée à la Faculté de Technologie

Département D'Electrotechnique

Pour l'Obtention du Diplôme de

**DOCTORAT en SCIENCES**

Filière : Electrotechnique

Option : Réseaux électriques

Présentée par :

**AMROUNE Mohammed**

**Thème :**

# Contribution à l'étude de la stabilité des réseaux électriques intelligents (smart grids)

Soutenue le : 28/06/2018 devant un Jury composé de:

| | | |
|---|---|---|
| Pr. GHERBI Ahmed | Université Ferhat Abbas Sétif 1 | Président |
| Pr. BOUKTIR Tarek | Université Ferhat Abbas Sétif 1 | Rapporteur |
| Pr. MUSIRIN Ismail | Universiti Teknologi MARA, Malaysia | Co-rapporteur |
| Pr. ARIF Salem | Université Amar Telidji Laghouat | Examinateur |
| Pr. BETKA Achour | Université Mohamed Kheider Biskra | Examinateur |
| Pr. RADJEAI Hammoud | Université Ferhat Abbas Sétif 1 | Examinateur |

**الجمهورية الجزائرية الديموقراطية الشعبية**

PEOPLE'S DEMOCRATIC REPUBLIC OF ALGERIA

وزارة التعليم العالي و البحث العلمي

MINISTERY OF HIGHER EDUCATION AND RESEARCH

جامعة فرحات عباس سطيف 1

UNIVERSITY OF FERHAT ABBES - SETIF 1

UFAS (ALGERIA)

A thesis presented to the Faculty of Technology

Department of Electrical Engineering

in fulfilment of the requirement for the degree of

**Doctor of Science**

in

Electrical Engineering

Presented by

**Mohammed AMROUNE**

Thesis Title:

# Contribution to the stability study of smart grids

Approved by:

| | | |
|---|---|---|
| Pr. GHERBI Ahmed | University of Ferhat Abbas Sétif 1 | Chair of committee |
| Pr. BOUKTIR Tarek | University of Ferhat Abbas Sétif 1 | Supervisor |
| Pr. MUSIRIN Ismail | Universiti Teknologi MARA, Malaysia | Co-Supervisor |
| Pr. ARIF Salem | University of Amar Telidji Laghouat | Examiner |
| Pr. BETKA Achour | University of Mohamed Kheider Biskra | Examiner |
| Pr. RADJEAI Hammoud | University of Ferhat Abbas Sétif 1 | Examiner |

June 2018

# Acknowledgments

In the name of Allah and all praise is for Allah.

I'd like to express my sincere gratitude and appreciation to my supervisor, Professor Tarek Bouktir, for his invaluable guidance, suggestions, support and encouragement throughout my Ph.D studies. I'd like also to sincerely thank my co-supervisor, Professor Ismail Musirin, for all his suggestions, motivation and constant support during this research work. It was a great honour for me to work with them.

I'm also indebted to the Department of Electrical Engineering, University of Ferhat Abbas Setif 1, Algeria, for allowing me to fully utilize the necessary facilities during my studies. Thanks are also extended to the Faculty of Electrical Engineering, Universiti Teknologi MARA (UiTM) Malaysia.

I'm particularly grateful to all staff members of the UiTM Office of International Affairs for their invaluable assistance during my stay at the UiTM. In addition, I'd like to express my special thanks to Dr. Muhammad Murtadha Othman from the Faculty of Electrical Engineering, UiTM, for his invaluable advice.

I also would like to thank my committee members, Pr. Ahmed Gherbi from University of Ferhat Abbas Sétif 1, Pr. Salem Arif from University of Amar Telidji Laghouat, Pr. Achour Betka from University of Mohamed Kheider Biskra and Pr. Hammoud Radjeai from University of Ferhat Abbas Sétif 1 for their important comments.

A lot of thanks to all my colleagues for the excellent work environment they created.

Finally, I'd like to give special appreciation and thanks to my parents and all my family for their patience, encouragement and support during my study.

# Contents

# List of Figures

# List of Tables

# List of Terms

## Acronyms:

| | |
|---|---|
| ANN | : Artificial Neural Network |
| MLP | : Multi-Layer Perceptron |
| RBF | : Radial Basis Function |
| ANFIS | : Adaptive Neuro-Fuzzy Inference System |
| SVR | : Support Vector Regression |
| AC | : Alternative Current |
| ALO | : AntLion Optimizer |
| DA | : Dragonfly Optimization |
| WOA | : Whale Optimization Algorithm |
| GA | : Genetic Algorithm |
| VSM | : Voltage Stability Margin |
| VSI | : Voltage Stability Index |
| OPF | : Optimal Power Flow |
| CPF | : Continuation Power Flow |
| SCADA | : Supervisory Control and Data Acquisition |
| PMU | : Phasor Measurement Unit |
| WAMS | : Wide Area Measurement System |
| GPS | : Global Positioning System |
| R | : Correlation coefficient |
| RMSE | : Root Mean Square Error |
| PRMSE | : Percentage Root Mean Square Error |

MAPE : Mean Absolute Percentage Error

PSAT : Power System Analysis Toolbox

EDR : Emergency Demand Response

EEDR : Event-driven Emergency Demand Response

## Symbols:

$P$ : Active power

$Q$ : Reactive power

$S$ : Apparent power

$R_l$ : Line resistance

$X_l$ : Line reactance

$V$ : Bus voltage magnitude

$\delta$ : Bus phase angle

$Y$ : Admittance matrix

$F$ : Regression function

$\varphi$ : High-dimensional input vector

$w$ : Weighting factor

$b$ : Bias

$L_\varepsilon$ : $\varepsilon$-insensitive loss function

$\xi$, $\xi^*$ : Positive slack variables

$\alpha_i$, $\alpha_i^*$ : Nonlinear Lagrangian multipliers

$K$ : Kernel function

$C$ : Penalty parameter

$\varepsilon$ : Non-sensitivity coefficient

$\gamma$ : Gaussian RBF kernel

$F_c$ : Fuel cost function

$N_g$ : Number of generators

$N_b$ : Number of branches

$N_{bus}$ : Number of buses

$a_i$, $b_i$, $c_i$ : Cost coefficient of the $i$th generator

$P_{loss}$ : Power losses

$C_d$ : Cost of demand reduction

# Chapter 1: Introduction

## 1.1 Overview of the Study

In the last decade, serious power grid blackouts have occurred throughout the world bringing with them important economic losses and affecting the lives of local residents. Voltage instability incidents have been identified as contributing factors in several recent worldwide blackouts such as the blackouts occurred in Sweden and Denmark in 2003, the great US Northeast blackout of 2003, the blackout affected the Algerian power system in 2003, the Athens blackout in 2004 and the Brazilian blackout in 2009 [1, 2].

Voltage instability phenomenon is generally associated with a gradual or uncontrollable drop in voltage magnitude after disturbances in the system, increase in load demand or incapacity to cover the demand for reactive power. The voltage collapse is the process by which voltage instability leads to loss of voltage in an important part of the system. When the power system is operating with insufficient voltage stability margin in one or more regions, it becomes more likely to voltage collapse. In order to mitigate the risk of voltage collapse, stability analysis should be considered during both planning and real-time operating of power systems. In contrast to the off-line planning, where the computational speed may not be important, in on-line analysis, real-time tools are of great importance for assessing the voltage stability of power system. On the other hand, if voltage stability margin leaves its permissible range, emergency actions should be applied to drive the operating condition of a power system away from the insecure points. Recently, with the emergence of computational intelligence techniques, the assessment of voltage stability in an on-line manner and the development of effective countermeasures against voltage collapses have attracted wide attention.

The present study mainly focuses on the development of fast and efficient voltage stability assessment and enhancement tools based on artificial intelligence techniques in order to mitigate the risk of voltage collapses.

## 1.2 Problem Statement

The on-line assessment of power system voltage stability becomes more and more important to evaluate and to improve the performance of system operation. Traditionally, voltage stability assessment is performed using *P–V* and *Q–V* curves, Continuation Power Flow (CPF) and voltage stability indices based on Supervisory Control and Data Acquisition (SCADA) system, which require large computations and are not effective for on-line applications. In recent years, Support Vector Regression (SVR) has been adapted to assess the voltage stability of power systems in an on-line manner. However, the performance of the SVR technique is highly dependent upon the selection of its parameters (i.e., the penalty parameter ($C$), the non-sensitivity coefficient ($\varepsilon$) and the kernel function parameters). Therefore, the selection of appropriate parameter values of the SVR model is considered as a key step to improve its prediction performance. In the past, although some researchers have applied various methods to select the SVR optimal parameters, thus, to obtain a good performance in on-line voltage stability assessment [3-5], the achieved results have not been so effective due to the complex nature of the SVR parameters.

In addition to the fast and accurate assessment of voltage stability, remedial measures must be implemented to protect the power system against contingencies, such as a sudden branch or generator outages, and to preclude voltage collapse following such events. Identification of weak buses in power system plays an important role in the voltage stability improvement as well as in the prevention of possible voltage instability problems [6]. Several methods have been reported in the literature to identify the weak buses in power system. CPF, *P-V* and *Q-V* curves and voltage stability indices are the typically applied methods [7]. However, the identification of the weak buses using these methods, which are based on graduation increasing of the load at each bus, requires a large computation time, particularly for large-scale power systems.

Emergency Demand Response (EDR) is one of the emergency measures that have been adopted by power system companies to protect the system against voltage collapse. EDR program is called upon when power generation is anticipated to experience a shortfall or during the contingency situations [8]. However, the application of such

programs to improve the power system security has not been completely addressed. The only work –as far as the author knows– discussed the use of EDR in power system security enhancement is that of Wang *et al.* [9]. In this work, an event-driven EDR strategy is proposed to improve the operating reserves of the power system under credible contingencies. A multistage optimization technique based on segmentation of the original nonlinear problem, associated with EDR program, into a series of linear optimization problems is proposed. However, this procedure needs to be repeated several times until a required security margin is achieved, which is time-consuming task. Another disadvantage of the proposed strategy is that it considers all loads in the system as EDR participants which results in high cost of implementation of such programs.

## 1.3 Objectives

The formulated objectives of this study can be presented in three main points:

1. To develop an on-line voltage stability assessment technique based on new hybrid models combining the SVR and the modern meta-heuristic optimization algorithms namely AntLion Optimizer (ALO), Dragonfly Algorithm (DA) and Whale Optimization Algorithm (WOA). The proposed techniques will be useful for the power system utility operators in taking the required measures to avoid large blackouts.
2. To develop new technique for the identification of weak buses in power system based on the optimal location of reactive power support using ALO, DA and WOA algorithms.
3. To develop an Event-driven Emergency Demand Response (EEDR) approach based on Voltage Stability Margin (VSM) using WOA algorithm to improve voltage stability as well as to avoid a risk of large blackouts by driving the operating condition of a power system away from the insecure points during emergency conditions.

## 1.4 Thesis outline

This thesis comprises six chapters and it is organized as follows:

**Chapter 2** introduces the fundamental of voltage stability phenomena, followed by a brief description of the methods used to assess the voltage stability. Finally, the on-line voltage stability assessment using Machine Learning (ML) techniques, the identification of weak buses in power system and the countermeasures employed to avoid a risk of voltage collapse are briefly reviewed.

**Chapter 3** initially presents the general background on synchronized PMUs and SVR technique, followed by the description of meta-heuristic optimization algorithms used in this study i.e., ALO, DA and WOA algorithms. The developed hybrid models combining the SVR and the aforementioned meta-heuristic optimization algorithms are then presented. Finally, the proposed voltage stability assessment techniques are implemented on the IEEE 14-bus and the Algerian 114-bus systems for validation purposes.

**Chapter 4** presents the implementation of ALO, DA and WOA optimization algorithms in the identification of the weak buses in the system for voltage stability enhancement. In order to demonstrate the validity and the effectiveness of the proposed methods, the IEEE 14-bus and the Algerian 114-bus systems are used-as the test platforms.

**Chapter 5** presents Event-driven Emergency Demand Response (EEDR) approach based-VSM to improve the voltage stability of power system and to mitigate the risk of large blackouts. Firstly, the EEDR is described and formulated as an optimization problem in which the goal is to minimize the demand reduction cost and the main constraint is the VSM. Then, the WOA optimization algorithm is adopted to solve this optimization problem. Several simulations are carried out on the IEEE 14-bus, and the Algerian 114-bus systems to assess the performances of the proposed approach.

**Chapter 6** concludes this study and cites few recommendations for future development and enhancement.

# Chapter 2: Literature review

## 2.1 Introduction

This chapter presents comprehensive theoretical concepts of voltage stability. It first gives a short overview of the voltage stability phenomena along with the different techniques used to assess power system voltage stability. Then, it presents a review of past research works related to the voltage stability assessment based on Machine Learning (ML) techniques, the identification of weak buses in power system and the countermeasures implemented to prevent a risk of voltage collapse.

## 2.2 Voltage stability phenomenon

Voltage stability is currently one of the most important research areas in the field of the electrical power system. Voltage instability problem is associated with a progressive or uncontrollable drop in voltage magnitude after a disturbance, increase in load demand, insufficient local reactive supply or change in operating condition.

### 2.2.1 Definition and classification

Several definitions of voltage stability can be found in the literature. The most general definition is that given by the IEEE/CIGRE Joint Task Force on Stability Terms and Definitions, where the voltage stability is defined as follows [10]:

*"Voltage stability is the capability of a power system to retain steady voltages at all nodes in the system after being subjected to a perturbation from a given initial operating condition"*.

According to the IEEE/CIGRE, voltage stability can be divided into two subcategories: *large-disturbance voltage stability* and *small-disturbance voltage stability*. The first category refers to the voltage stability of power system after being subjected to a large disturbance, such as an outage of system components, loss of transmission line and faults in transformers or generation units. The second one refers to the voltage stability

when subjected to small perturbations such as incremental load changing. In addition to this classification, the voltage stability can be fast (*short-term voltage stability*) or slow (*long-term voltage stability*) as demonstrated in Figure 2.1.

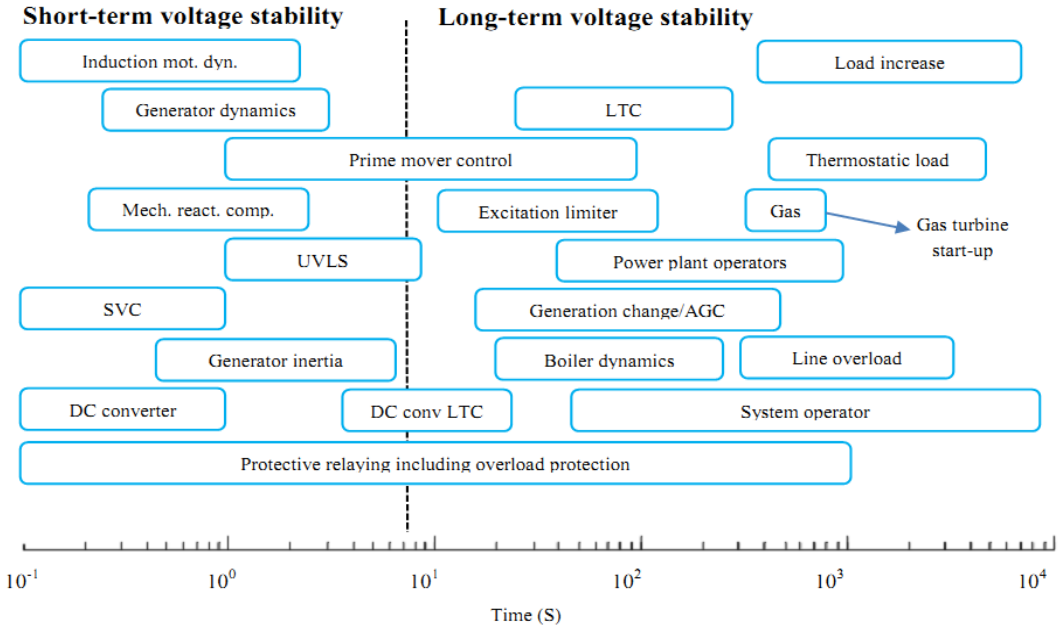


**Figure 2.1** Different time responses for voltage stability phenomenon [11]

### 2.2.2 Voltage collapse

Voltage collapse in power systems is one of the main security concerns for power system operations, as several large-scale system blackouts around the world have been related to this phenomenon. The definition and the factors that cause voltage collapse will be discussed in the next subsections.

#### 2.2.2.1 Definition

The static voltage instability problem becomes a serious type of voltage instability which is essentially related to the increased loading of the power system and the incapacity to cover the demand for reactive power. It is characterized by an initial progressive decrease of voltage magnitude and a final rapid decline. Figure 2.2 depicts the relationship between the load bus voltage and the active power transfer through a transmission line denoted as a *P-V* curve. As the loading increases, the voltage at the load bus decreases. The edge of the curve is the maximum active power ($P_{max}$) that can be

transmitted over the transmission line and it is considered as the *voltage collapse point*. Consequently, the voltage collapse can be defined as follows:

*"Voltage collapse is the process by which voltage instability causes the loss of voltage in an important part of the system"* [12].

One of the most frequent terms related to the voltage collapse is the *Voltage Stability Margin* (VSM), which corresponds to a measure of the distance from the current operating point to the collapse point.

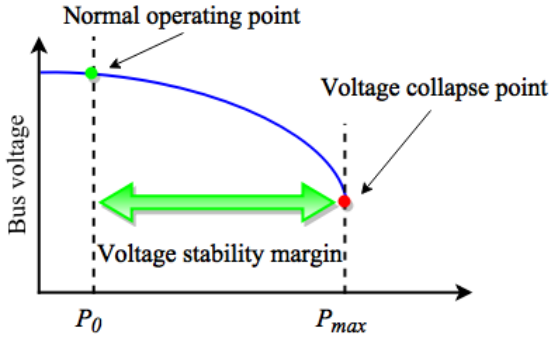


**Figure 2.2** *P-V* curve for the simple two-bus system

### 2.2.2.2 Causes of voltage collapse

The primary factors that cause voltage collapse and lead to voltage instability are described as follows:

- **Increase in the load demand**

  The increase in the load is a serious factor causing voltage collapse. It is well-known that the increase in the load demand leads to inequality between the reactive power supply and demand. As consequence of the gradual increases in the load, the reactive power demand will be higher than supply and the voltage magnitude will progressively decrease until a very small value. The example of this kind of problems is the Tokyo blackout on 23$^{rd}$ July 1987 [13], where the load was gradually increased by around 1% per minute and the voltages started to drop at 500 kV. After 20 minutes, the voltages dropped to very small values (close to 0.75 p.u) and about 800 MW of load was disconnected by the protective relays.

According to [14], load characteristics of air conditioners were a contributing factor.

- **Transmission system**

  Another factor contributing to voltage collapse is the transmission system (lines and transformers). Lines and transformers have a limited transfer capacity, which is related to many factors such as their impedance, the nature of the load and the presence/absence of the reactive power compensators (capacitors, reactors or Flexible AC Transmission Systems (FACTS) devices).

- **Generation system**

  The loss of generation or their inability to meet the demand for reactive power in heavily stressed systems can cause a large increase of reactive power losses in the power grid, which leads to the occurrence of instability problems. The example of this kind of problems is the incidence of Zealand in Denmark [16], where the loss of only one production source of 270 MW in the southern part of the island caused a gradual voltage decline (to around 0.75 after 15 minutes), which prevented the synchronization of 75 MW gas turbine.

## 2.3 Voltage stability assessment

Voltage stability assessment is one of the important parts of the planning and operating of power systems. Voltage stability assessment methods are categorized into off-line and on-line studies. The first category is conducted in the power system planning and the second category is conducted during the system operation. The on-line assessment is to justify whether the current operating point is secure or insecure, and to determine how close the system is to voltage collapse point which is called the VSM.

### 2.3.1 Methods of voltage stability assessment

Many different methods have been introduced to assess the voltage stability and to find the VSM among them [16]:

#### 2.3.1.1 Methods based on modal analysis

The modal analysis method proposed by Gao *et al.* [17] in 1992 depends on the power flow Jacobian matrix and it can predict the voltage collapse in complex power systems. This method, in addition to providing a good estimation of the system proximity to the voltage collapse [18, 19], it is used as a tool to identify the critical load buses [20, 21].

#### 2.3.1.2 Methods based on energy function

The energy function method has been initially applied to determine the transient stability of one machine-infinite bus system or two-machine system based on the equal area criterion [22]. Albeit that the energy function method is more appropriate for transient stability assessment, many authors have associated this technique with measure voltage stability margin in the static cases. The first application of energy function for voltage collapse analysis was performed by DeMarco and Overbye [23, 24]. The energy function technique is, also, used to rank the system buses according to their participation in voltage collapse [22].

#### 2.3.1.3 Methods based on loading margins

One of the important tools to assess voltage stability is the methods based on loadability margins. This loadability margin can be computed by *P-V* and *Q-V* curves, CPF method or by using voltage stability indices.

- ***P-V* and *Q-V* curves**

The *P-V* and *Q-V* curves are the most used methods to evaluate the voltage stability [25]. They are used to determine the VSM of the power system. The *P-V* curve can be obtained by gradually increasing the active power, by constant power factor, at load bus or area and executing consecutive power flow equations. An example of such curves is the Figure 2.2 which depicted the relationship between the load bus voltage and the active power transfer through a transmission line. The edge point or voltage stability collapse point is the point where the power flow process will diverge due to the singularity of the Jacobian matrix. The distance between the voltage collapse point and the normal operating point or the so-called VSM is used as the voltage stability criterion.

In the same manner, the *Q-V* curves are used to indicate the sensitivity and variation of bus voltage magnitude with respect to reactive power injections and absorptions. The *Q-V* curves (see Figure 2.3) can be used as voltage stability assessment tools, taking the edge point of the curve as the collapse point and the MVar distance between this point and the normal operating point as the reactive power margin [26].

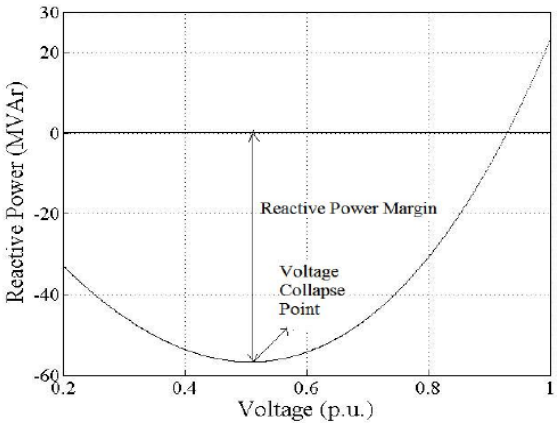


**Figure 2.3** *Q-V* curve

- **Continuation Power Flow (CPF)**

CPF is an iterative process that finds a gradation of power flow solutions at different operating points by using branch tracing methods or also called predictor-corrector methods [27]. CPF is utilized to determine the steady-state voltage stability limits. These limits are determined by drawing the nose curve where the nose represents the maximum power that can be transmitted over the transmission line. The nose curve can be drawn by the variation of load voltage magnitude with the automatic changes of the loading parameter. From a known base solution, a tangent predictor is used so as to estimate next solution for a specified pattern of load increase. Then, the corrector step determines the exact solution using Newton-Raphson technique. After that, a new prediction technique is made for a specified increase in load based upon the new tangent vector. Then corrector step is applied. This process goes until a critical point is touched [28].

- **Voltage stability indices**

The methods based on voltage stability indices are very popular due to the uncomplicated interpretation of the index used. Many indices have been proposed in the

literature to assess the static voltage stability of power systems and to find VSM. Among these indices the Line stability factor (LQP) [29], the Line stability index ($L_{mn}$) [30], the Fast Voltage Stability Index (FVSI) [31] and the Voltage Stability Index (VSI) [32].

## 2.4 Machine Learning (ML) techniques applied to voltage stability assessment

As abovementioned, there are numerous tools that have been developed to conduct a comprehensive analysis of the voltage stability assessment, such as *P–V* and *Q–V* curves, CPF and voltage stability indices. However, the developed software tools have the scarcity to be used in a real-time or on-line operation as they are computationally time-consuming due to its reliant on a complex mathematical modelling of a power system. The aforementioned predicament of enormous computational requirements could be resolved by utilizing the Machine learning (ML) techniques such as the Artificial Neural Networks (ANNs), Adaptive Neuro-Fuzzy Inference System (ANFIS) and Support Vector Machines (SVMs).

A neural network is a computational model proposed in the late 1940s by Hebb [33]. It was inspired by the operations of biological neural systems. In 1954, Farley and Wesley [34] first employed computational machines to simulate a Hebbian network at Massachusetts Institute of Technology (MIT) and then called calculators. Frank Rosenblat [35] developed the perceptron in 1958, and in 1975 the back-propagation algorithm was introduced by Paul Werbos [36]. In 1982 and 1984, the Hopfield and the Kohonen neural networks were provided by Hopfield [37] and Kohonen [38]. In 1986 [39], Rumelhart and McClelland introduced the back-propagation learning algorithm. In 1987, several research programs based on ANNs were initiated and the list of their application has been extended to large practical tasks [40]. Between 2009 and 2012, the recurrent and the deep feed-forward ANNs were developed in the research group of Jurgen Schmidhuber at the Swiss AI Lab [41].

Several ANN architectures and various neural network combinations have been proposed in the literature for on-line voltage stability assessment. Multi-Layered Perceptron (MLP) neural network trained by the back-propagation algorithm is firstly introduced by Jeyasurya [42] and El-Keib *et al.* [43] for computing the VSM using

energy method. An extended work on the MLP has been employed to assess the voltage stability for a dynamic power system model [44, 45]. Further improvement of MLP performance in on-line monitoring of voltage stability could be realized by reducing the input data at an optimal size [46]. In the same context, Ying and Chung [47] proposed the use of hybrid MLP networks and ward equivalent approach network reduction. The proposed approach possesses the properties of ward equivalent method to update the parameters of the equivalent model for representing real-time topology change of the power system. In tandem with the input data minimization, this can also be perpetrated by using several feature extraction methods such as the principal component analysis that augment the performance of MLP to assess the voltage stability in an on-line manner [48, 49]. In [50], a systematic way to train separate MLP network for various contingencies is presented. In this work, the load active and reactive powers are used as the input features for the MLP. In [51], an MLP based input features selection using mutual information method is proposed to estimate the voltage stability level at various load conditions and contingencies. Jayasankar *et al.* [52] used a sequential learning strategy to design a single feed-forward back-propagation network to estimate the line voltage stability index for different load conditions. In [53], a regression-based method of selecting features for training a separate ANNs is proposed to assess the voltage stability considering deferent contingencies. Mithra and Bhuvaneshwari [54] proposed the application of MLP based approach for fast voltage contingency ranking. In the proposed approach, the off-line load flow studies are adopted to find the Minimum Singular Value (MSV) and the results from load flow study are used to train the MLP network to estimate the MSV. Authors in [55] developed a new extreme learning machine model for precise and fast prediction of voltage stability under different loading conditions and under contingencies. Authors in [56] proposed a new MLP network-based algorithm that requires only a minimum number of inputs to estimate the voltage magnitude of each critical bus in a power system under normal and contingency states. Another approach to find the fewest input variables required to approximate the VSM with sufficient accuracy and high execution speed is proposed in [57]. In [58], a Z-score based bad data processing algorithm is implemented to enhance the estimation accuracy of the feed-forward ANNs.

The application of Radial Basis Function (RBF) neural network for on-line voltage stability assessment has also been performed by several researchers. Jain *et al.* [59] applied both supervised and unsupervised learning to RBF network in order to reduce the number of neural networks required for voltage contingency screening and ranking. Sahari *et al.* [60] used the active and reactive loads on all load buses as input set of RBF network for on-line monitoring of voltage stability. Authors in [61] proposed the application of RBF network-based energy method for on-line estimation of VSM. Arya *et al.* [62] proposed the use of RBF network to get the probabilistic risk of voltage collapse for various operating conditions. In this work, the training and testing instances have been generated using Monte-Carlo simulation. RBF neural network is also applied by Moradzadeh *et al.* [63] to predict the static voltage stability index and to rank the critical line outage contingencies. In this study, three distinct feature extraction algorithms are used to speed-up the training process via reducing the input training vectors dimensions. In [64], several dimensionality reduction techniques are employed to enhance the predictive ability of the RBF network in the estimation of the voltage stability level. In [65], a comparison between ANNs trained using linear basis function and RBF in the estimation of line voltage stability index ($L_{mn}$) has been presented. The results show that both the ANNs paradigms are suitable for $L_{mn}$ index prediction. In [66] the RBF network is adapted to estimate the VSM using the dominant extracted features of the voltage profile by multi-resolution wavelet transform and principal component analysis.

The application of self-organizing Kohonen-neural network for fast indication and visualization of voltage stability has been discussed in [67]. In [68], a new ANN architecture called the parallel self-organizing hierarchical neural network is proposed to estimate the loadability margin with Static Var Compensator (SVC). Chen *et al.* [69] proposed a new approach to compute a risk of low voltage using Neural Network Ensemble (NNE). In this work, the probability model of system contingency and the impact model of low voltage are built, first, and then the corresponding risk index is computed to form the NNE system. Chakraborty *et al.* [70] incorporated a self-organizing feature map with RBF network for determination and classification of the power system voltage stability level. Notwithstanding the fact that the ANN has gained attention from researchers as a tool for on-line voltage stability assessment, it has some drawbacks. The

problem of sticking to local minima and the greater computational burden are the main disadvantages of ANNs [71].

The ANFIS model introduced by Jang in 1993 [72] has emerged as a strong tool for power system applications. It is based on the combination of the advantages of ANNs capability in learning from processes and fuzzy interpretation of the fuzzy logic system. One of the first voltage stability approaches in which ANFIS algorithms were applied is reported in [73]. In this work, a novel architecture based on ANFIS system and three-dimensional voltage, real power and reactive power surfaces is proposed. The approach was found to be very effective, with the system providing good predictions of voltage collapse under a wide range of scenarios. ANFIS system has been also applied to compute the loadability margin of the power system incorporating FACTS devices [74]. In [75], the ANFIS model is constructed in conjunction with the input information of voltage stability indices called VOSTA (VOltage STAbility) to perform a comprehensive risk assessment of voltage collapse. Torres *et al.* [76], uses the subtractive clustering and ANFIS methods based various voltage stability indices to estimate the loadability margin of the power system. More recently, a fuzzy inference engine is developed and optimized by two different approaches (ANN and genetic algorithm) to evaluate the security margins of the power system [77]. The simulation results show that the proposed approach allows the correct estimation of the voltage security margin with a high level of reliability, accuracy, and robustness. The complexity of proper parameters selection and the high computational cost are the main drawbacks of the ANFIS technique.

Support Vector Machine (SVM) [78] is a supervised learning technique with different learning algorithms that are used for developing of classification and regression models. In recent years, SVM is emerged to be an effective computational technique due to their many advantages and has already been applied to different engineering areas, except in power system stability monitoring where its application is still very limited. Cortés *et al.* [79] employed the SVM based Bayesian rule to classify the status of power system either it is secure, alert and emergency. This approach has been applied relatively analogous to the proposed multi-class SVM used for security assessment as highlighted in [80]. In the proposed approach, four different statuses of system security namely normal, alert,

emergency_1 and emergency_2 are considered. Further amelioration of multi-class SVM has been undertaken by consolidating the pattern recognition approach for security assessment [81]. Support Vector Regression (SVR), the most common application form of SVM, has also been applied to evaluate the voltage stability of a power grid [82-84]. In [82], the SVR model has been used to assess the voltage stability of power system incorporating Flexible Alternating Current Transmission Systems (FACTS) devices. In [83], the $v$-SVR and $\varepsilon$-SVR models with RBF and polynomial kernel functions have been used in on-line prediction of voltage stability margin. Recently, Sajan *et al.* [84] proposed a hybrid model combining Genetic Algorithm (GA) with SVR for voltage stability monitoring. It was reported that the proposed GA-SVR model has better performance compared to the MLP neural networks. However, the performance of GA is imperfect, it encloses a sequence of processes i.e., coding, selection, crossover, and mutation, which could affect the speed and the accuracy of the optimization. Another problem is related to the difficulty of choosing of GA operators such as population size, selection method, crossover rate and mutation rate, which have a significant impact on the convergence to the optimum solution.

## 2.5 Weak buses identification for voltage stability improvement

In recent years, due to the economic and environmental issues, modern power systems often operate proximate to the technical restraints enlarging the probable level of voltage instability risks. In such situations, any disturbance or increase in load demand can lead to a progressive or uncontrollable fall in system buses' voltage magnitudes which causes voltage instability. The main challenge of this problem is to identify the system buses where voltage instability could be started and to understand the origin of the problem. One effective method to know the voltage instability origin is to identify weak buses in the system.

In order to identify the weak buses in the power system, several methods have been reported in the literature. Han and Song [85] proposed an improved singular value decomposition method based on a Continuation Power Flow (CPF) for identifying weak buses in the power system. The proposed approach uses uniform reactive loading for all power system loads, a binomial searching method in order to speed up the computation

process and a polar form optimal multiplier to enhance power flow convergence. Peng *et al.* [86] proposed a new index combining the bus voltage margin and reactive power margin information for identifying the weak buses. The proposed multi-criteria integrated voltage stability index employed *P-V* and *Q-V* curves to determine bus voltage changes and reactive power margins.

The weak buses could also be determined using voltage stability indices. In [31], a novel line stability index designated as Fast Voltage Stability Index (FVSI) is proposed to determine the maximum reactive loadability and the weakest buses. He *at al.* [87] developed a new method based on the combination of voltage stability and buses voltage angle differences to find the weak locations in large-scale power systems. In this work, Voltage Stability Margin Index (VSMI) is taken as an indicator of voltage stability. Qin et *al.* [88] proposed a method to identify weak buses based on three voltage stability indicators i.e., Voltage Change Index (VCI), Minimum Voltage Index (MVI) and Voltage Collapse Proximity Indicator (VCPI). In [89], the bus voltage ranking index of $V/V_0$ is applied to identify the weak buses of the unbalanced multi-phase smart grid during 24 hours taking account the influence of plug-in electric vehicle charging stations. Moger and Dhadbanjan [90] proposed a new weak buses identification index called Reactive Power Loss Index (RPLI). The newly proposed index is extracted from the reactive power support and loss allocation algorithm using computed admittance matrix of the system. The identification of the weak buses using most of the aforementioned methods is based on graduation increasing the load at each bus and computing the voltage stability indices. However, this process requires a large computation time, particularly for large-scale power systems.

Fuzzy logic is another technique that used to identify the weak buses in the power system. In [91], a new approach based on fuzzy set theory is proposed to identify the weak buses in a power system. In this work, two membership functions are assumed for every bus; the first one for the voltage and the second one for the global reactive system losses of the branches joined to that bus. A decision function is selected based on the fuzzy multiplication of the two membership functions. The bus with the weakest decision value is selected as a weak bus in the system.

The amalgamation of fuzzy logic and ANN with other techniques in hybrid form was proven as an effective way of weak buses identification [92, 93]. Kumar *et al.* [92] proposed a new scheme based on the combination of MLP neural network and CPF to estimate the post-contingency loadability margin as well as to identify the weak bus in the system. Isaac *et al.* [93] suggested another combination between ANN surrogate model and sensitivity of the total bus voltage magnitudes to reactive power changes, where the objective is the identification of weak buses for proper placement of reactive power compensation.

Other options were the application of optimization algorithms to determine the weak buses. These methods are based on the formulation of optimization problems with incorporating the determination of weak locations in the power system. Examples of optimization procedures applied to the power system weak buses/area identification are presented in [94-96]. In [94], real coded Security Constraint Genetic Algorithm (SCGA) is developed to solve Maximum Loadability Limit (MLL) problem considering the security constraints. Weak buses are identified for the implementation of FACTS devices to improve MLL. It was reported that the proposed SCGA technique outperformed the General Particle Swarm Optimization (GPSO) technique in test systems of IEEE 14, 30, 57 and 118 buses. Similarly, both MLL and weak buses are identified by using four meta-heuristic optimization algorithms namely GA, GPSO, Adaptive PSO (APSO) and Chaotic PSO (CPSO) [95]. In this work, the performance of PSO is enhanced when its parameters are made adaptive, in APSO, for the MLL problem. It was reported that the CPSO algorithm offered the best success rate, the more maximum loadability factors and provides reliable convergence. On the other hand, GPSO gives worst performances in the case of success rate as well as in convergence time. Amroune *et al.* [96] proposed a technique to identify the weak buses in a large-scale power system based on the optimal location of reactive power supports using Differential Evolutionary (DE) algorithm.

## 2.6 Countermeasures against voltage collapse in power system

After serious blackouts occurred around the world, voltage instability prevention has become an important aspect of power system companies and researchers. Thus, a number of emergency controls have been adopted to protect the system against voltage collapse.

Adjustment of Load Tap Changer (LTC) transformer taps is the well-known emergency action for containing voltage instability. Different emergency schemes may be applied using the LTCs. One of the popular forms of emergency actions using LTCs is the tap blocking, which is an indirect way of load reduction [97]. However, this technique avoids an extra deterioration of the stability [98]. Otomega *et al.* [99] proposed an LTC control logic strategy that can be used in emergency voltage conditions. The principle of the proposed tap-reversing strategy is to inverse the tap actions once the power system voltages fall below some threshold. Vournas and Karystianos [100] discussed how tap-blocking and tap-reversing based LTC techniques can avoid an approaching voltage collapse, as well as the advantages and drawbacks of these techniques. Another type of LTCs was the voltage set-point reduction, which is based on the lowering of the reference voltage to improve voltage stability [101].

The generation rescheduling was another technique to prevent voltage collapse. Several approaches reported in the literature concerning the implementation of generation rescheduling to avoid voltage instability of a power system. Kumar *et al.* [102] proposed a zonal/cluster-based congestion management approach, in which the generators belongs to most sensitive zones are identified for rescheduling their real power output. Talukdar *et al*. [103] presented a technique for generation rescheduling based on the sensitivities of the overloaded branches to the bus injections. Yesuratnam and Thukaram [104] proposed a new approach for real power generation rescheduling based on relative electrical distance concept for overload mitigation. The generator sensitivities to the power flow of the congested lines have been used as indices for optimal selection of candidate generators [105]. Raouf and Kalantar [106] proposed a new method called reactive power rescheduling with generator ranking to improve power system voltage stability. In the proposed method, the generators were divided into two groups: important and less-important generators. Then, the VSM was enhanced by increasing and reducing reactive power generation at the two groups, respectively. Particle Swarm Optimization (PSO) was applied to determine the amount and the most suitable generators for reactive power rescheduling [107]. Verma and Mukherjee [108] proposed a generation rescheduling method for congestion management in electricity market using Ant Lion Optimizer (ALO) algorithm. In this study, contingencies such as branch outage and sudden load

variation are considered. A comparative analysis of the proposed technique with several recent algorithms is carried out on three test systems i.e., IEEE 30-bus, IEEE 57-bus and IEEE 118-bus and the results show the superiority of the proposed technique. In [109], Firefly Algorithm (FFA) has been successfully implemented to optimize the amount of real power generation rescheduling incorporating pumped storage hydro unit. Nesamalar *et al.* [110] proposed an energy management methodology based generation rescheduling, on day-ahead and hour-ahead basis, using Cuckoo Search (CS) algorithm. It was reported that the proposed CS algorithm can reduce energy rescheduling cost, energy loss, and energy generation cost.

Load Shedding (LS) technique was also identified as an effective emergency action against voltage collapse because it results in an instantaneous voltage stability enhancement. However, due to the disturbance affected the consumers that have been shed; this action must be the latest protection applied method. LS techniques are generally divided into three main types i.e., conventional, adaptive, and computational intelligence-based LS [111]. Conventional load shedding techniques are of two types Under Frequency Load Shedding (UFLS) and Under Voltage Load Shedding (UVLS). UFLS involve shedding determined amounts of the load if the system frequency falls below its specified range. It has been first introduced by Lokay and Burtnyk [112] and ameliorated by some other authors [113, 114]. UFLS is based on the determination of the worst probable system contingency, then, the size and number of LS required to ensure the minimum permissible frequency would be determined. In the same manner, UVLS is applied by power utilities to avoid a risk of voltage collapse and restore voltage to its nominal value [115]. The major drawback of the conventional LS techniques is that are limited by their incapability to deliver optimum LS [116]. Adaptive LS is another type of LS techniques. It based on the use of power swing equation to shed the desired amount of load as reported in [117]. Albeit the Adaptive LS techniques improve the reliability of conventional LS, they suffer from un-optimum LS due to the variations in the rate of change of frequency. The application of computational intelligent techniques was another alternative for solving LS problem. The benefits of the application of computational intelligence in LS over the conventional ones are outlined in [111]. The ANN is one of the most applied techniques in power system LS [118-121]. The high influence of the

training data size in the training time and the problem of sticking to local minima are the major drawbacks of the application of ANN [6]. ANFIS model has been also applied to LS in a power system [122-123]. The combination of ANFIS with decision tree technique in hybrid form was applied in [124] to shed a load of the power system under stressed conditions and with the integration of wind power generation. Meta-heuristic optimization algorithms have some application in LS problem in power systems. Among the implemented meta-heuristic methods to minimize the LS, the GA-based method [125], the PSO algorithm [126], the PSO-Simulating Annulling (PSO-SA) optimization technique [127], the Differential Evolution (DE) algorithm [128], the Glowworm Swarm Optimization (GSO) algorithm [129] and the Harmony Search Algorithm (HSA) [130].

In recent years, under the paradigm of the smart grids, in which the major operations are executed in a coordinated and efficient manner, the focus for solving power system problems has moved more from the supply-side to the demand-side. Such concept is known as demand-side management (DSM), which the main purpose is the adjustment of consumer demand to increase efficiency and reliability of power system. Among the DSM solutions, demand response (DR) strategy is gaining increasing interest after several successful implementations in real power systems and their indubitable benefits [131]. DR programs aimed to electricity price reduction, transmission lines congestion resolving, security enhancement and improvement of market liquidity [132]. Emergency Demand Response (EDR) is one of the most widely used DR programs. It is called upon when power generation is anticipated to experience a shortfall or during the contingency situations [17]. In EDR programs, the EDR participants are contractually obligated to provide a set amount of capacity and they receive payments for being available and face financial penalties for non-attendance. A number of works have been reported in the literature on the implementation of EDR programs. The application of EDR program in the spinning reserve markets has been reported in [133]. In [134], the AC load flow based on customer interruption load cost has been used to evaluate the impacts of EDR program on the reliability of a deregulated power system. The obtained results confirm that the EDR program has a good impact on system reliability. Shayesteh *et al*. [135] examined the influence of EDR program on available transfer capability enhancement considering system reliability. Rajesh and Jason [136] proposed an EDR program that empowers the

use of residential load resources to respond to contingencies down to the distribution level. Sahebi *et al.* [137] proposed the use of Unit Commitment (UC) as a platform to implement both EDR and interruptible load contracts programs. Mixed Integer Linear Programming (MLIP) has been implemented in order to solve the optimization problem. To overcome the limitations of MLIP method, the nonlinear and nonconvex UC–EDR problem has been solved using simulated annealing method [138]. The authors of Ref. [139] have proposed a novel approach to formulate customer-oriented demand response employing analytic hierarchy process for selecting and prioritizing DR programs. Aalami and Khatibzadeh [140] conducted several simulations to show the effectiveness of the proposed nonlinear EDR-based price elasticity concept in the reduction of the wholesale electricity price in the spot market. Focusing on the implementation of EDR for security enhancement, Wang *et al.* [9], proposed an event-driven EDR strategy to improve the operating reserves under a credible contingency. In the proposed method, a multistage optimization technique is used to solve the nonlinear problem associated with EDR program. The proposed multistage technique is based on segmentation of the original problem into a series of linear optimization problems. However, this procedure needs to be repeated several times until a required security margin is achieved, which is time-consuming. On the other hand, the proposed strategy considers all loads in the system as EDR participants which results in high demand reduction costs.

## 2.7 Conclusion

This chapter has presented for the first time the voltage stability phenomenon, the basic concepts related to this phenomenon and the main analysis techniques used to evaluate the voltage stability. Then, a literature review of machine learning techniques applied to analyze power system voltage stability, weak buses identification for voltage stability improvement and countermeasures against voltage collapses are presented.

# Chapter 3: On-line voltage stability assessment using hybrid meta-heuristics-SVR models based on PMU measurements

## 3.1 Introduction

In recent years, due to the economic and environmental issues, modern power systems often operate close to their voltage stability limits enlarging the probable level of voltage instability risks. Therefore, fast and efficient methods to assess power system voltage stability are of great importance to experts and industrials in order to avoid a risk of large blackouts.

In order to assess the voltage stability in an on-line manner, it is indispensable that the measurement, the estimation, and the analysis be attained during a short period of time. Traditionally, the voltage phasors at system buses are provided by Supervisory Control and Data Acquisition (SCADA) based state estimator, typically every few minutes. In addition to the slow nature of SCADA system, the conventional methods of voltage stability assessment such as $P$–$V$ and $Q$–$V$ curves, continuation power flow and voltage stability indices require comparatively large computations and are not efficient for real-time or on-line applications.

Nowadays, Phasor Measurement Unit (PMU) is employed in many countries to enhance the security, reliability, and the efficient monitoring of the power system. Compared to the SCADA, PMU devices are able to provide the measurement data (voltages and currents), with great accuracy, 100 times faster than SCADA system [5]. The PMU technology, in cooperation with the advanced computational intelligence (CI) techniques, has opened new perspectives for on-line voltage stability analysis.

This chapter presents the development of new hybrid models for on-line voltage stability assessment. The developed models are based on the combination of the SVR with the recently proposed optimization algorithms namely Ant Lion Optimizer (ALO),

Dragonfly Algorithm (DA) and Whale Optimization Algorithm (WOA). The rest of this chapter is organized as follow: the basic theory of PMUs, the formulation of voltage stability index and the SVR model concepts are first presented. Then, the proposed hybrid models and their application for on-line voltage stability assessment are explained. Finally, numerical applications are carried out on the IEEE 14-bus and the real Algerian 114-bus systems for testing the efficiency of the proposed methods.

## 3.2 Phasor Measurement Unit (PMU) technology

Phasor Measurement Unit (PMU) is a power system device that provides real-time synchronized measurements of voltage, current and frequency in terms of magnitude and phasor. Recently, PMU is becoming an important element of the modern power system. A number of PMUs are installed in several countries around the world for different applications such as state estimation, monitoring, protection and control of power systems.

### 3.2.1 Synchrophasors definition

The synchrophasors are accurate time-synchronized measurements of some power system's parameters (voltage, current and frequency) provided by the PMUs. A phasor is a complex number that represents a sinusoidal waveform with magnitude and phase angle at a specific point in time [141].

An AC waveform can be mathematically represented by the following equation:

$$V(t) = V_1 \cos\left(2\pi f t + \delta_1\right) \tag{3.1}$$

where $V_1$ is the magnitude of the AC waveform, $\delta$ is the angular starting point for the AC

Where $f$ is the instantaneous frequency.

In a phasor notation, the AC waveform is commonly represented as follows (see Figure 3.1):

$$V = V_m \angle \delta_1 \tag{3.2}$$

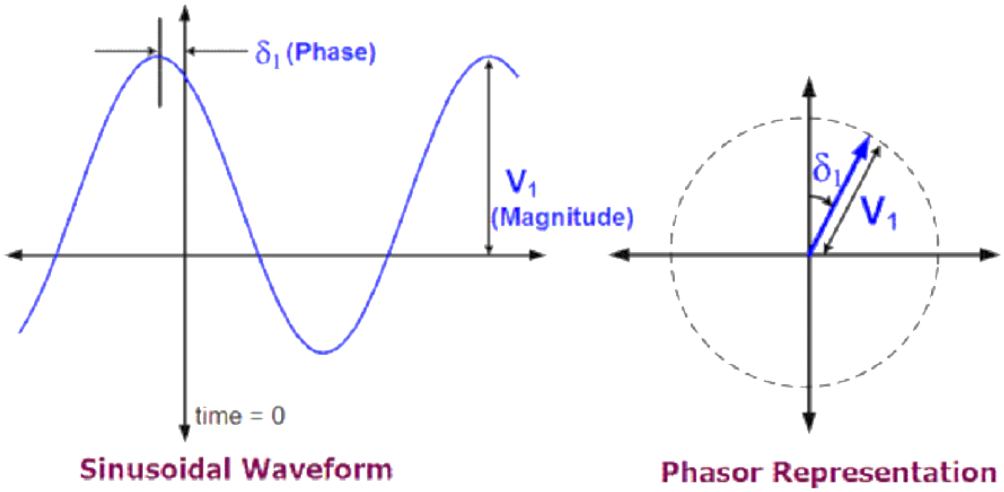


**Figure 3.1** Phasor representation [141]

### 3.2.2 Phasor Measurement Unit (PMU) devices

PMU was first developed and introduced into the power system in the 1980s [142]. It is a smart metering device that measures a voltage phasor of the power system's bus, a local frequency as well as the current phasor of the lines emanating from that bus, with respect to the global time reference received from the GPS of satellites [143]. With the introduction of PMUs, the timely comparison of measurements (magnitudes and angles) obtained over widely detached locations in power grids is consequently possible, which is considered as the main advantage of PMUs.

### 3.2.3 PMU based Wide Area Measurement System (WAMS)

Wide Area Measurement System (WAMS) is a novel locution introduced to power system literature in the late 1980s by Bonneville Power Administration and first implemented in the Western North American power system [144, 145]. Previously, the WAMS was defined as follows [144]:

*"The WAMS effort is a strategic effort to gather significant information required to change power system"*.

In recent years, as consequence of the wide commercialization of PMU devices, the high speed and the low cost of communication systems, the definition of WAMS had

become different. A newly definition of WAMS could be presented as follows: *"The WAMS is a network of PMUs and conventional measurement devices together with the new communication systems, which the fundamental aims are the monitoring, centralized control, and protection of power systems in wide geographical areas"* [146]. The simplified architecture of WAMS based PMUs is represented in Figure 3.2. The PMUs installed in different locations in the power system send the time synchronized data to control center (s). The precise and accurate real-time measurements (current, voltage and frequency) offered by PMUs help the operators in taking the required control actions for more security and better operation of power system.

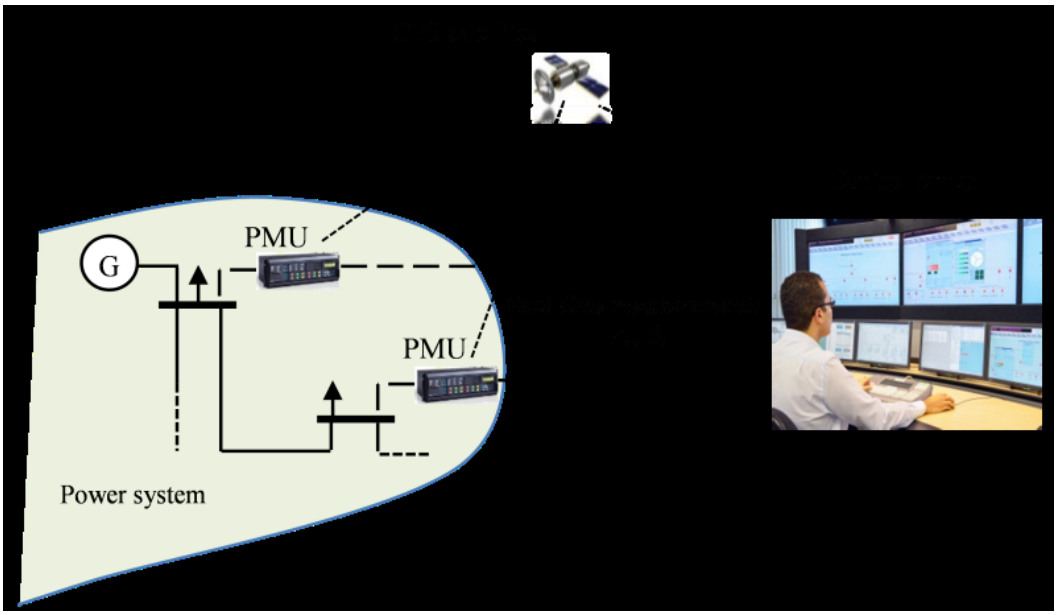


**Figure 0.2** Simplified structure of WAMS based PMUs

### 3.3 Support Vector Regression (SVR)

Support vector regression (SVR), the extended version of support vector machine was proposed by Vapnik in 1995 [147]. It has become a paramount computational tool due to its prosperous applications in the regression and prediction problems. The SVR model is based on a non-linear transformation of the input variables into a higher-dimensional feature space. The main idea of SVR is briefly reported here considering a regression function $F$ which is estimated based on the training data in the form of $\{(x_i, y_i)$ $i=1, 2,\ldots, n\}$, where $x_i$ and $y_i$ are the input and output sets, respectively; $n$ is the overall

number of the dataset. In SVR method, the regression function is approximated utilizing the following function [147]:

$$F = w^{T}\varphi(x) + b \tag{3.3}$$

where $F$ is the predicted output, $w$ is the weight vector, $b$ is the bias and $\varphi(x)$ is the high-dimensional input vector. The coefficients $w$ and $b$ were computed by minimizing the risk function, as given below.

$$R(F) = \frac{1}{2}\|w\|^2 + C\frac{1}{n}\sum_{i=1}^{n} L_{\varepsilon}(y_i, F_i) \tag{3.4}$$

$L_{\varepsilon}(y_i, F_i)$ is called the $\varepsilon$-insensitive loss function. This function is defined as follows:

$$L_{\varepsilon}(y_i, F_i) = \begin{cases} 0 & \text{if } |y_i - F_i| \le \varepsilon \\ |y_i - F_i| - \varepsilon & \text{otherwise} \end{cases} \tag{3.5}$$

where $\varepsilon$ represents the maximum deviation allowed during the training. This allowed deviation can be viewed as a tube around the regression function where all points located on the exterior of the tube are considered as training errors as shown in Figure 3.3. The penalty parameter $C$ is used to determine the trade-off cost between the minimization of the training error and the model complexity. In order to estimate $w$ and $b$, the Equation (3.4) is converted to the constrained form given by Equation (3.6) by introducing two positive slack variables $\xi$ and $\xi^*$. These variables represent the stated excess positive and negative deviations, respectively, and assume non-zero values on the exterior of the $\varepsilon$-tube and zero inside [147].

$$\text{minimize} \quad \frac{1}{2}\|w\|^2 + C\sum_{i=1}^{n}(\xi_i + \xi_i^*) \tag{3.6}$$

$$\text{Subject to} \quad \begin{cases} w \cdot \varphi(x) + b - y_i \le \varepsilon + \xi_i \\ (y_i - (w \cdot \varphi(x) + b) \le \varepsilon + \xi_i^* \\ \xi_i, \xi_i^* \ge 0, \quad i = 1, 2, \ldots, n \end{cases} \tag{3.7}$$

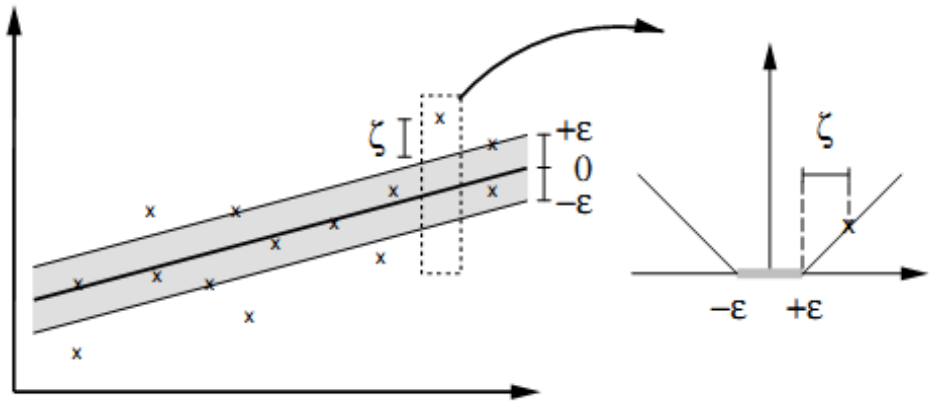


**Figure 0.3** Regression with the $\varepsilon$-insensitive tube [148]

The optimization problem in Equation (3.6) can be solved more easily in its dual formulation. Therefore, a standard dualization technique using Lagrangian multipliers has been employed. Using the Lagrangian multipliers, this problem can be written in the dual formulation as follows [148]:

$$\text{Maximize}\left\{-\frac{1}{2}\sum_{i,j=1}^{n}(\alpha_i-\alpha_i^*)(\alpha_j-\alpha_j^*)(\varphi(x_i)\cdot\varphi(x_j))-\varepsilon\sum_{i=1}^{n}(\alpha_i-\alpha_i^*)+\sum_{i=1}^{n}y_i(\alpha_i-\alpha_i^*)\right\} \tag{3.8}$$

$$\text{Subject to}\quad \begin{cases}\sum_{i=1}^{n}(\alpha_i-\alpha_i^*)=0\\ 0\le\alpha_i,\alpha_i^*\le C \qquad i=1,2,\ldots,n\end{cases} \tag{3.9}$$

where $\alpha$, $\alpha^*$ represent the Lagrangian multipliers.

The SVR function can be obtained by solving the dual maximization problem in Equation (3.8) as follows:

$$F(x,\alpha_i,\alpha_i^*)=\sum_{i=1}^{n}(\alpha_i-\alpha_i^*)(\varphi(x_i)\cdot\varphi(x_j))+b \tag{3.10}$$

The vector inner-product $(\varphi(x_i)\cdot\varphi(x_j))$ can be replaced by a kernel function $K(x_i,x_j)$. Hence, the Equation (3.10) becomes:

$$F(x,\alpha_i,\alpha_i^*)=\sum_{i=1}^{n}(\alpha_i-\alpha_i^*)K(x_i,x_j)+b \tag{3.11}$$

The prevalent kernel functions provided by SVR are:

Linear:

$$K(x_i, x_j) = x_i^T x_j \tag{3.12}$$

Polynomial:

$$K(x_i, x_j) = \left(t + x_i^T x_j\right)^d \tag{3.13}$$

Radial Basis Function (RBF):

$$K(x_i, x_j) = \exp\left(\frac{-\left\|x_i - x_j\right\|^2}{2\gamma}\right) \tag{3.14}$$

where $\gamma$ represent the bandwidth of the RBF function.

### 3.3.1 Necessity of SVR parameters optimization

In order to build an effective SVR model with high prediction accuracy, there are three parameters that need to be chosen carefully. These parameters include [149]:

- *Penalty parameter C*: Parameter *C* determines the trade-off cost between the minimization of the model complexity and the training error.
- *Non-sensitivity coefficient*$\varepsilon$: Parameter $\varepsilon$ controls the width of the $\varepsilon$-insensitive zone and its value affects the number of support vectors employed to construct the regression function.
- *Kernel function*: The kernel function is employed to build a nonlinear decision hyper-surface on the SVR input space. As mentioned before, several kernel functions have been proposed in the literature, however, the choice of the suitable kernel function dramatically depends on the nature of the data representing the problem. In this work, the RBF kernel function has been used. This kernel function is characterized by its ability to analyze a higher dimensional data and its simplicity.

The above-cited parameters, known in some literature as *hyper-parameters*, have considerable influence on the regression accuracy and generalization performance of the SVR model. The following example represents the impact of those parameters on the predictive ability of the SVR. In this example, a simple data set is used to train the SVR.

As shown in Figure 3.4, the small value of penalty parameter $C$ ($C$ = 1 in our example) leads to disagreement between the training data and the values predicted by SVR model. Contrariwise, with the big value of $C$ ($C$ = 20) the predicted values are in good agreement with the actual ones, which emphasizes the great impact of the penalty parameter $C$ in the predictive capability of the SVR. In the same manner, Figures 3.5 and 3.6 show the impact of $\varepsilon$ and $\gamma$ RBF kernel function parameter in the regression accuracy. Generally, various parameter settings can lead to considerable differences in SVR performance, which emphasizes the great importance of SVR parameters optimization.

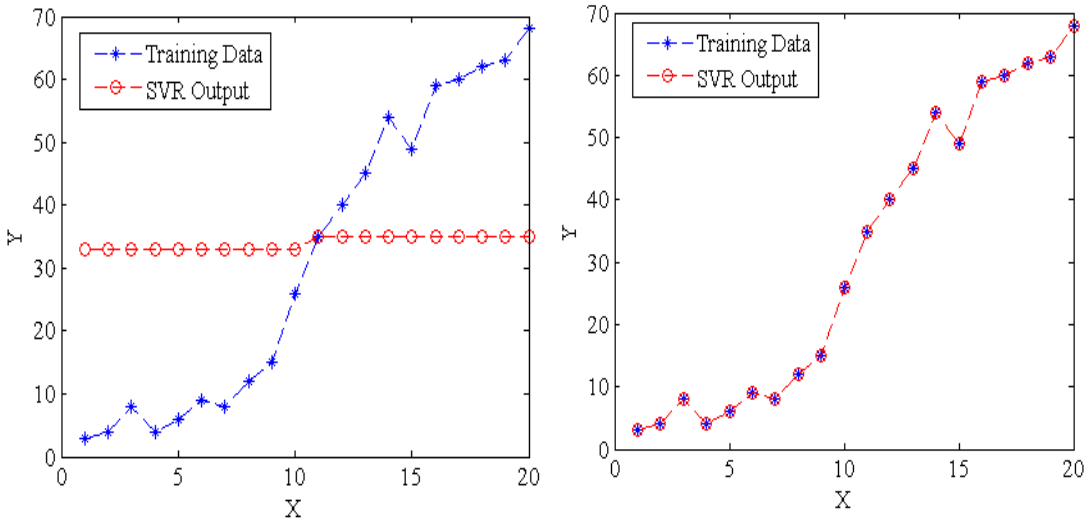


**(a)** **(b)**

**Figure 0.4** The effect of penalty parameter $C$ in the SVR performance, **(a)** $C$=1, **(b)** $C$=20

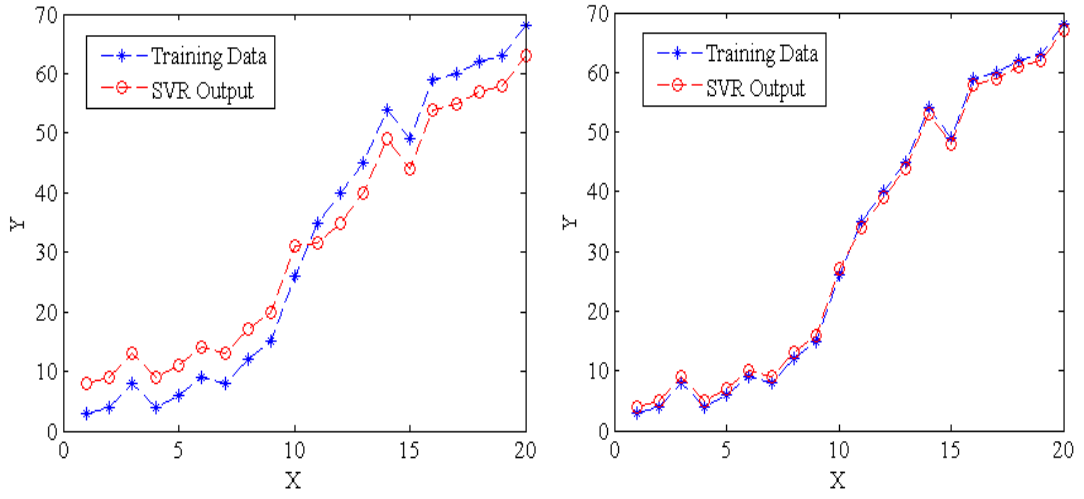


**(a)** **(b)**

**Figure 0.5** The effect of the $\varepsilon$ parameter in the SVR performance, **(a)** $\varepsilon$= 5, **(b)** $\varepsilon$= 1

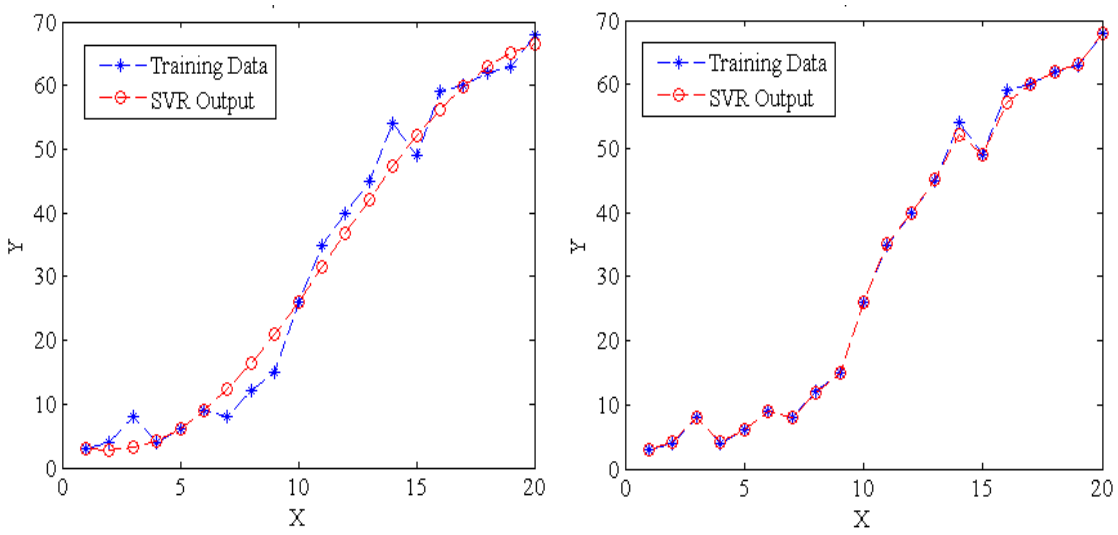


**(a)** **(b)**

**Figure 0.6** The effect of the RBF parameter ($\gamma$) in the SVR performance, **(a)** $\gamma$=10, **(b)** $\gamma$=1

### 3.4 SVR parameters optimization using meta-heuristic optimization algorithms

As shown in the previous section, the SVR parameters need to be selected properly by the user, because the regression performance of the SVR model heavily depends on the right set of these three parameters. Hence, a reliable and robust optimization strategy for SVR parameter selection is a pre-requisite to obtain a well-performing and robust SVR regression model.

Optimization is the process/methodology of finding the best possible solution for a particular problem under a set of given constraints. Many algorithms have been proposed in the past to solve various optimization problems, most of them were deterministic approaches (e.g., linear programming, nonlinear programming, and mixed-integer nonlinear programming, etc.). Deterministic optimization is the classical branch of mathematic optimization algorithms that based on the iterative enhancement of the initial solution using some algorithms. Over the last few decades, due to the technological advancement in computers, meta-heuristic optimization algorithms have appeared and a great importance has reported to these methods.

The term meta-heuristic was introduced by Glover in 1986 [150]. It refers to the family of methods that generate and use random variables for minimizing/maximizing an objective function. According to [151], meta-heuristic optimization methods can be

regrouped into four main categories: evolution-based algorithms, physics-based algorithms, human-based algorithms and swarm-based algorithms as shown in Figure 3.7.

Evolutionary-based methods simulate the process of natural evolution where the search for an optimum value starts by the generation of a random population which is then improved through a number of iterations or generations. Among these methods: Genetic Algorithm (GA), Evolution Strategy (ES), Genetic Programming (GP) and Biogeography-Based Optimizer (BBO). Physics-based meta-heuristic algorithms are inspired by the phenomenon of physics. Among these methods: Gravitational Search Algorithm (GSA), Big-Bang Big-Crunch (BBBC), Black Hole (BH) and Galaxy-based Search Algorithm (GbSA). Swarm-based algorithms mimic the social comportment of groups of animals. The most popular Swarm-based algorithms are Particle Swarm Optimization (PSO), Artificial Bee Colony optimization (ABC) and Ant Colony Optimization (ACO). Human-based algorithms are inspired by human behaviours. Some of the most popular human-based algorithms are Group Search Optimizer (GSO), Teaching Learning Based Optimization (TLBO), Firework Algorithm (FA) and Interior Search Algorithm (ISA).

Recently, novel flexible and efficient stochastic optimization algorithms have been proposed and used in a significant number of practical applications. In this section, the recently developed algorithms called Antlion Optimizer (ALO), Dragonfly Algorithm (DA) algorithm and Whale Optimization Algorithm (WOA) have been used to find the most appropriate values of SVR parameters.

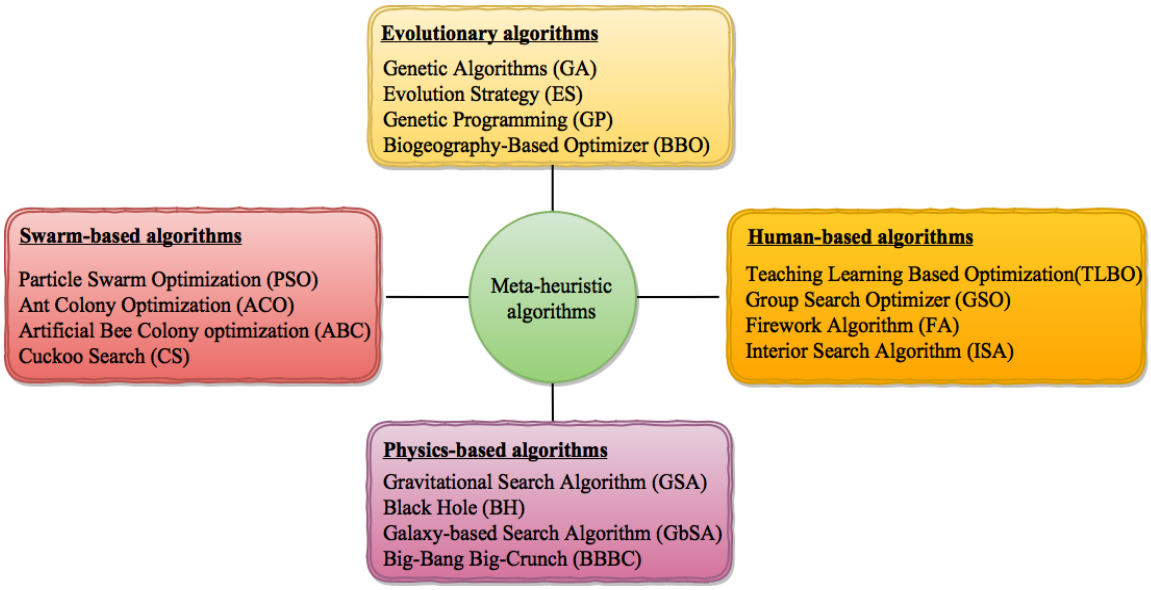


**Figure 0.7** Classes of meta-heuristic optimization algorithms

### 3.4.1 SVR optimized by Antlion Optimization (ALO) algorithm

#### 3.4.1.1 ALO algorithm

ALO is a recently established new and efficient swarm intelligence optimization technique proposed by Mirjalili in 2015 [152]. It was inspired by the intelligent demeanour of Antlion hunting mechanism for ants in nature. Antlions belong to Myrmeleontidae family of class net-winged insects. Figure 3.8 shows an Antlion in nature. The Antlion larvae dig a cone-shaped pit in the sand by moving along a circular path and throwing out sands with its massive jaw [152]. Figure 3.9 shows several cone-shaped pits with different sizes. The edge of the cone is sharp enough for insects to fall to the bottom of the trap easily. Figure 3.10 illustrates the hunting demeanour in which Antlion wait for the ants to be trapped in the cone-shaped pit. When an ant or other preys (e.g., small insects) fall into the pit, the Antlion catches it and pull it under the sand.

**Figure 0.8** Antlion in nature

**Figure 0.9** Cone-shaped traps

**Figure 0.10** Sliding ants toward Antlion

The mathematical modelling of the demeanour of Antlion hunting mechanism can be summarized in the follows procedures [152].

**Random walks of ants:** In nature, the ants walk in a random way when seeking for food. This stochastic movement is given by Equation (3.15).

$$X(t) = \begin{bmatrix} 0, cumsum\begin{pmatrix} 2r(t_1)-1, cumsum(2r(t_2)-1), \ldots, \\ cumsum(2r(t_n)-1) \end{pmatrix} \end{bmatrix} \tag{3.15}$$

where *cumsum* is the cumulative sum, $t$ represents the step of a stochastic walk (iteration), $n$ is the maximum number of iterations and $r(t)$ is a random function expressed by the following equation.

$$r(t) = \begin{cases} 1 & if \quad rand > 0.5 \\ 0 & if \quad rand \le 0.5 \end{cases} \tag{3.16}$$

where *rand* is a random number generated with uniform distribution in the range of [0 1].

To confine that the random walks are within the search space, the ant movement must be normalized at every iteration as follows.

$$X_i^t = \frac{(X_i^t - a_i) \times (d_i - c_i^t)}{(d_i^t - a_i)} + c_i \tag{3.17}$$

where $X_i^t$ is the normalized value of the $i$th variable, $t$ represents the iteration, $a_i$ and $d_i$ are respectively the min-max of the stochastic walk of the $i$th variable, $c_i^t$ and $d_i^t$ are the min-max of the stochastic walk of the $i$th variable at $t$th iteration, respectively.

**Trapping in antlion's pits:** The ant's stochastic walk is influenced by ant-lions' traps, which can be modelled as follows.

$$\begin{cases} c_i^t = Antlion_j^t + c^t \\ d_i^t = Antlion_j^t + d^t \end{cases} \tag{3.18}$$

where $c^t$ and $d^t$ are the min-max of variables at $t$th iteration, respectively, $Antliont_j^t$ indicates the position of the $j$th Antlion at the $t$th iteration.

**Building trap and sliding ants toward ant lion:** The antlions' hunting capability can be modelled using the roulette wheel. The slipping of ants into Antlions pits is given by the Equation (3.19).

$$\begin{cases} c^t = \frac{c^t}{I} \\ d^t = \frac{d^t}{I} \end{cases} \tag{3.19}$$

where $I$ is a ratio given as follows:

$$I = \begin{cases} 10^2 \times \frac{t}{T} & if \ \frac{t}{T} > 0.1 \\ 10^3 \times \frac{t}{T} & if \ \frac{t}{T} > 0.5 \\ 10^4 \times \frac{t}{T} & if \ \frac{t}{T} > 0.75 \\ 10^5 \times \frac{t}{T} & if \ \frac{t}{T} > 0.9 \\ 10^6 \times \frac{t}{T} & if \ \frac{t}{T} > 0.95 \end{cases} \tag{3.20}$$

where $t$ and $T$ are the current iteration and the total number of iterations, respectively.

**Catching ants and rebuilding the pit:** when an ant reaches the lowest part of the pit, the Antlion consumes it. To increase the opportunities for catching another ant, the Antlion takes the position of the latest caught prey and rebuild a novel pit. This process can be modelled as follows.

$$Antlion_j^t = Ant_i^t \quad if \quad f\left(Ant_i^t\right) > f\left(Antlion_j^t\right) \tag{3.21}$$

where $Ant_i^t$ is the position of $i$th ant at $t$th iteration.

**Elitism:** The elite Antlion, which is the best Antlion obtained at every iteration, is saved and it must be competent to influence the locomotion of all the ants. Thus, it presumed that each ant unsystematically walks around a chosen Antlion by the roulette wheel and the elite at the same instant as follows:

$$Ant_i^t = \frac{R_A^t + R_E^t}{2} \tag{3.22}$$

where $R_A^t$ and $R_E^t$ are respectively the stochastic walks around the Antlion chosen by the roulette wheel and round the elite at $t$th iteration.

### 3.4.1.2 Hybrid ALO-SVR model

In this sub-section, the ALO technique is applied to optimize the SVR parameters. Figure 3.11 shows the flowchart of the new hybrid ALO-SVR-based model, which is explained by the steps below.

**Step 1:** Set the values of ALO parameters including:

- The number of ants and Antlions;
- The maximum number of iterations;
- The number of variables (number of SVR parameters);
- The upper and lower bounds of SVR parameters ($C$, $\gamma$ and $\varepsilon$).

**Step 2:** Initialize the random walks of ants as the initial population using Equation (3.15).

**Step 3:** Read the dataset and create two sets, i.e., training and testing sets.

**Step 4:** Train SVR model using training set and compute the fitness value of ants and Antlions. The root mean squared error (RMSE) was used as the fitness function.

$$Fitness = \sqrt{\frac{1}{n}\sum_{i=1}^{n}(a_i - p_i)^2} \tag{3.23}$$

where $a$ and $P$ are the actual and the predicted outputs, respectively; $n$ is the overall number of data.

**Step 5:** Find the best Antlion and consider it as the elite.

**Step 6:** For every ant:

- Choose an Antlion based on the roulette wheel
- Update the values of $c$ and $d$ utilizing the Equation (3.19).
- Generate a stochastic walk and normalize it using the Equations (3.15) and (3.17).
- Update the position of ant based on the Equation (3.22).

**Step 7:** (Fitness evaluation): Compute the fitness of all ants.

**Step 8:** Substitute an Antlion with its corresponding ant if it becomes fitter using Equation (3.21).

**Step 9:** Update the elite if an Antlion becomes better.

**Step 10:** Check the stopping criterion: if the stopping criterion, which is the maximum number of iterations, is achieved go to the step 11. Otherwise, loop to the step 6.

**Step 11:** When the stopping criterion was achieved, the elite comprised the optimized SVR parameters was selected. Then the SVR model was tested and evaluated using testing set and performance evaluation indices.

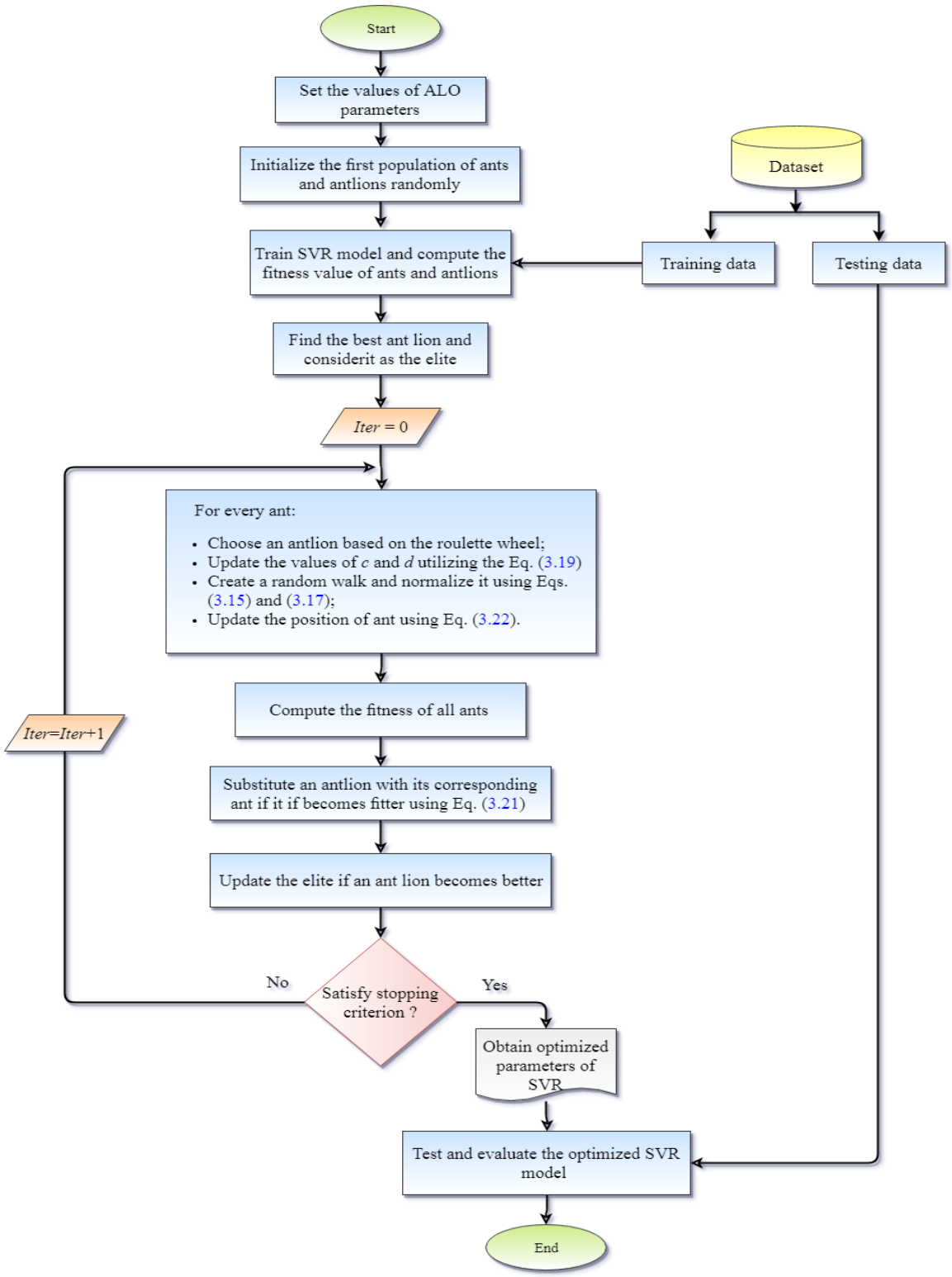


**Figure 0.11** Flowchart of the new hybrid ALO-SVR model

### 3.4.2 SVR optimized by Dragonfly Algorithm (DA)

#### 3.4.2.1 DA algorithm

DA algorithm is a recently established new and efficient swarm intelligence optimization technique proposed by Mirjalili in 2015 [153]. It was inspired by the dynamics of dragonflies in nature. Dragonflies are carnivorous insects which catch and eat a wide variety of small insects from gnats and mosquitoes to wasps and butterflies. Generally, the Dragonfly swarms are both dynamic and static in the natural world. Dynamic swarms, or migratory swarms, form as large groups (hundreds of thousands of dragonflies) and flying in a single direction and travelling for long distance as shown in Figure 3.12. During the process of static swarms, in which the dragonflies hunting prey, they fly in small groups frequently over a well-determined small area and much closer to the land as shown in Figure 3.13. Naturally, the instinct of each individual in the swarm imposes to attract to the nurturing sources and distract outward enemies. From these two conducts that the DA algorithm is inspired.

**Figure 0.12** Dynamic dragonfly swarms

**Figure 0.13** Static Dragonfly swarms

The position updating of each individual in the swarm is represented in Figure 3.14 and mathematically explained as follows [153].

***Separation*** **(S):**

The aim of this step is to eschew the collision of individuals with their neighbours in the static swarm. This separation is expressed by the following equation.

$$S_i = \sum_{j=1}^{n} X - X_j \tag{3.24}$$

where $X$ and $X_j$ are the positions of the current individual and the $j$th neighbouring individual, respectively; $n$ is a number of neighbouring individuals.

***Alignment*** **(A):**

The purpose of this step is to match the velocity of each individual with the other. The alignment is given by Equation (3.25).

$$A_i = \frac{\sum_{j=1}^{n} V_j}{n} - X \tag{3.25}$$

where $V_j$ is the velocity of neighbouring individual $j$.

***Cohesion*** **(C):**

It refers to the movement of individuals towards the centre of the swarm's group.

$$C_i = \frac{\sum_{j=1}^{n} X_j}{n} - X \tag{3.26}$$

***Attraction towards the food*** **(F):**

All individuals tend to move towards the food.

$$F_i = X^+ - X \tag{3.27}$$

where $X^+$ shows the position of the food source.

***Distraction outwards an enemy*** **(E):**

It is calculated as follows:

$$E_i = X^- - X \tag{3.28}$$

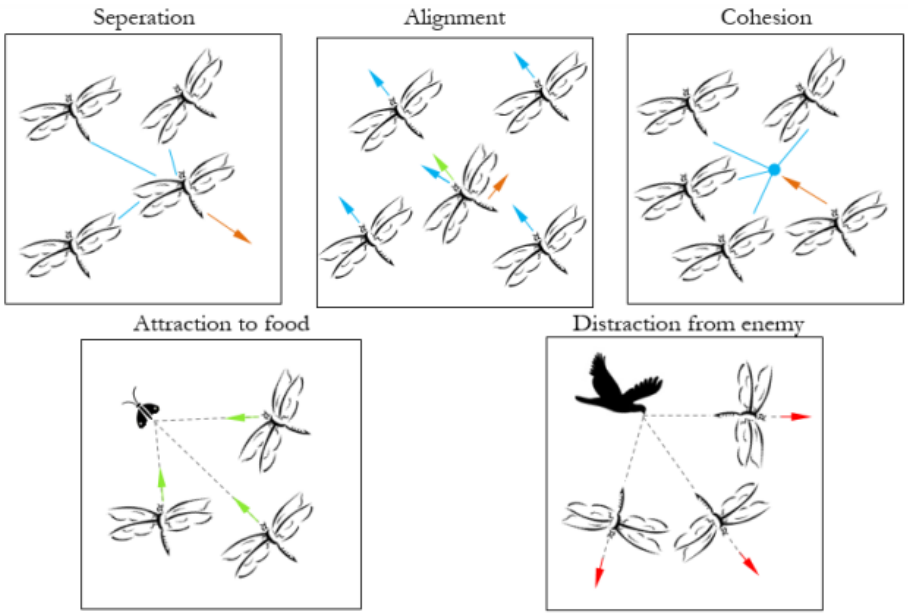


**Figure 0.14** Primitive corrective patterns between individuals in a swarm [153]

where $X^-$ shows the position of the enemy.

The position of each dragonfly is updated based on step vector $\Delta X$, which is calculated as follows.

$$\Delta X_i = \left(sS_i + aA_i + cC_i + fF_i + eE_i\right) + w\Delta X_t \tag{3.29}$$

where *s, a,* and *c* represent respectively the separation, alignment, and cohesion weights; *f* and *e* are the food and the enemy factors, respectively; *w* is the inertia weight and *t* is the iteration counter. The updated position vector is calculated as follows.

$$X_{t+1} = X_t + \Delta X_{t+1} \tag{3.30}$$

In the case of no neighbouring solutions founded, Dragonflies fly around the search space using a random walk, or Lévy flight, to ameliorate their randomness, stochasticity, and exploration. In this case, the dragonflies update their position based on the following equation:

$$X_{t+1} = X_t + Lévy(d) + X_t \tag{3.31}$$

where *t* is the current iteration, and *d* is the dimension the dimension of the search space. Lévy flight is given by:

$$Lévy\ (x) = 0.01 \times \frac{r_1 \times \sigma}{|r_2|^{\frac{1}{\beta}}} \tag{3.32}$$

where $r_1$ and $r_2$ are random numbers in the range of [ 0,1]; $\beta$ is a constant (equal to 1.5 in this work) and $\sigma$ is given by the following equation.

$$\sigma = \left( \frac{\Gamma(1+\beta) \times \sin\left(\frac{\pi\beta}{2}\right)}{\Gamma\left(\frac{1+\beta}{2}\right) \times \beta \times 2^{\left(\frac{\beta-1}{2}\right)}} \right)^{\frac{1}{\beta}} \tag{3.33}$$

where $\Gamma(x)=(x-1)!$.

### 3.4.2.2 Hybrid DA-SVR model

In this section, the recently developed dragonfly algorithm has been deployed to optimize the SVR parameters. Figure 3.15 shows the flowchart of this new hybrid DA-SVR-based model. The processing steps are described as follows:

**Step1:** Set the values of DA parameters such as:

- The number of dragonflies (candidate solutions);
- The maximum number of iterations;
- The upper and the lower bounds of *C,* $\gamma$ and $\varepsilon$.

**Step2:** Initialize the step vectors $\Delta X_i$ ($i=1, 2, ..., n$), the values of $s$, $a$, $c$, $f$, $e$ and $w$, and the values of SVR parameters ($C$, $\gamma$ and $\varepsilon$).

**Step 3:** Train the SVR model using the training set and compute the fitness value of every dragonfly. The RMSE was used as a fitness function.

**Step 4:** Update the values of $s$, $a$, $c$, $f$, and $e$.

**Step 5:** For all individuals, calculate the values of $S$, $A$, $C$, $F$ and $E$ using Equations (3.24) to (3.28).

**Step 6:** Update the neighbouring radius.

**Step 7:** If the Dragonfly has at least one neighbouring dragonfly, the velocity and the position of the dragonfly are updated based on the Equations (3.29) and (3.30). Otherwise, the position vector is updated using Equation (3.31).

**Step 8:** Correct the new positions taking into account the upper and lower values of variables $C$, $\gamma$ and $\varepsilon$.

**Step 9:** Check the stopping criterion: if the stopping criterion is achieved go to the Step 10. Otherwise, loop to the step 3.

**Step 10:** The best position of all individuals comprised the optimized SVR parameters is selected, then the SVR model was tested and evaluated using a testing set and performance evaluation indices.

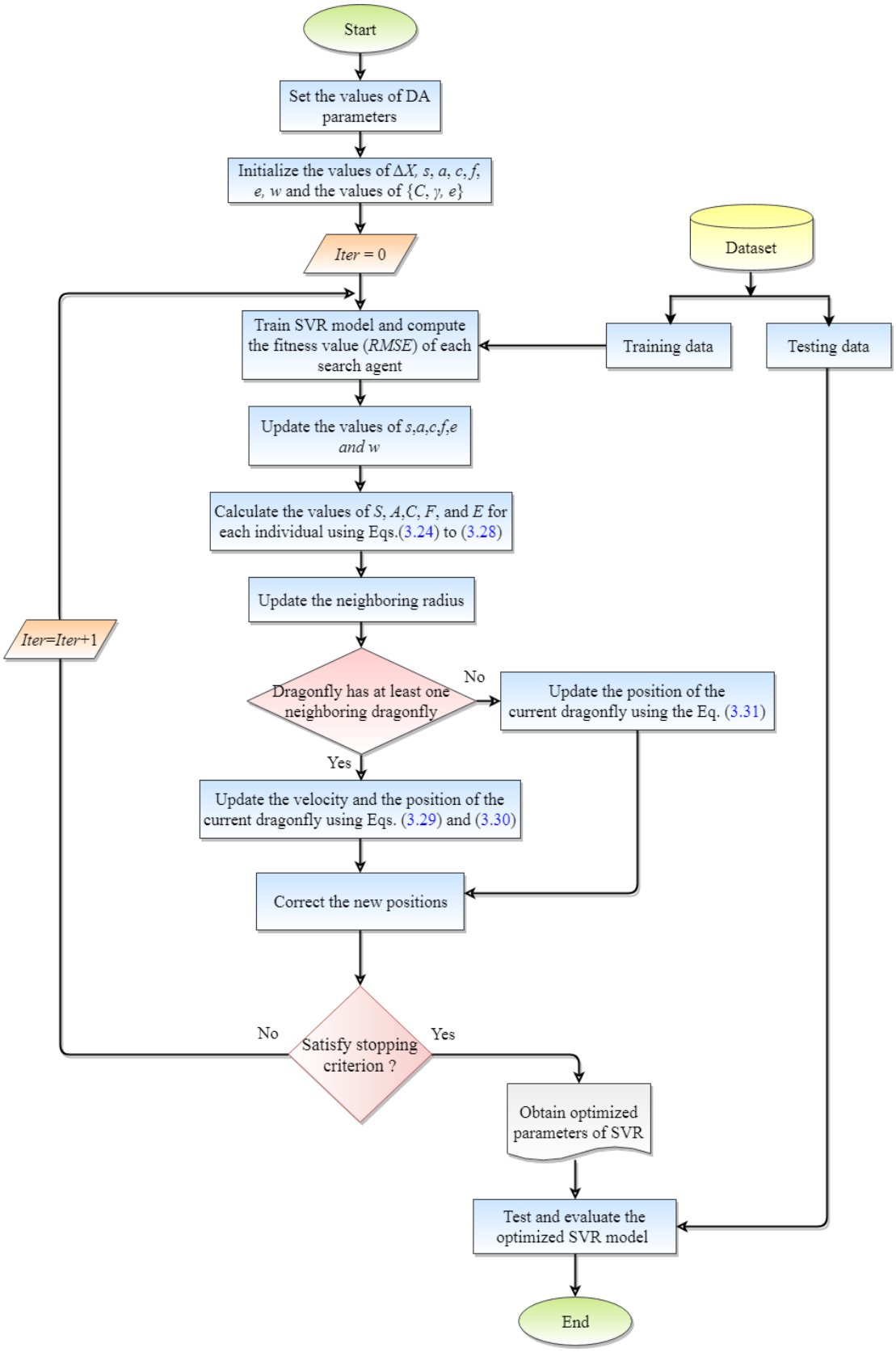


**Figure 0.15** The flowchart of the proposed DA-SVR model

### 3.4.3 SVR optimized by Whale Optimization Algorithm (WOA)

#### 3.4.3.1 WOA algorithm

WOA optimization algorithm is a novel bio-inspired optimization technique proposed by Mirjalili in 2016 [151]. It is based on the simulation of the special hunting method of one of the biggest baleen whales called humpback whales. This kind of whales feeds a small prey as krill, herrings, and other small fishes near the surface, their demeanour to find and hunt the prey is called "bubble-net feeding". The humpback whales dive down and then start to create a ring of bubbles to encircle the fishes, which are too frightened to pass through the bubbles as shown in Figure 3.16, in meantime the whales swim upward to the surface through the bubble net and swallowing a huge number of fishes in one swig.

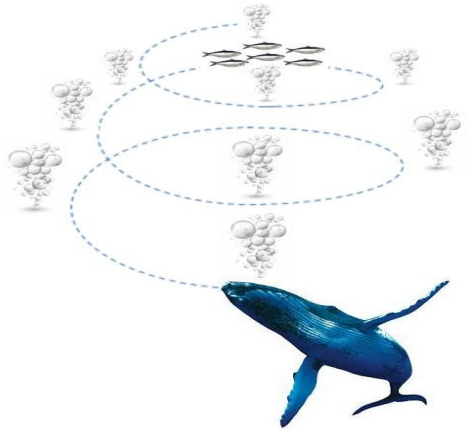

**Figure 0.16** Humpback whales bubble-net feeding technique

The bubble-net feeding behaviour is mathematically modelled as follows.

**Searching for prey:**

Humpback whales search for prey randomly according to the position of each other. The mathematical model is as follows:

$$D = \left| C \cdot X_{rand} - X \right| \tag{3.34}$$

$$X(t+1) = X_{rand} - A \cdot D \tag{3.35}$$

where $t$ indicates the current iteration; $X$ is the position vector; $X_{rand}$ is a random position vector (a random whale) chosen from the current population; $A$ and $C$ are coefficient vectors computed as follows:

$$A = 2a.r - a \tag{3.36}$$

$$C = 2r \tag{3.37}$$

where $a$ is linearly decremented from 2 to 0 along with the iterations, $r$ is a random vector in [0, 1]. Therefore, $A$ is used with the random values $|A|>1$ in order to guarantee the global search for the WOA algorithm. The position of every search agent is renewed according to a randomly chosen search agent [151].

**Prey encircling technique:**

After locating the prey, humpback whales circle around this prey to start hunting them. The WOA presumes that the current best candidate solution is the target prey or is close to the optimum. Accordingly, the overall search agents will renew their new positions towards the best-determined search agent. This demeanour is represented as follows:

$$D = \left| C.X^{*}(t) - X(t) \right| \tag{3.38}$$

$$X(t+1) = X^{*}(t) - A.D \tag{3.39}$$

where $X^*$ is the position vector of the best solution obtained so far. Figure 3.17 illustrates the rationale behind Equation (3.39). The position ($X$, $Y$) of a search agent can be updated, according to the position of the current best record ($X^*$, $Y^*$), by adjusting the values of $A$ and $C$ vectors.

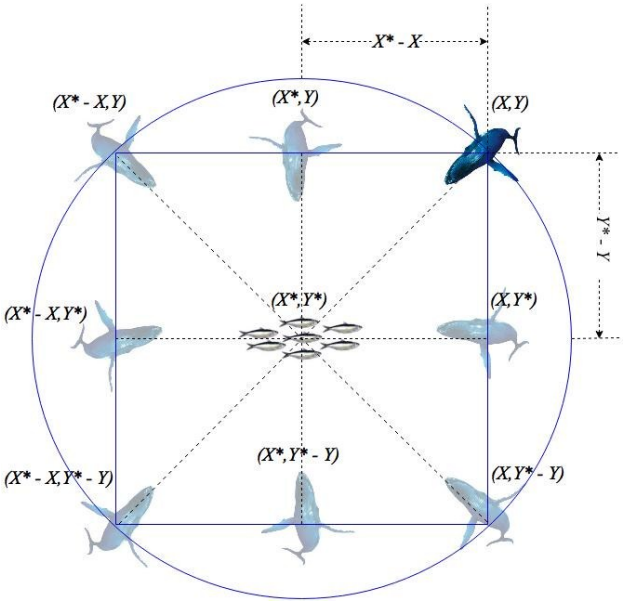


**Figure 0.17** Principle of prey encircling technique used by humpback whales

**Bubble-net attacking technique:**

As above-mentioned, after locating the prey and encircling them, humpback whales start the hunting step using the bubble-net mechanism. Two approaches to model the bubble-net demeanour of humpback whales are proposed as represented below.

*Shrinking encircling technique*:

This behaviour is achieved by decrementing the value of $a$ in the Equation (3.36), consequently, the value of $A$ is also decreased by $a$. Figure 3.18 shows the possible positions from ($X$, $Y$) towards ($X^*$, $Y^*$) that can be achieved by $0 \leq A \leq 1$.

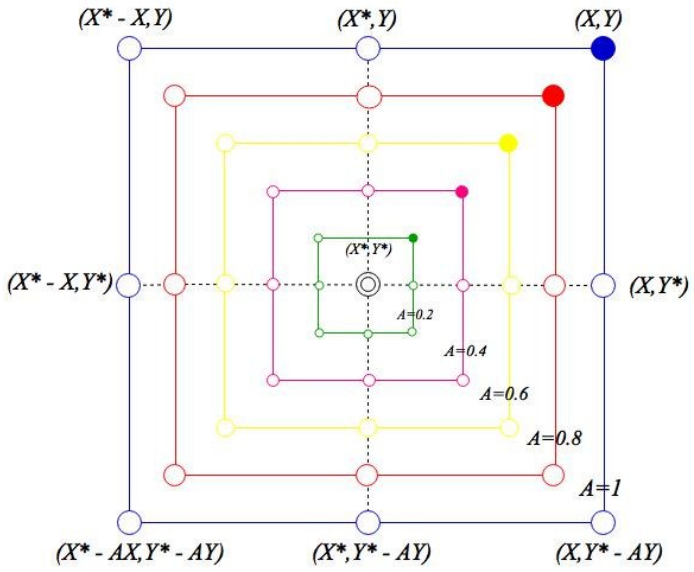


**Figure 0.18** Shrinking encircling technique

*Spiral updating position*:

In this approach the distance between the whale located at ($X$, $Y$) and the prey located at ($X^*$, $Y^*$) is first calculated (see Figure 3.19), then the spiral equation to imitate the helix-shaped movement of humpback whales is formed as follows [151]:

$$X(t+1) = D' \cdot e^{bl} \cdot \cos(2\pi l) + X^*(t) \tag{3.40}$$

where $D' = |X^*(t) - X(t)|$ indicates the distance between the $i$th whale and the prey (best solution obtained so far); $b$ is a constant that determines the form of the logarithmic spiral; $l$ is a randomly chosen number in the range [−1, 1].

The humpback whales swim around the prey within a shrinking circle and along a spiral path at the same time. To model this simultaneous behaviour, we suppose that there is a probability of 50% to choose the technique that will be used to update the position of whales during optimization. The mathematical model is as follows:

$$X(t+1) = \begin{cases} X^*(t) - A.D & \text{if } p < 0.5 \\ D'.e^{bl}.\cos(2\pi l) + X^*(t) & \text{if } p \geq 0.5 \end{cases} \tag{3.41}$$

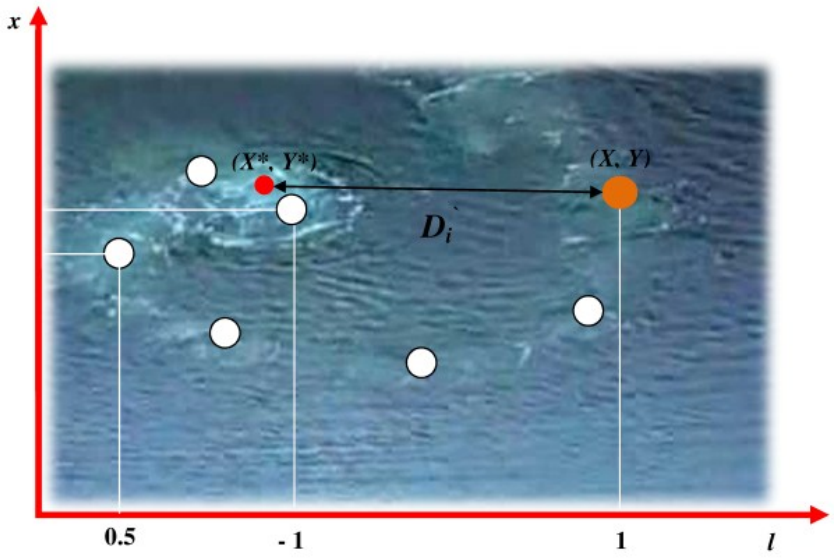


**Figure 0.19** Spiral updating position

### 3.4.3.2 Hybrid WOA-SVR model

In this sub-section, the WOA technique is applied to optimize the SVR parameters. Figure 3.20 shows the flowchart of this new hybrid WOA-SVR-based model. The processing steps are described below.

**Step 1:** Set initial parameters: In WOA, there are four parameters that must be set, which are:

- Number of search agents (whales);
- Maximum number of iterations;
- Problem dimensions or variables number;
- Upper bound *lb* and lower *up* bound of SVR parameters ($C$, $\gamma$ and $\varepsilon$).

**Step 2:** Initialize the whale's population $\{C, \gamma, \varepsilon\}$.

**Step 3:** Train SVR model using training set and compute the fitness value for every search agent. The RMSE is employed as a fitness function.

**Step 4:** Update the values of $a$, $A$, $C$, $l$ and $p$.

**Step 5:** Update the search agent's positions according to the values of $A$ and $p$ using the Equations (3.35), (3.38) and (3.40). Accordingly, update the best position ($X^*$).

**Step 6:** Check the stopping criterion: if the stopping criterion is achieved the best solution comprised the optimal SVR parameters was selected, otherwise, repeat steps 3 to 6.

**Step 7:** The trained SVR model was tested and evaluated using a testing set and performance evaluation indices.

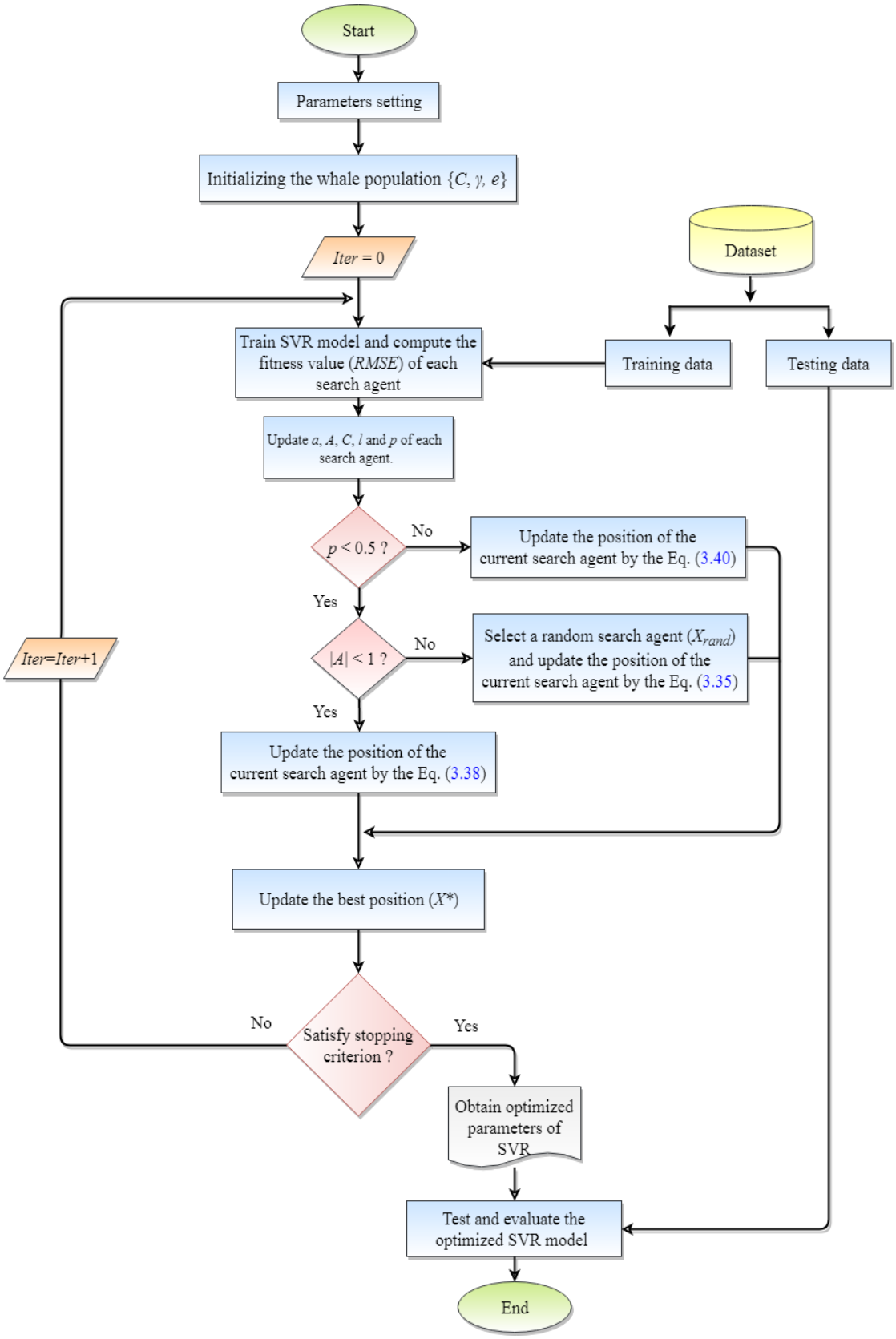


**Figure 0.20** The detailed flowchart of the proposed WOA-SVR model

## 3.5 Voltage stability assessment using meta-heuristics−SVR models

### 3.5.1 Voltage Stability Index (VSI) formulation

Voltage stability assessment is one of the important parts of the planning and operating of power systems. This assessment is for objective to identify whether the current operating point is secure or not, as well as to determine how close the system is to the voltage instability. Several indices have been introduced to assess the voltage stability and to determine the stability margins such as line stability factor (LQP) [29], line stability index ($L_{mn}$) [30], Fast Voltage Stability Index (FVSI) [31] and Voltage Stability Index (VSI) [32]. A comparative study of these indices has been presented in [154]. Based on this comparison, the VSI is found to be the best index since the mathematical formulation is derived considering all of the system margins, including real, reactive and apparent power margins. The derivation of VSI formulation is originated from a 2-bus system illustrated in Figure 3.21.

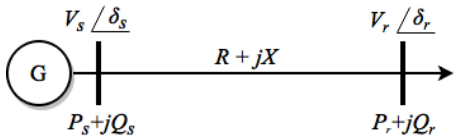


**Figure 0.21** A simple two-bus system

The current *I* that flows in the line given by:

$$\bar{I} = \frac{V_s \angle \delta_s - V_r \angle \delta_r}{R_l + jX_l} \tag{3.42}$$

The apparent power *S* at receiving end bus can be written as:

$$\bar{S}_r = \bar{V}_r \bar{I}^* \tag{3.43}$$

Rearranging the Equation 3.43 yields:

$$\bar{I} = \left( \frac{\bar{S}_r}{\bar{V}_r} \right)^* = \frac{P_r - jQ_r}{V_r \angle -\delta_r} \tag{3.44}$$

Equating Equations (3.42) and (3.44)

$$\frac{V_s \angle \delta_s - V_r \angle \delta_r}{R_l + jX_l} = \frac{P_r - jQ_r}{V_r \angle -\delta_r} \tag{3.45}$$

Separating the real and imaginary parts yields:

$$V_s V_r \cos\delta - V_r^2 = R P_r + X Q_r \tag{3.46}$$

And,

$$-V_s V_r \sin\delta = X_l P_r + R Q_r \tag{3.47}$$

where $\delta=\delta_s-\delta_r$.

From Equations (3.46) and (3.47), the real and reactive powers at the receiving end bus can be given by:

$$P_r = \left[ \left( V_s \cos\delta - V_r \right) \frac{R_l}{R_l^2 + X_l^2} + V_s \sin\delta \frac{X_l}{R_l^2 + X_l^2} \right] V_r \tag{3.48}$$

$$Q_r = \left[ \left( V_s \cos\delta - V_r \right) \frac{X_l}{R_l^2 + X_l^2} - V_s \sin\delta \frac{R_l}{R_l^2 + X_l^2} \right] V_r \tag{3.49}$$

$$V_r = \sqrt{\frac{V_s^2}{2} - \left( Q_r X_l + P_r R \right)_l \pm \sqrt{\frac{V_s^4}{4} - \left( Q_r X_l + P_r R_l \right) V_s^2 - \left( P_r X_l + Q_r R_l \right)^2}} \tag{3.50}$$

where, $V$ is the voltage magnitude; $s$ and $r$ are the sending and receiving buses, respectively; $R_l$ and $X_l$ are the line resistance and reactance, respectively. The maximum transmitted power $S_{max}$ through the line is attained as the internal root phrase equals to zero [32]. There will be a unique solution for $V_s$ and $V_r$ at the collapse point. The maximum transferred active power $P_{max}$, the maximum transferred reactive power $Q_{max}$ and the maximum transferred power $S_{max}$ can be expressed by equations (3.51) – (3.53), respectively:

$$P_{\max} = \frac{Q_r R_l}{X_l} - \frac{V_s^2 R_l}{2 X_l^2} + \frac{\left| Z_L \right| V_s \sqrt{V_s^2 - 4 Q_r X_l}}{2 X_l^2} \tag{3.51}$$

$$Q_{\max} = \frac{P_r X_l}{R_l} - \frac{V_s^2 X_l}{2 R_l^2} + \frac{\left| Z_L \right| V_s \sqrt{V_s^2 - 4 P_r R}}{2 R_l^2} \tag{3.52}$$

$$S_{\max} = \frac{V_s^2 \left[ \left| Z_L \right| - \left( \sin(\theta) X_l + \cos(\theta) R_l \right) \right]}{2 \left( \cos(\theta) X_l - \sin(\theta) R_l \right)^2} \tag{3.53}$$

where, θ is the load power angle, $\theta = \tan^{-1}\left[\frac{Q_r}{P_r}\right]$.

These equations can be simplified by supposing high $X$ to $R$ ratio.

$$P_{\max} = \sqrt{\frac{V_s^4}{4X_l} - Q_r \frac{V_s^2}{X_l}} \tag{3.54}$$

$$Q_{\max} = \frac{V_s^2}{4X_l} \frac{P_r^2 X_l}{V_s^2} \tag{3.55}$$

$$S_{\max} = \frac{\left(1 - \sin(\theta)\right) V_s^2}{2\cos(\theta)^2 X_l} \tag{3.56}$$

Therefore, based on these relations, the total VSI can be computed as [32]:

$$VSI = \min\left(\frac{P_{\max} - P_r}{P_{\max}}, \frac{Q_{\max} - Q_r}{Q_{\max}}, \frac{S_{\max} - S_r}{S_{\max}}\right) \tag{3.57}$$

To maintain a secure operating condition, the value of VSI index should be maintained greater than 0.

### 3.5.2 The proposed on-line voltage stability approach

The proposed methodology deployed for an on-line assessment of voltage stability based PMUs measurement using the obvious developed hybrid models is illustrated in Figure 3.22. It incipient with an off-line training of meta-heuristics–SVR models and the outcomes will be an on-line monitoring of power system voltage stability. During the off-line phase, the sufficient and convenient inputs and outputs required for the training and testing of SVR model are generated based on the conventional power flow. In the on-line phase, the real-time information or data obtained from the PMUs is applied to the well trained SVR models to estimate the VSI index.

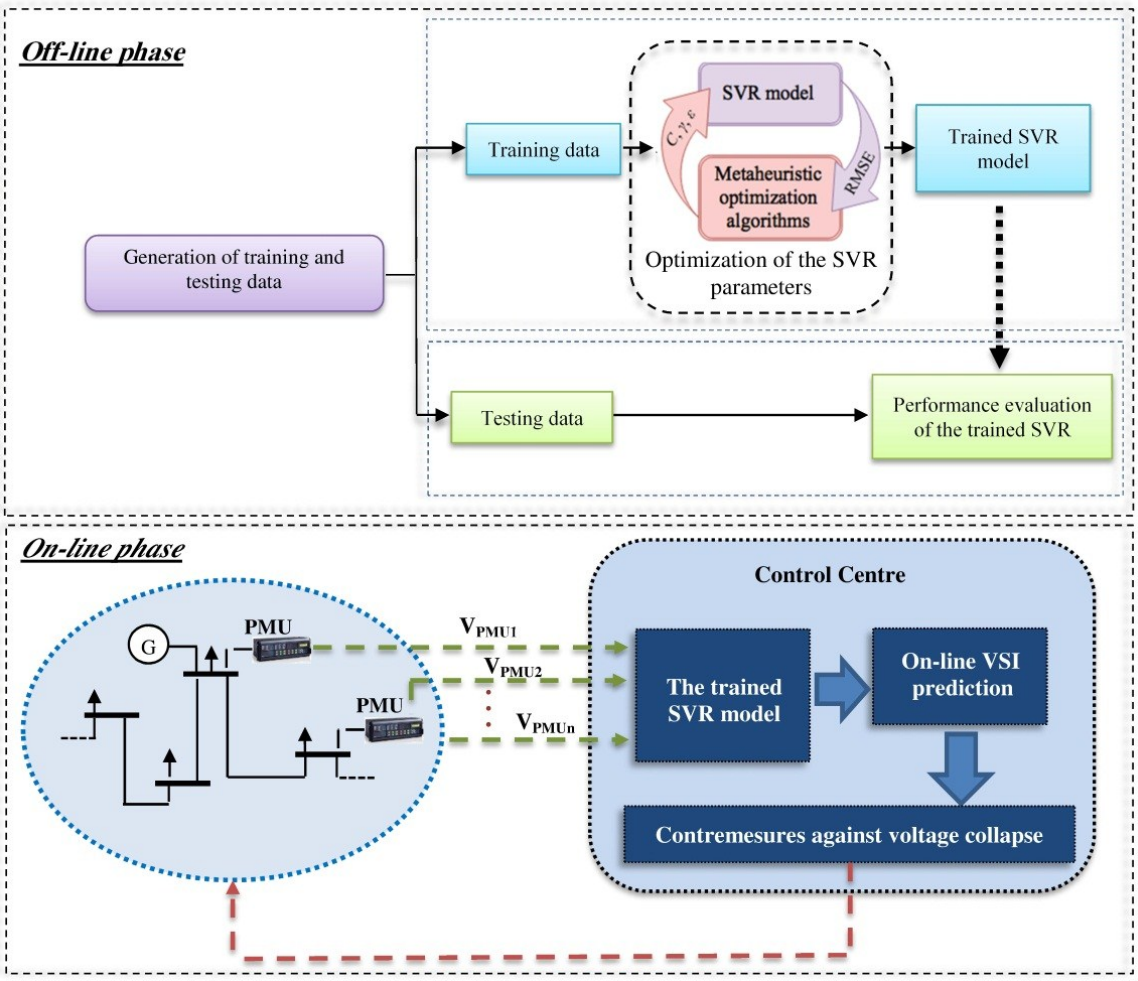


**Figure 0.22** Block diagram of the proposed on-line voltage stability assessment method

### 3.5.2.1 Generation of training and testing data

In order to train and to evaluate the performance of the proposed hybrid models, it is a prerequisite to prepare enough and appropriate training and testing data. These data are generated through off-line simulation process by varying both real and reactive power loads at all buses in the system. The load is increased randomly from the base case until the system reached the collapse point, and then the VSI is computed for each operating point. In order to meet the increased power demand, the active and reactive powers of all generators should be adjusted. The adjustment of the generators outputs is achieved using the optimal power flow method.

### 3.5.2.2 Contingencies ranking

During its operation, the power system encountered a wide range of contingencies such as the loss of transmission line contemplated as the most frequent contingency that can appear recurred in a system. In the present study, a single line outage is considered in the analysis. For a large power system, it is impractical and unnecessary to train the SVR model for all possible contingencies. Therefore, contingencies should be ranked and selected according to their voltage severity with the reason to focus merely on the analysis having critical situations of power system operation. The flowchart reasserts on the contingency ranking procedure is presented in Figure 3.23.

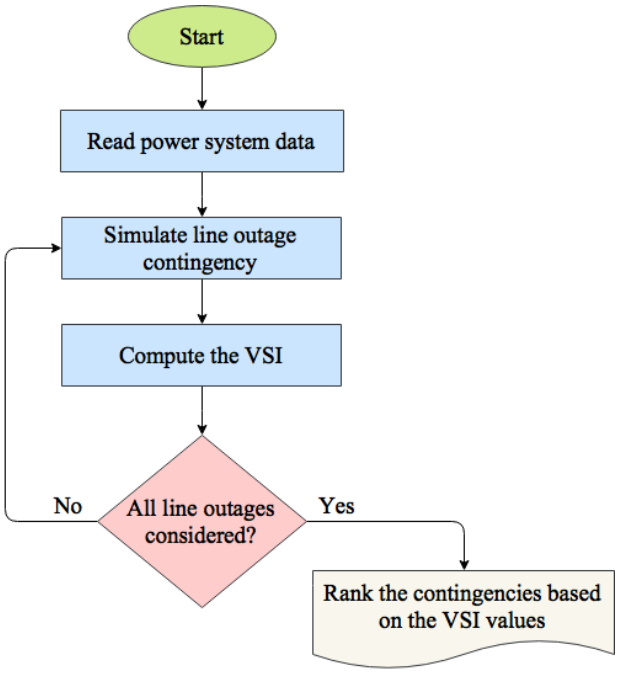


**Figure 0.23** Flowchart of contingency ranking procedure

### 3.5.2.3 Performance evaluation

In order to evaluate the performance of each model, the difference between the predicted and actual output values were evaluated according to the correlation coefficient (R), the mean absolute percentage error (MAPE), the root means square error (RMSE) and the percent root means square error (PRMSE). The statistical indices are calculated by the following equations:

$$R = \frac{\sum_{i=1}^{n}\left(a_i - \bar{a}\right)\left(P_i - \bar{P}\right)}{\sqrt{\sum_{i=1}^{n}\left(a_i - \bar{a}\right)^2 \sum_{i=1}^{n}\left(P_i - \bar{P}\right)^2}} \tag{3.58}$$

$$MAPE = \frac{100}{n}\sum_{i=1}^{n}\left|\frac{a_i - p_i}{a_i}\right| \tag{3.59}$$

$$RMSE = \sqrt{\frac{1}{n}\sum_{i=1}^{n}\left(a_i - p_i\right)^2} \tag{3.60}$$

where, $a$ and $P$ are the actual and the predicted outputs, respectively; $n$ is the number of data; $\bar{a}$ and $\bar{P}$ are the average of the actual and predicted values, respectively. The prediction model can be considered as robust in its performance if the correlation coefficient (R) value is close to unity. Thus, R = 1 indicates the good prediction and R = 0 the poor one. MAPE and RMSE are the most used indices in the literature; the criteria to evaluate the best model using these indices are relatively small for MAPE and RMSE in training and testing phases.

The PRMSE in percent is computed by the following Equation.

$$PRMSE = \frac{RMSE}{\sqrt{\frac{1}{n}\sum_{i=1}^{n} p_i^2}} \times 100 \tag{3.61}$$

Various ranges of PRMSE can be defined to determine the model precision [155]:

- Excellent for PRMSE < 10%;
- Good for 10% < PRMSE < 20%;
- Reasonable for 20% < PRMSE < 30%;
- Low for PRMSE > 30%.

### 3.6 Simulation and results

In this section, the effectiveness of the proposed voltage stability assessment methods has been validated on the IEEE 14-bus and real Algerian 114-bus power systems. The IEEE 14-bus test system, shown in Figure 3.24, consists of 14 buses, 5 generators, and 20 lines [156]. The Algerian 114-bus system, shown in Figure 3.25, contains 114 buses, 15 generators and 175 branches [157]. The IEEE 14-bus system data and the data of the Algerian power system can be found in Appendix A.

The simulations are done using MATLAB programming language, MATPOWER [156] and Power System Analysis Toolbox (PSAT) [158]. MATPOWER and PSAT are package of MATLAB M-files for electric power system analysis and simulation. The simulations are performed on a computer with specification Intel® Core™ i5-2540M CPU@2.60 GHz.

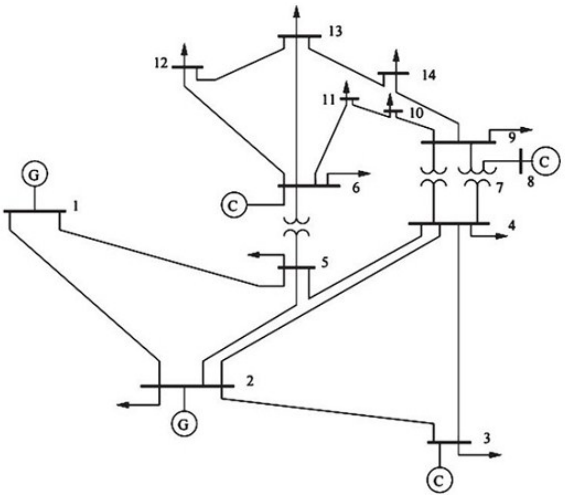


**Figure 0.24** Single line diagram of the IEEE 14-bus test system

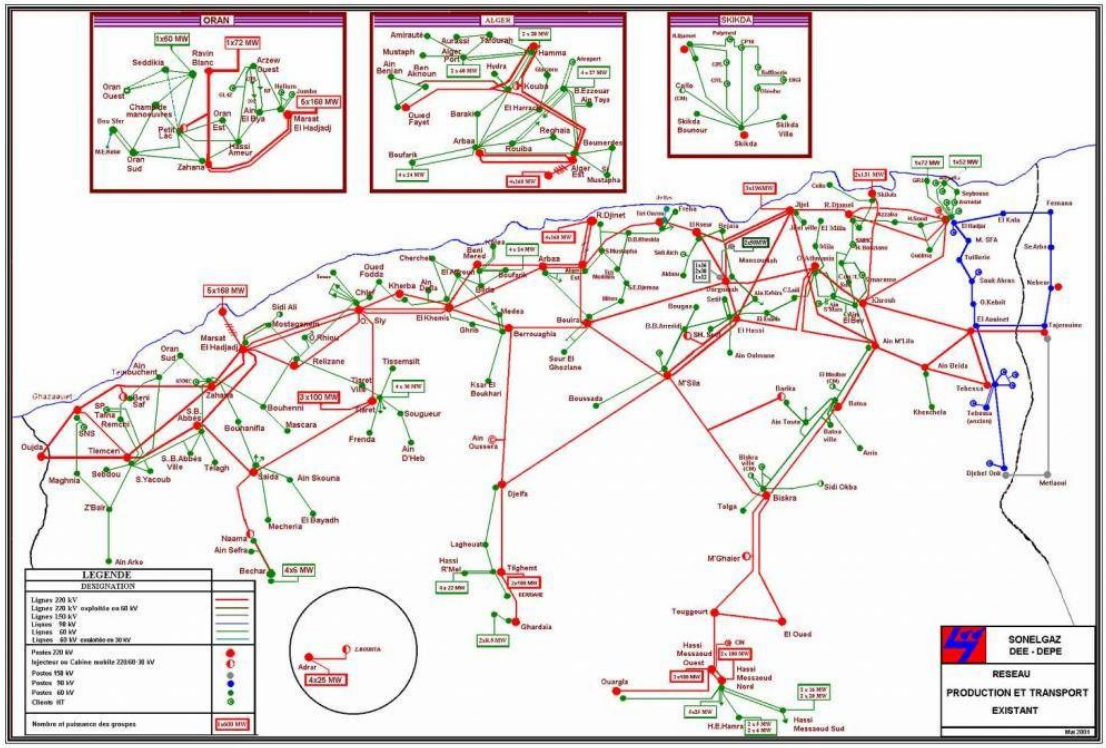


**Figure 0.25** Topology of the Algerian 114-bus power system [157]

In the on-line assessment of voltage stability based PMUs measurements, the optimal number and locations of PMUs should be specified beforehand. In order to obtain the optimal number and locations of PMUs with the aim of power system observability, the systems were simulated in PSAT software. The obtained appropriate buses to implement the PMUs are tabulated in Table 3.1. The gathered voltage magnitudes and voltage phase angles from PMU buses have been used as the input information for the hybrid meta-heuristics–SVR models. While the corresponding minimum values of voltage stability index ($VSI_{min}$) are used as the output variables. In order to generate the training and testing data, random sets of loads and corresponding generations are created using the power flow method to ensure that only the acceptable cases are considered. These data sets are generated by varying both real and reactive powers at load buses for the base case configuration and critical branch outage contingencies. As above-mentioned, it is impractical and time-consuming to evaluate the system performance considering all possible line outages. Therefore, it is better to reduce them to only the most critical ones.

To identify the most critical contingencies, contingency analysis was carried out for all single line outages in both systems. The selected contingencies along with their corresponding VSI in the base loading condition are shown in Table 3.2. In the present work, 900 random patterns were generated for the IEEE 14-bus system and 720 for the Algerian 114-bus system. From these generated patterns, 80% are employed to train the SVR model and the rest 20% are used to evaluate the performance of the proposed models.

**Table 0.1** Number and locations of the required PMUs

| Power system | Number of required PMUs | Locations of PMUs |
|---|---|---|
| IEEE 14-bus | 4 | 2, 4, 11, 13 |
| Algerian 114-bus | 35 | 2, 3, 10, 12, 15, 20, 22, 26, 36, 38, 39, 42, 46, 49, 50, 54, 57, 60, 61, 63, 69, 70, 73, 78, 79, 82, 89, 93, 96, 100, 101, 103, 109, 112, 113 |

**Table 0.2** Set of the critical contingencies of IEEE 14-bus and Algerian 114-bus systems

| Power system | Contingency N° | Line outage | VSI |
|---|---|---|---|
| IEEE 14-bus | 1 | Line between bus 1 and bus 2 | 0.0381 |
| | 2 | Line between bus 2 and bus 3 | 0.6468 |
| | 3 | Line between bus 5 and bus 6 | 0.6753 |
| | 4 | Line between bus 7 and bus 9 | 0.6857 |
| | 5 | Line between bus 4 and bus 7 | 0.7057 |
| | 6 | Line between bus 2 and bus 4 | 0.7122 |
| | 7 | Line between bus 2 and bus 5 | 0.7122 |
| | 8 | Line between bus 3 and bus 4 | 0.7152 |
| | 9 | Line between bus 4 and bus 5 | 0.7161 |
| | 10 | Line between bus 7 and bus 8 | 0.7389 |
| | Intact condition | All lines are in service | 0.7573 |
| Algerian 114-bus | 1 | Line between bus 63 and bus 66 | 0.1261 |
| | 2 | Line between bus 81 and bus 90 | 0.1720 |
| | 3 | Line between bus 85 and bus 87 | 0.2438 |
| | 4 | Line between bus 81 and bus 82 | 0.2950 |
| | 5 | Line between bus 87 and bus 100 | 0.3359 |
| | 6 | Line between bus 82 and bus 83 | 0.3440 |
| | 7 | Line between bus 80 and bus 82 | 0.3557 |
| | 8 | Line between bus 105 and bus 101 | 0.3560 |
| | 9 | Line between bus 103 and bus 105 | 0.3591 |
| | 10 | Line between bus 87 and bus 99 | 0.3600 |
| | Intact condition | All lines are in service | 0.3674 |

### 3.6.1 Application of ALO-SVR model in on-line voltage stability assessment

As described earlier, the proposed ALO-SVR model, to estimate VSI, was trained using voltage magnitudes and voltage phase angles of PMUs buses as the input vector and the corresponding minimum values of VSI as the output vector. When using the ALO algorithm for identifying the optimal SVR parameters, some parameters must be determined such as the maximum number of iterations, the number of search agents (candidate solutions), the fitness function, the number of variables, and the upper/lower bounds of variables. In the present study, the maximum number of iterations and the number of search agents were set to 100 and 30, respectively. The RMSE was considered as a fitness function in the optimization process. Moreover, the stopping criterion in this study is the maximum number of iteration. The ranges of $C$, $\gamma$ and $\varepsilon$ parameters are as follows: [1 1000], [0.1 1] and [0.0001 0.1] [84], respectively. The fitness curves of ALO algorithm for finding optimal SVR parameters, in both IEEE 14-bus and Algerian 114-bus systems, are displayed in 3.26(a) and (b). The optimal found values of $C$, $\gamma$ and $\varepsilon$ parameters are shown in Table 3.3.

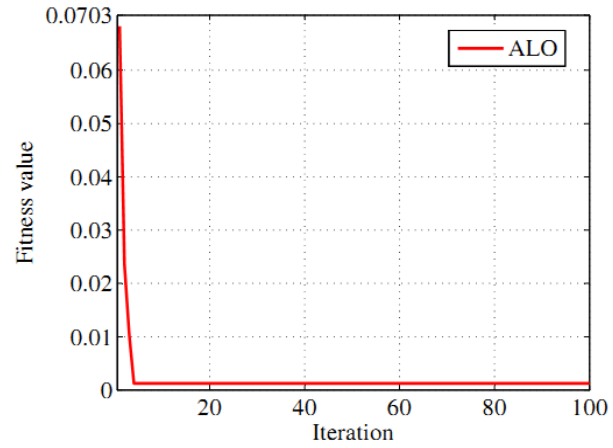


**(a)**

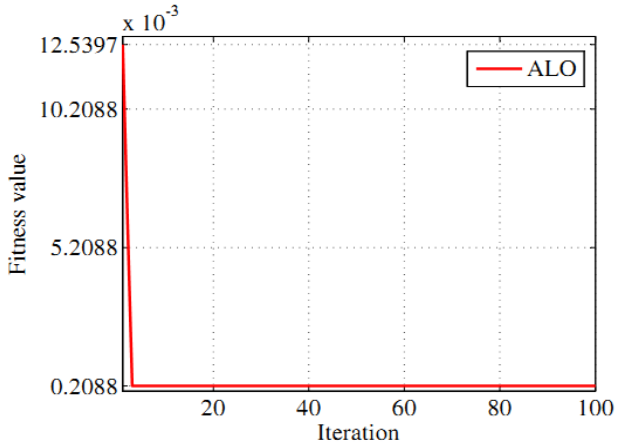


**(b)**

**Figure 0.26** Convergence curves of ALO for **(a)** IEEE 14-bus system, **(b)** Algerian 114-bus system

**Table 0.3** SVR parameters optimized by ALO algorithm

| SVR parameters | Optimal values of SVR parameters | |
|---|---|---|
| | **IEEE 14-bus** | **Algerian 114-bus** |
| $C$ | 520.5673 | 54.1874 |
| $\gamma$ | 0.1 | 0.1 |
| $\varepsilon$ | 0.0001 | 0.0001 |

Once the optimal parameters of SVR model are obtained, the ability of this proposed hybrid model to predict the VSI was evaluated. The actual values of VSI, calculated using conventional load flow, and the predicted values by ALO-SVR model in training and testing phases are plotted in Figure 3.27(a) and (b). Figure 3.28 shows the absolute error between the VSI index estimated by ALO-SVR model and the VSI index calculated by the conventional load flow. These Figures evince that the ALO-SVR model provides

the results that are in good agreement with the actual values and this is referring to the case study of the IEEE 14-bus system.

The above-mentioned discussion can be generalized to the results, shown in Figures 3.29(a) and (b) and 3.30, obtained by the application of ALO-SVR model to assess the voltage stability of the Algerian 114-bus system.

Figures 3.31 and 3.32 show the correlation plots of predicted versus actual values of VSI for both systems in the training and testing phases. For the IEEE 14-bus system (Figure 3.31(a) and (b)), the statistical characteristic of R=0.99998 was obtained in the training phase and R=0.99998 in the testing phase. For the Algerian 114-bus system (Figure 3.32(a) and (b)), the proposed technique managed to yield R=1 in the training phase and R=0.99996 in the testing phase. According to these results, it can be noted that the proposed ALO-SVR model has a good predicting performance. Computation time is also a significant aspect when applying machine learning techniques to a practical system. In the case of IEEE 14-bus, the computational time required in the training phase is 14.5689 (s) and in the testing phase is 0.008225 (s). In the case of Algerian system, the training and the testing time was 3.1798 (s) and 0.003294 (s), respectively.

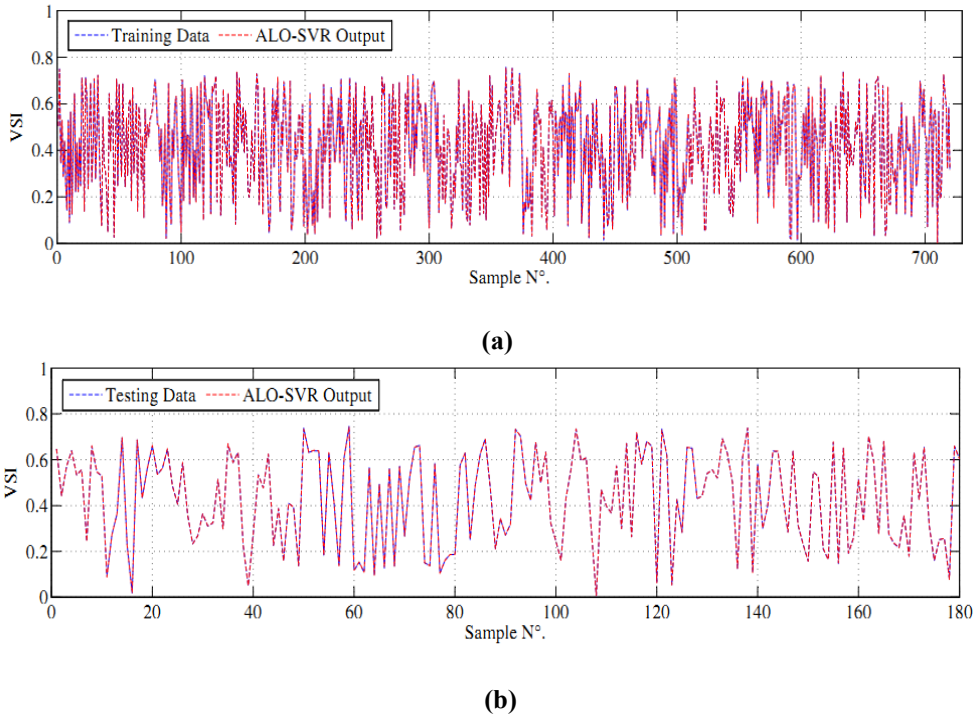


**Figure 0.27** Comparison between actual and predicted values using ALO-SVR in the case of IEEE 14-bus system: **(a)** Training phase, **(b)** Testing phase.

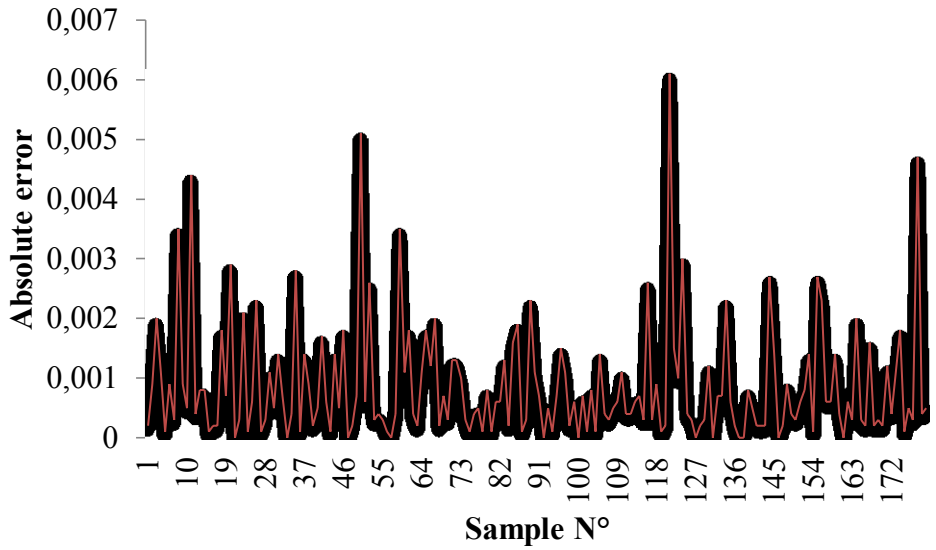


**Figure 0.28** Testing absolute error in the case of IEEE 14-bus system using ALO-SVR

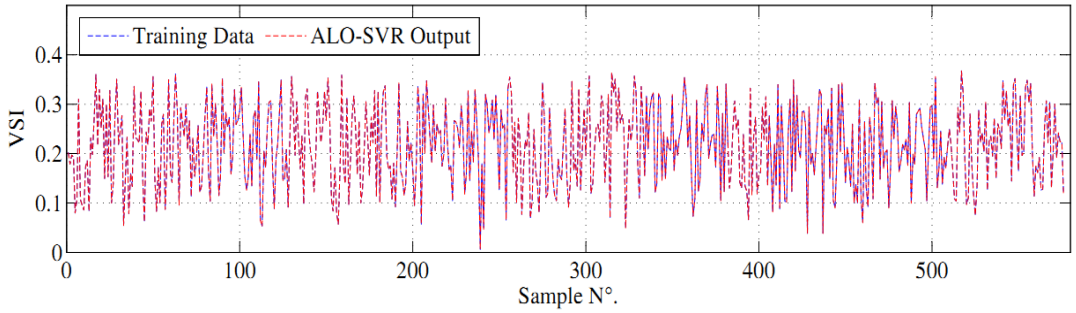


**(a)**

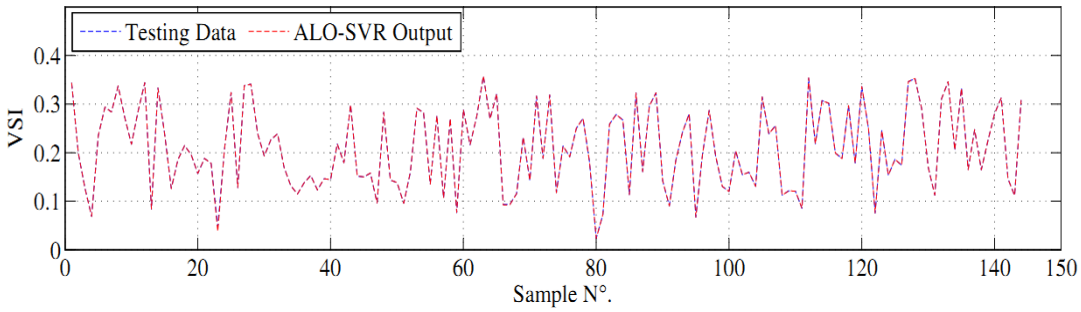


**(b)**

**Figure 0.29** Comparison between actual and predicted values using ALO-SVR in the case of Algerian 114-bus system: **(a)** Testing phase **(b)** Training phase

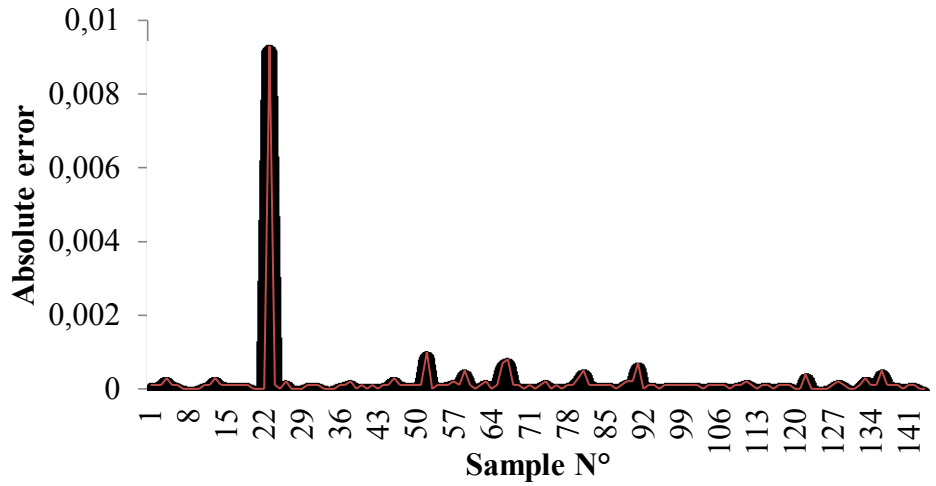


**Figure 0.30** Testing absolute error in the case of Algerian 114-bus system using ALO-SVR

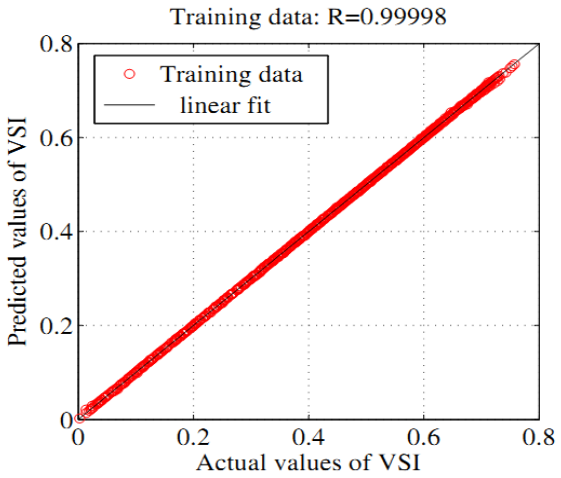


**(a)**

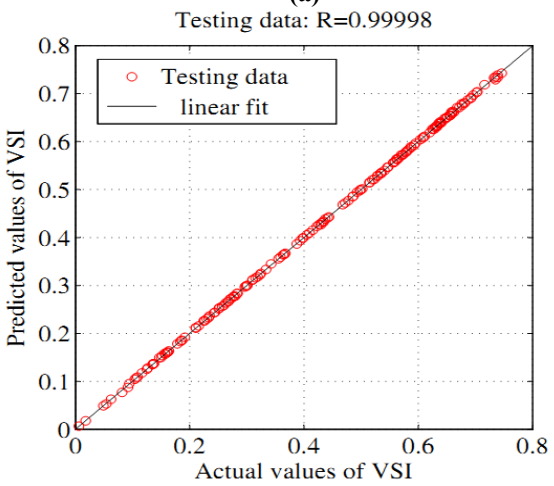


**(b)**

**Figure 0.31** Scatter plots of actual and predicted values using ALO-SVR in the case of IEEE 14-bus system: **(a)** Training phase, **(b)** Testing phase

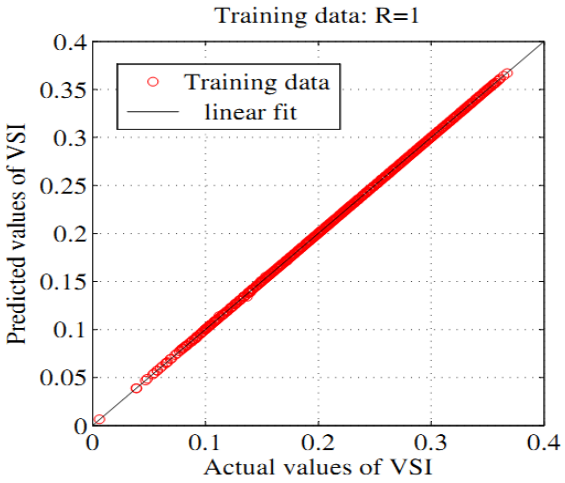


**(a)**

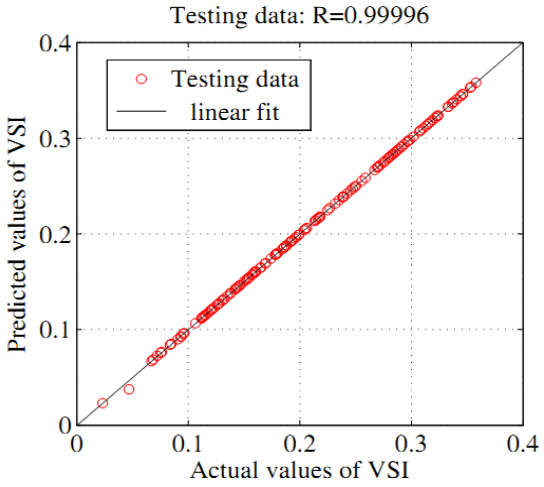


**(b)**

**Figure 0.32** Scatter plots of actual and predicted values using ALO-SVR in the case of Algerian 114-bus system: **(a)** testing phase **(b)** training phase

### 3.6.2 Application of DA-SVR model in on-line voltage stability assessment

In this section, the proposed DA-SVR model will be used to assess the voltage stability in an on-line manner. For DA optimization algorithm, the number of search agents (dragonflies) and the maximum number of iterations were taken also as 30 and 100, respectively. The RMSE is taken as the fitness function and the maximum number of iterations is considered as the stopping criterion. The DA algorithm seeks for the best $C$, $\gamma$ and $\varepsilon$ in the ranges mentioned in the previous section. The iterative RMSE trend of the DA algorithm when searching for the optimal SVR parameters is shown in Figure 3.33(a) and (b). Table 3.4 shows the optimal found values of $C$, $\gamma$ and $\varepsilon$ parameters for

both the IEEE 14-bus and the Algerian 114-bus systems. In Figures 3.34 and 3.35, the conventional load flow solution inflicting to the actual values of VSI is compared with the predicted values of VSI determined by the DA-SVR model in both test systems. These Figures show that the DA-SVR model provides the results that are in agreement with the actual values.

Figure 3.36 and 3.37 show the testing absolute error between the VSI index estimated by DA-SVR model and the VSI index calculated by the conventional load flow in the case of IEEE 14-bus and Algerian 114-bus systems, respectively. The Figures show that the DA-SVR output values are very close to the target values with maximum absolute error equal to 0.0061 in the case of IEEE 14-bus and 0.0093 in the case of Algerian power system.

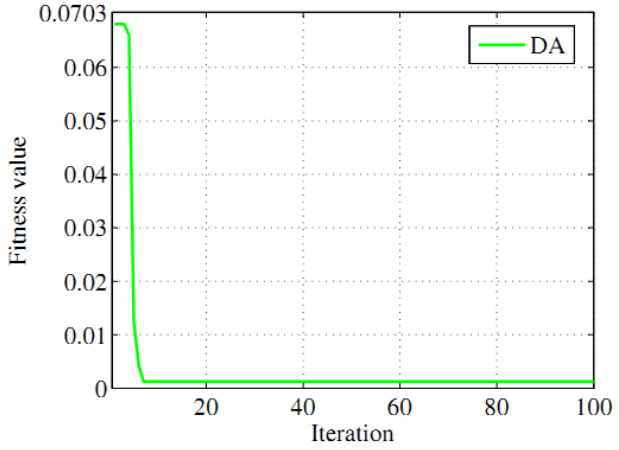


**(a)**

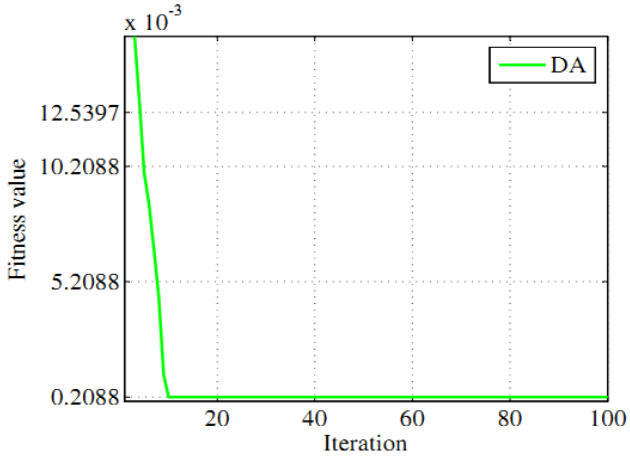


**(b)**

**Figure 0.33** Convergence curves of DA for: **(a)** IEEE 14-bus system, **(b)** Algerian 114-bus system

**Table 0.4** SVR parameters optimized by DA algorithm

| SVR parameters | Optimal values of SVR parameters | |
|---|---|---|
| | **IEEE 14-bus** | **Algerian 114-bus** |
| $C$ | 518.1321 | 54.8965 |
| $\gamma$ | 0.1 | 0.1 |
| $\varepsilon$ | 0.0001 | 0.0001 |

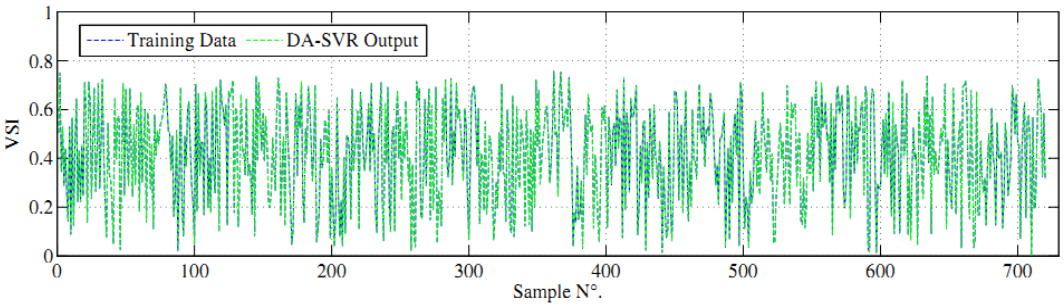


**(a)**

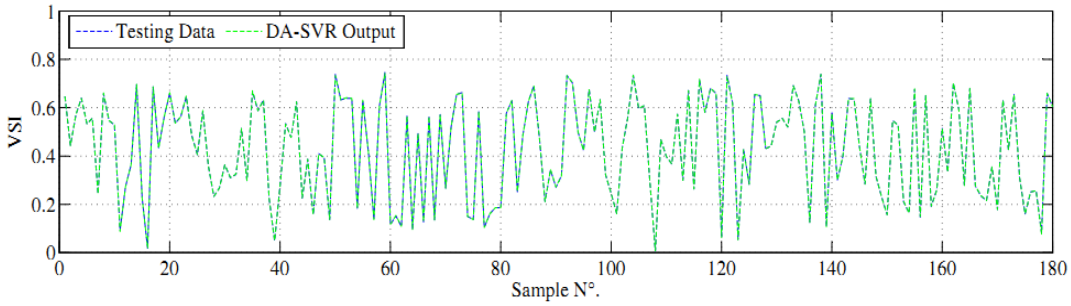


**(b)**

**Figure 0.34** Comparison between actual and predicted values using DA-SVR in the case of IEEE 14-bus system: **(a)** Training phase, **(b)** Testing phase

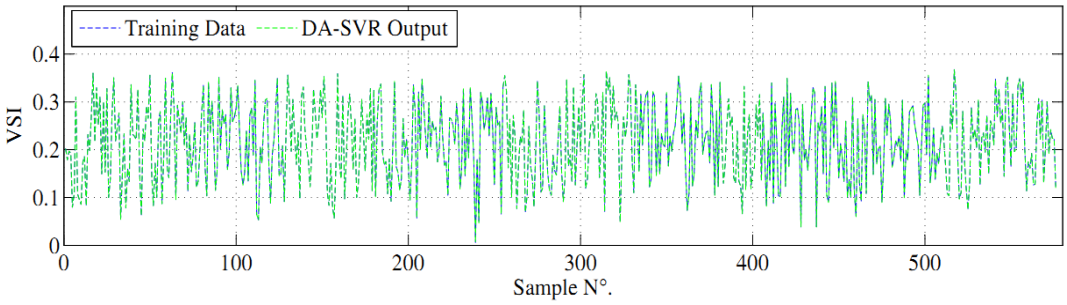


**(a)**

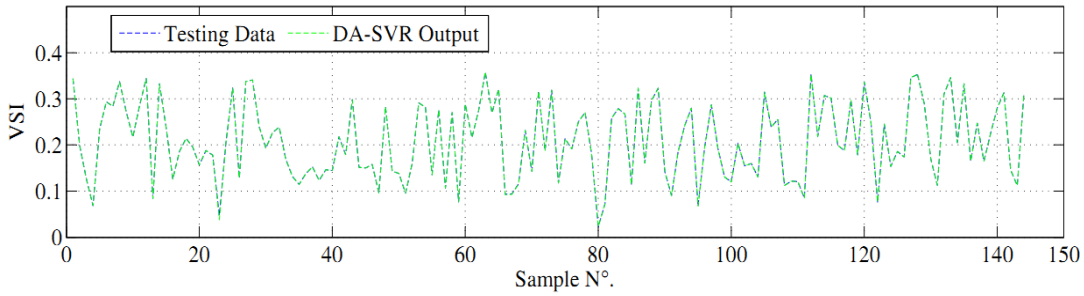


**(b)**

**Figure 0.35** Comparison between actual and predicted values using DA-SVR in the case of IEEE 14-bus system: **(a)** Training phase, **(b)** Testing phase

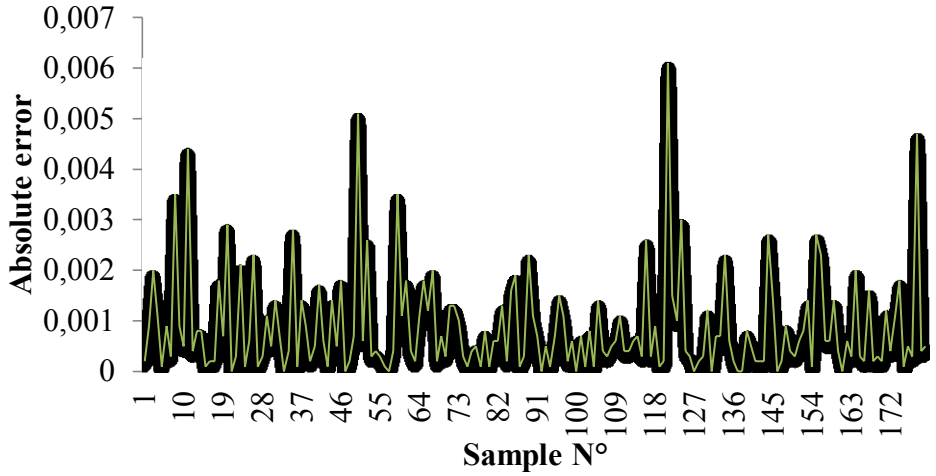


**Figure 0.36** Testing absolute error in the case of IEEE 14-bus using DA-SVR

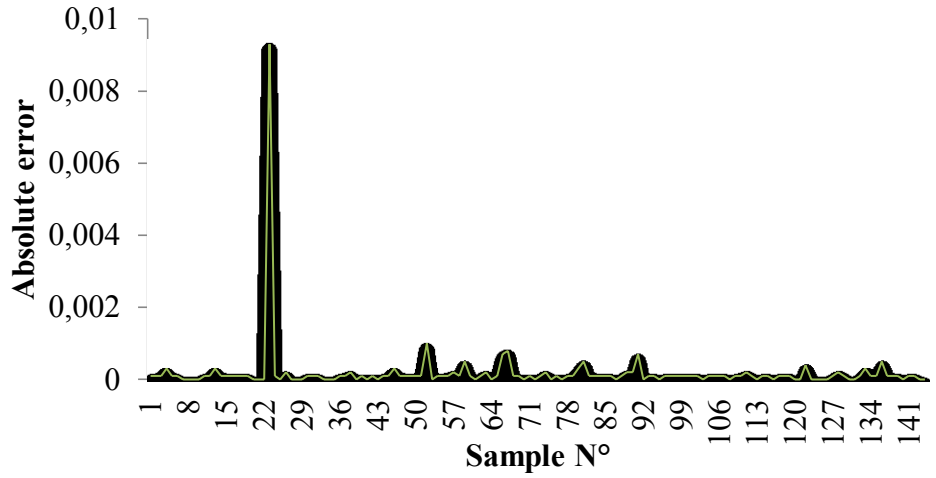


**Figure 0.37** Testing absolute error in the case of Algerian 114-bus using DA-SVR

Figures 3.38 and 3.39 show the correlation plots of predicted values versus actual values of VSI for both systems in the training and testing processes. For the IEEE 14-bus

system (Figure 3.38(a) and (b)), the statistical characteristic of R=0.99998 was obtained in both the training phase and the testing phase. For the Algerian 114-bus system (Figure 3.39(a) and (b)), the proposed model managed to yield R=1 in the training phase and R=0.99996 in the testing phase. Accordingly, it can be noted that the proposed DA-SVR model has a good predicting performance. In addition, the training and testing of SVR optimized by DA required only a short time. The computational time required in the training phase, in the case of IEEE 14-bus test system, was 14.2249 (s) and in the testing phase was 0.008671 (s). Similarly, in the case of Algerian power system, the training and the testing time was 3.0912 (s) and 0.003317 (s), respectively.

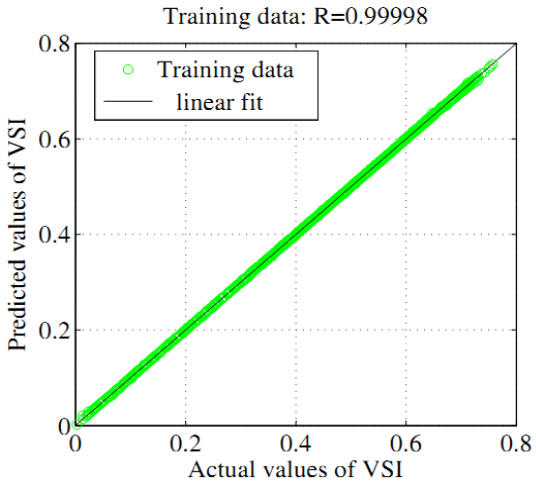


**(a)**

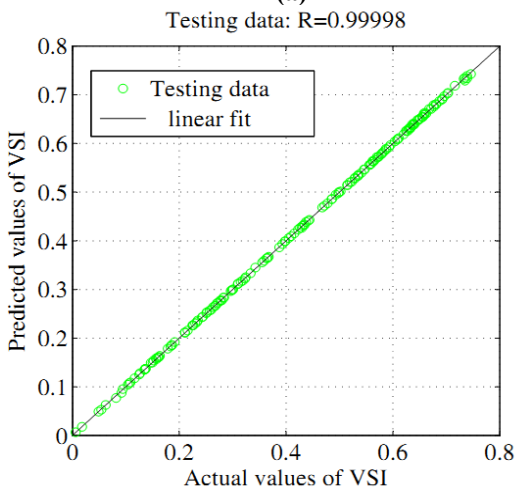


**(b)**

**Figure 0.38** Scatter plots of actual and predicted values using DA-SVR in the case of IEEE 14-bus system: **(a)** Training phase, **(b)** Testing phase

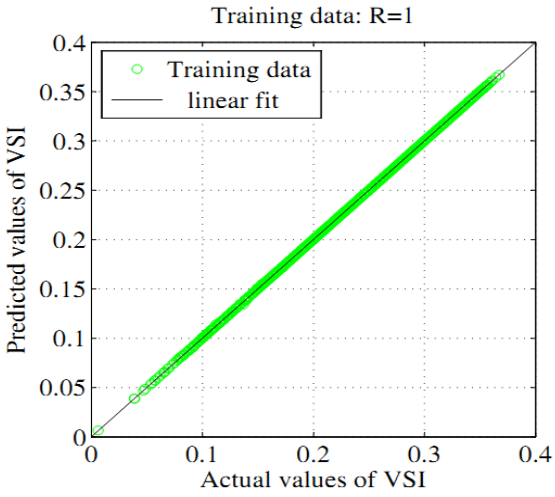


**(a)**

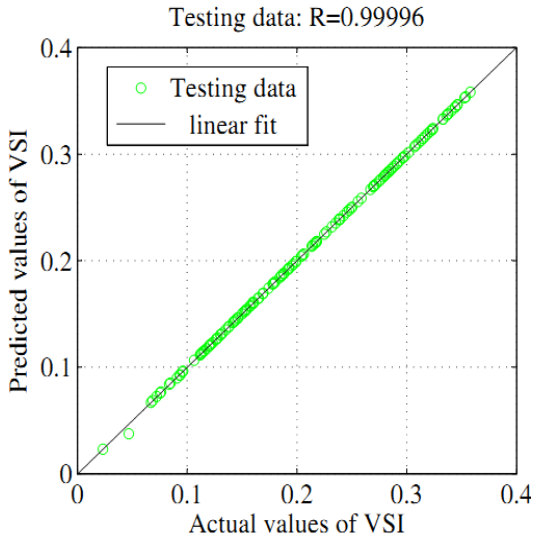


**(b)**

**Figure 0.39** Scatter plots of actual and predicted values using DA-SVR in the case of Algerian 14-bus system: **(a)** Training phase, **(b)** Testing phase

### 3.6.3 Application of WOA-SVR model in on-line voltage stability assessment

When using the WOA algorithm for identifying the optimal SVR parameters, the number of search agents and the maximum number of iterations were taken as 30 and 100, respectively. The stopping criterion was the set number of maximum iteration and the SVR parameters ($C$, $\gamma$ and $\varepsilon$) are in the search range cited before. The iterative WOA convergence curves for both test systems are displayed in Figures 3.40(a) and (b). Table 3.5 shows the optimal found values of $C$, $\gamma$, and $\varepsilon$ parameters.

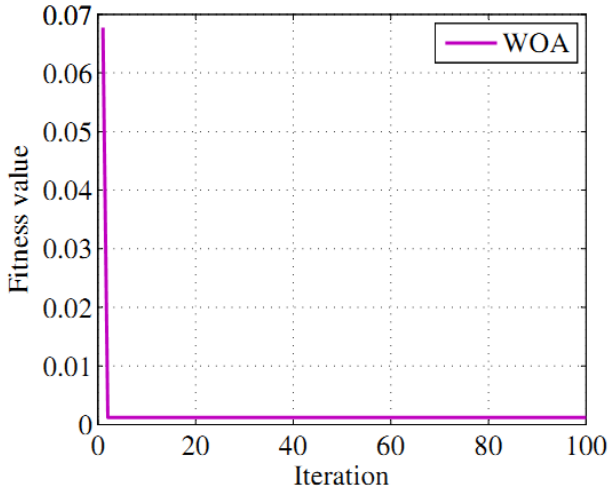


**(a)**

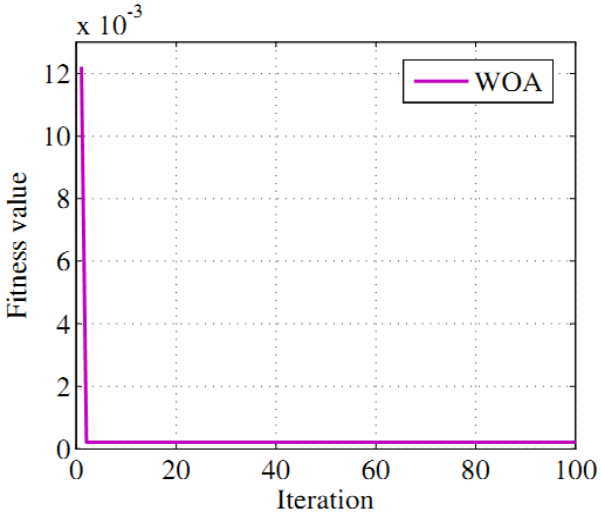


**(b)**

**Figure 0.40** Convergence curves of WOA for: **(a)** IEEE 14-bus system, **(b)** Algerian 114-bus system

**Table 0.5** SVM parameters optimized by WOA

| SVR parameters | Optimal values of SVR parameters | |
|---|---|---|
| | **IEEE 14-bus** | **Algerian 114-bus** |
| $C$ | 516.0472 | 52.1689 |
| $\gamma$ | 0.1 | 0.1 |
| $\varepsilon$ | 0.0001 | 0.0001 |

Once the optimal parameters of SVR model are obtained, the ability of the proposed WOA-SVR model was evaluated. Figures 3.41 and 3.42 show the plots of the predicted values of VSI via WOA-SVR model versus the actual values in both training and testing processes for the cases of IEEE 14-bus and Algerian 114-bus systems. It is clearly seen

that the WOA-SVR predictions are in good agreement with the actual values. The absolute error between the actual and the estimated values of VSI by WOA-SVR model in the case of IEEE 14-bus and Algerian 114-bus systems are represented in the Figures 3.43 and 3.44, respectively. It is clear from these figures that the WOA-SVR model has a very small deviation between the actual and the predicted values of VSI.

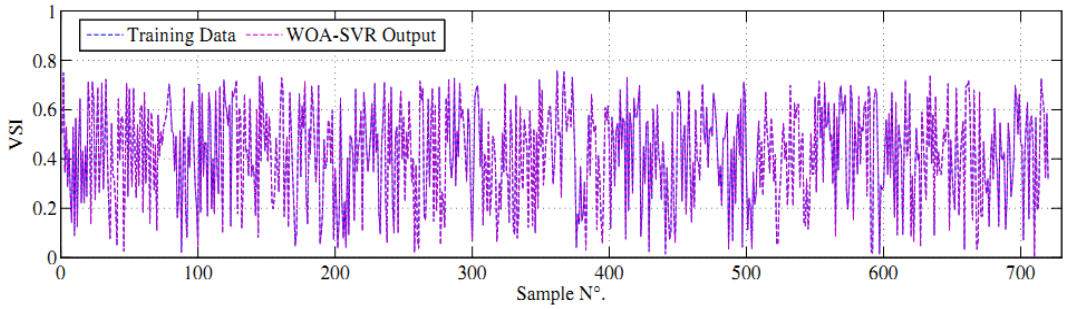


**(a)**

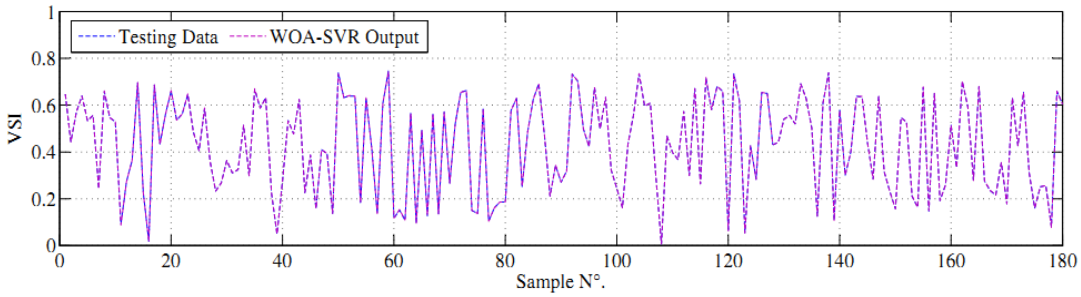


**(b)**

**Figure 0.41** Comparison between predicted and actual values of VSI in the case of IEEE 14-bus system: **(a)** Training phase, **(b)** Testing phase

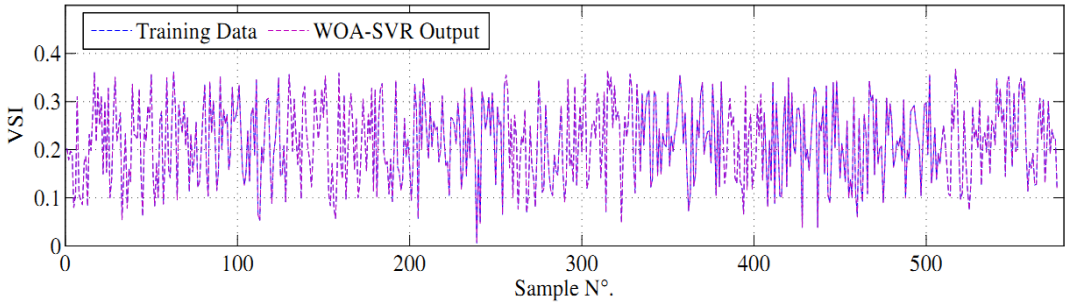


**(a)**

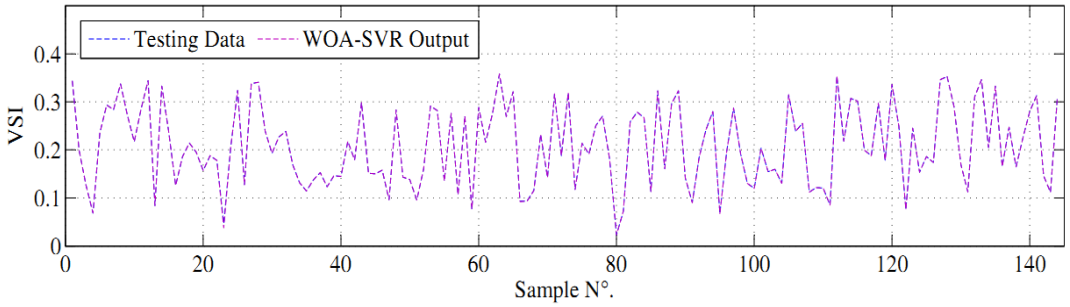


**(b)**

**Figure 0.42** Comparison between predicted and actual values of VSI in the case of Algerian 114-bus system: **(a)** Training phase, **(b)** Testing phase

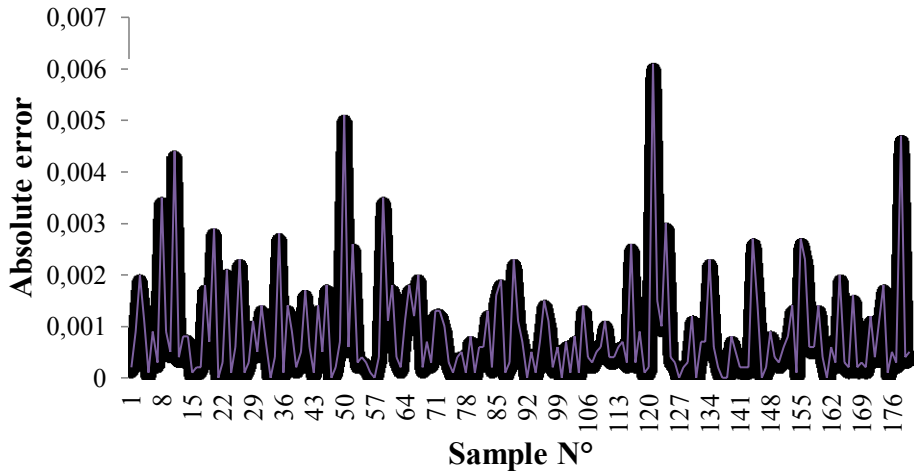


**Figure 0.43** Testing absolute error in the case of IEEE 14-bus system using WOA-SVR

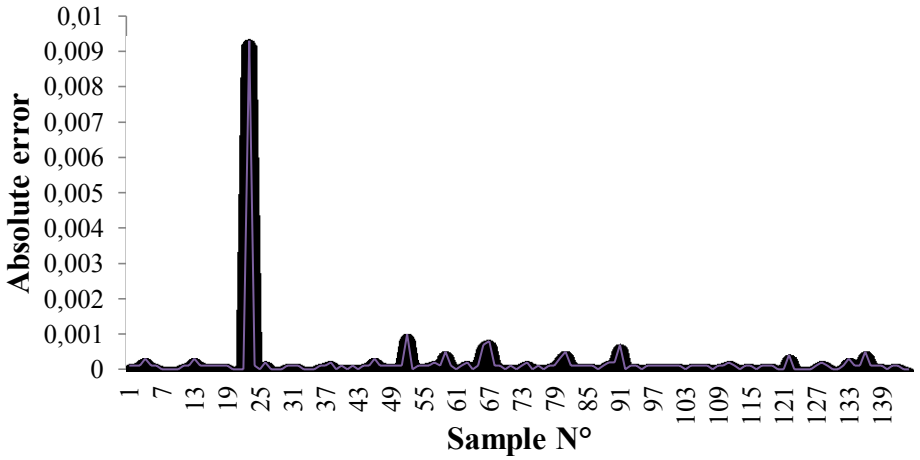


**Figure 0.44** Testing absolute error in the case of Algerian 114-bus system using WOA-SVR

Figure 3.45(a) and (b) depicts the scatter plots of the predicted VSI values against actual ones in the training and testing phases. For IEEE 14-bus system the correlation

coefficients (R) between the predicted and the actual values were found to be 0.99998 in both training and testing phases. In the case of Algerian power system (Figure 3.46(a) and (b)), the predictions result in a correlation coefficient of 1 and 0.99995 in training and testing phases, respectively. According to the obtained results, it can be noted that the proposed WOA-SVR model has a good predicting performance.

The time taken for training and testing the SVR, in the case of IEEE 14-bus system was, respectively, 15.6116 (s) and 0.0101 (s). In the case of Algerian 114-bus the training and testing time was 3.0772 (s) and 0.003361 (s), respectively.

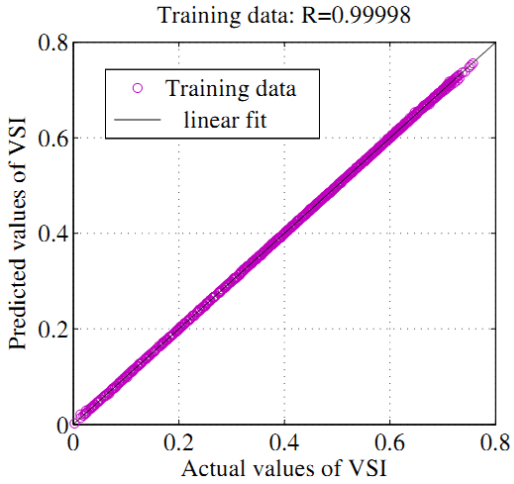


**(a)**

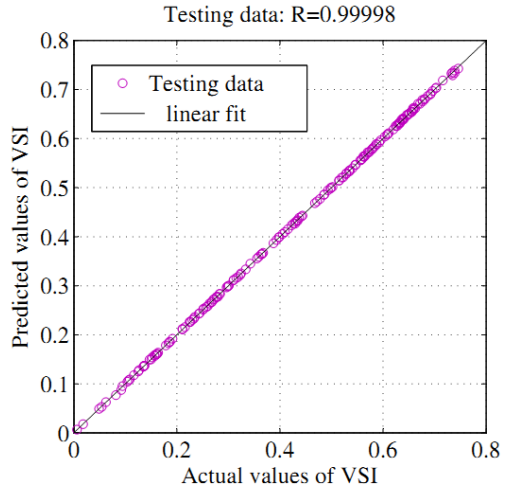


**(b)**

**Figure 0.45** Scatterplots of actual against predicted values of VSI for the IEEE 14-bus system in: **(a)** Testing phase, **(b)** Training phase

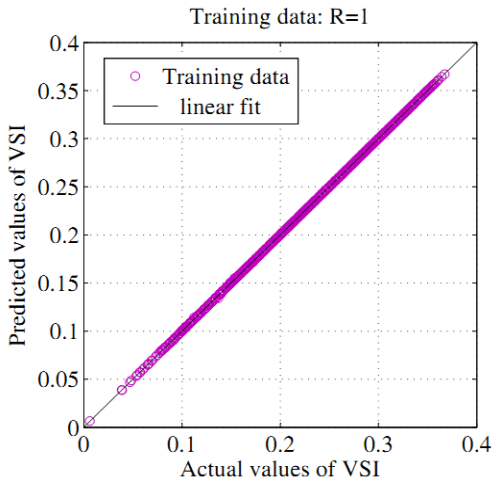


**(a)**

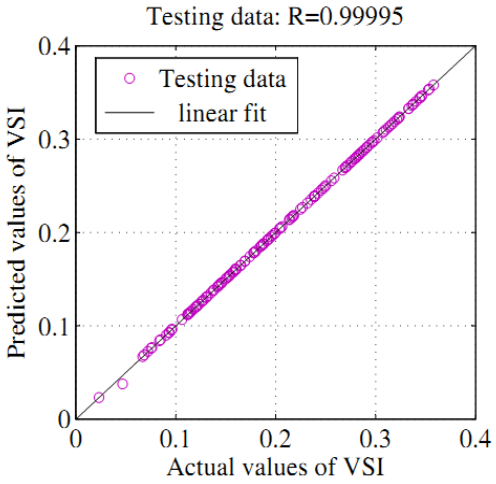


**(b)**

**Figure 0.46** Scatterplots of actual against predicted values of VSI for the Algerian 114-bus system in: **(a)** Testing phase, **(b)** Training phase

### 3.6.4 Performance comparison of different models

In order to verify the superior prediction performance of the proposed models, the obtained results are compared, using the same dataset, with that of Genetic optimization based SVR (GA-SVR) and ANFIS-based subtractive clustering model [159, 160]. In order to adapt the GA technique to the studied problem, some of its parameters must be tuned. The number of generation, the crossover probability, and the mutation probability were set to 100, 0.8 and 0.05, respectively [84].

Figures 3.47(a) and (b) show a comparison between the convergence graphics of ALO, DA, WOA and GA algorithms in the cases of the IEEE 14-bus and Algerian power systems. It can be seen that the GA has a slow convergence rate compared to the other algorithms and the fitness value obtained by GA was worse than that obtained using ALO, DA and WOA algorithms. The optimal SVR parameters found by using GA algorithm can be seen in Table 3.6. A comparison between the performance of the different models i.e., ALO-SVR, DA-SVR, WOA-SVR, GA-SVR and ANFIS based on the statistical indicators of RMSE, PRMSE and MAPE is performed and tabulated in Table 3.7. It is clearly seen, for both case studies of IEEE 14-bus and Algerian 114-bus systems, that the proposed models acquired relatively lower values of RMSE, MAPE and PRMSE when compared to the GA-SVR and ANFIS. Accordingly, it can drown the conclusion that the proposed hybrid models would be an appealing option for voltage stability assessment since the obtained results are superior to those of the other well-known models for the considered case studies.

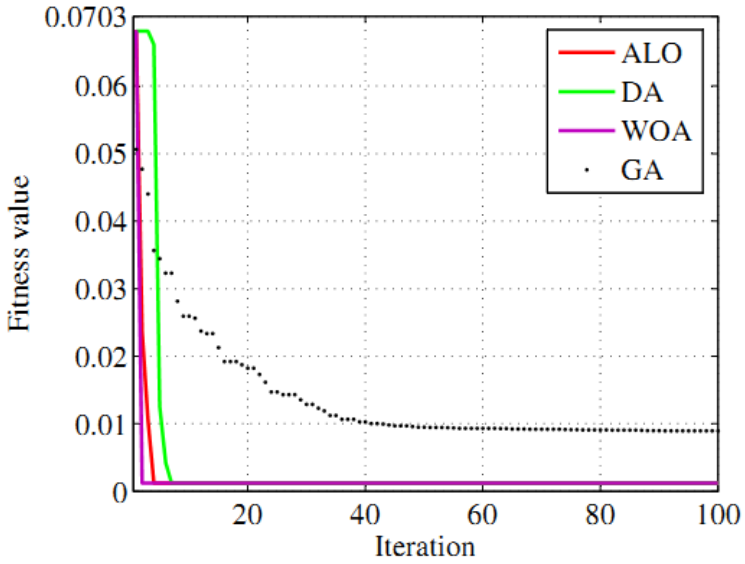


**(a)**

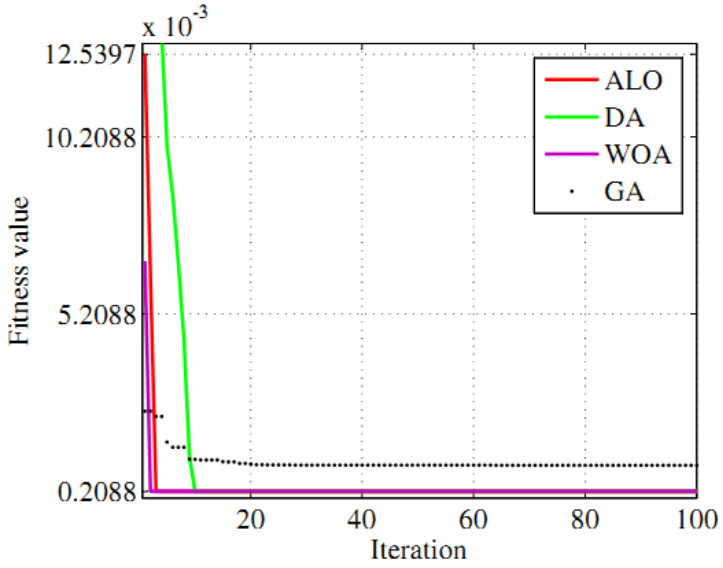


**(b)**

**Figure 0.47** Comparison of the convergence characteristics of ALO, DA, WOA and GA algorithms: **(a)** IEEE-14 bus system, **(b)** Algerian 114-bus system

**Table 0.6** SVR parameters optimized by GA algorithm

| SVR parameters | Optimal values of SVR parameters | |
|---|---|---|
| | IEEE 14-bus | Algerian 114-bus |
| $C$ | 34.9253 | 21.1671 |
| $\gamma$ | 0.1129 | 0.4248 |
| $\varepsilon$ | 0.0101 | 0.0013 |

**Table 0.7** Performance comparison between different models

| Test system | | Performance indices | ALO-SVR | DA-SVR | WOA-SVR | GA-SVR | ANFIS |
|---|---|---|---|---|---|---|---|
| IEEE 14-bus | Training phase | RMSE | 0.0012 | 0.0012 | 0.0012 | 0.0089 | 0.0297 |
| | | MAPE | 0.3463 | 0.3463 | 0.3463 | 3.2423 | 5.9258 |
| | | PRMSE | 0.2964 | 0.2964 | 0.2964 | 2.1465 | 7.1561 |
| | Testing phase | RMSE | 0.0013 | 0.0013 | 0.0013 | 0.0093 | 0.0308 |
| | | MAPE | 0.3470 | 0.3470 | 0.3463 | 3.7790 | 5.9040 |
| | | PRMSE | 0.3062 | 0.3062 | 0.3062 | 2.1521 | 7.1892 |
| Algerian 114-bus | Training phase | RMSE | $2.082\times10^{-4}$ | $2.088\times10^{-4}$ | $2.088\times10^{-4}$ | 0.0015 | $7.558\times10^{-4}$ |
| | | MAPE | 0.0867 | 0.0867 | 0.0867 | 0.6006 | 0.2524 |
| | | PRMSE | 0.0962 | 0.0962 | 0.0962 | 0.6722 | 0.3481 |
| | Testing phase | RMSE | $7.974\times10^{-4}$ | $7.974\times10^{-4}$ | $7.974\times10^{-4}$ | 0.0031 | 0.0014 |
| | | MAPE | 0.2621 | 0.2278 | 0.2621 | 0.8403 | 0.5998 |
| | | PRMSE | 0.3815 | 0.3815 | 0.3815 | 1.4986 | 0.6742 |

## 3.7 Conclusion

In this chapter, new hybrid approaches are proposed for on-line voltage stability assessment. The proposed approaches are based on the combination of Support Vector Regression (SVR) and three among the recently proposed optimization algorithms i.e., Antlion Optimization (ALO) algorithm, Dragonfly Algorithm (DA) and Whale Optimization Algorithm (WOA). These optimization algorithms are adopted as search strategies to seek for the optimal parameters of SVR. The developed models were trained based on the voltage magnitudes and voltage phase angles obtained from PMU buses, for different operating conditions and contingencies, as the input vector and the minimum values of voltage stability index (VSI) as the output vector. The proposed hybrid models were successfully implemented to estimate the VSI, which means that these optimization techniques are potential tools that can be employed for searching the appropriate SVR parameters and to ameliorate its prediction accuracy. Through the comparison with the GA-SVR and ANFIS models, the proposed hybrid ALO-SVR, DA-SVR and WOA-SVR models are confirmed to have more excellent performance.

# Chapter 4: Weak buses identification for voltage stability improvement

## 4.1 Introduction

The voltage instability phenomena usually start from some buses which are called weak buses and then spread to other buses, finally may lead to the collapse of the whole power system. Therefore, it is important and imperative to determine and monitor these weak buses in avoiding voltage instability and even voltage collapse occurrences rapidly and efficiently.

In this chapter, the ALO, DA and WOA optimization algorithms are used to identify the weak buses in the power system based on the optimal location of reactive power support. Firstly, the problem of identification of weak buses is formulated as an optimization problem. Then the procedures to solve this optimization problem using the ALO, DA and WOA algorithms are described. Finally, in order to demonstrate the validity and the efficiency of the proposed methods, the IEEE 14-bus and the Algerian 114-bus systems are used as benchmarks to carry out the corresponding simulations and comparisons.

## 4.2 Formulation of the weak buses identification problem

As it is known, the main reason for the voltage collapse is the sag in reactive power at various locations in power system. Therefore, the most sensitive buses in the power system, from the voltage stability viewpoint, can be identified as the buses which necessitate reactive power support. In this context, the identification of the weak locations can be mathematically formulated as a non-linear constrained optimization problem, where the main goal is the determination of the optimal location for reactive

power support. The objective function which has been handled by using meta-heuristic algorithms includes the fuel cost, real power losses and voltage stability margin.

***Fuel cost*:**

It is assumed to be a function of the real power generated by *i*th unit, and it is represented by quadratic curves.

$$f_i = a_i P_{gi}^2 + b_i P_{gi} + c_i \tag{4.1}$$

In this equation, $P_{gi}$ is the real power produced by the *i*th generator; $a_i$, $b_i$ and $c_i$ are the fuel cost coefficients of the *i*th generator; $N_g$ is the number of generators in the system.

The cost of the entire power system generation can be expressed as the sum of the quadratic cost at each generator.

$$F_1 = \sum_{i=1}^{N_g} f_i \left( \$ / h \right) \tag{4.2}$$

***Real power loss*:**

The second part of the objective function represents the real power losses and it is given by the following equation.

$$F_2 = P_{loss} = \sum_{i=1}^{N_b} \sum_{j=1, j \neq i}^{N_b} \left[ V_i^2 + V_j^2 - 2 V_i V_j \cos\left(\theta_i - \theta_j\right) \right] Y_{ij} \cos \varphi_{ij} \tag{4.3}$$

where $N_b$ is the number of transmission lines; $V_i$, $V_j$, $\theta_i$ and $\theta_j$ are the voltage magnitudes and the phase angles of the *i*th and *j*th buses, respectively; $Y_{ij}$ and $\varphi_{ij}$ are the magnitudes and the phase angles of the lines admittance, respectively.

***Voltage stability margin* (*VSM*):**

Under power systems planning and operation the voltage stability is one of the most significant security indices. Therefore, the VSM which would be maximized (i.e., ($1/VSI_{min}$) would be minimized) is considered as the third part of the objective function.

$$F_3 = \left( 1 / VSI_{\min} \right) \tag{4.4}$$

where $VSI_{min}$ is the minimum value of VSI.

The optimization problem can be formulated as follows:

$$\text{minimize } \left(F_1 + F_2 + F_3\right) \tag{4.5}$$

Subject to the equality and inequality constraints described by Equations (4.6) – (4.12).

The equality constraints represent the real and reactive power equations, which are expressed as follows:

$$P_{gi} - P_{di} - V_i \sum_{j=1}^{N_{bus}} V_j \left(g_{ij} \cos\delta_{ij} + b_{ij} \sin\delta_{ij}\right) = 0 \tag{4.6}$$

$$Q_{gi} - Q_{di} - V_i \sum_{j=1}^{N_{bus}} V_j \left(g_{ij} \sin\delta_{ij} - b_{ij} \cos\delta_{ij}\right) = 0 \tag{4.7}$$

where $N_{bus}$ is the number of buses; $N_g$ is the number of generator buses; $P_{gi}$ and $Q_{gi}$ are the real and reactive power generations at the $i$th bus. $P_{di}$ and $Q_{di}$ are the real and reactive load on the $i$th bus; $g_{ij}$, $b_{ij}$ and $\delta_{ij}$ are the conductance, the admittance and the phase difference of voltages between the $i$th and $j$th bus.

The inequality constraints include:

*Generator constraints*:

$$V_{gi}^{\min} \le V_{gi} \le V_{gi}^{\max}, \qquad i = 1, 2, \ldots, N_g \tag{4.8}$$

$$P_{gi}^{\min} \le P_{gi} \le P_{gi}^{\max}, \qquad i = 1, 2, \ldots, N_g \tag{4.9}$$

$$Q_{gi}^{\min} \le Q_{gi} \le Q_{gi}^{\max}, \qquad i = 1, 2, \ldots, N_g \tag{4.10}$$

where $V_{gi}^{min}$ and $V_{gi}^{max}$ are the minimum and maximum voltage limits; $P_{gi}^{min}$ and $P_{gi}^{max}$ are the minimum and maximum limits of real power generation; $Q_{gi}^{min}$ and $Q_{gi}^{max}$ are the minimum and maximum limits of reactive power generation.

*Load bus constraints*:

$$V_{li}^{\min} \le V_{li} \le V_{li}^{\max}, \qquad i = 1, 2, \ldots, N_{lb} \tag{4.11}$$

where $V_{li}^{min}$ and $V_{li}^{max}$ are minimum and maximum load voltage of $i$th load bus; $N_{lb}$ is the number of load buses.

*Transmission line constraints*:

$$S_{li} \le S_{li}^{\max}, \qquad i = 1, 2, \ldots, N_b \tag{4.12}$$

where $S_{li}$ is the apparent power flow of $i$th branch; $S_{li}^{max}$ is the maximum apparent power flow limit of the $i$th branch.

## 4.3 Meta-heuristic algorithms applied to weak buses identification

In this section, the ALO, DA and WOA algorithms have been deployed to determine the best locations for reactive power support which can be considered as the weak buses in the system. The proposed methodologies have been described in the following sub-sections.

### 4.3.1 Implementation of ALO algorithm

The implementation of ALO optimization algorithm in weak locations identification can be summarized into the steps below. The proposed flowchart is illustrated in Figure 4.1.

**Step 1:** Read power system data i.e., bus data, line data, and generator data;

**Step 2:** Set the values of ALO parameters which are:

- The number of ants and Antlions;
- The maximum number of iterations;
- The number of variables;
- The upper and lower bounds of variables (the real power outputs and the location of reactive power support). The candidate locations are in the range [1 $N_{lb}$], where $N_{lb}$ is the number of load buses in the system.

**Step 3:** Initialize the random walks of ants as the initial population using Equation (3.26).

**Step 4:** Run power flow; compute VSI for all branches in the power system and find the minimum value of VSI ($VSI_{min}$).

**Step 5:** Compute the fitness value of each search agent according to the objective function in Equation (4.5);

**Step 6:** Find the best Antlion and consider it as the elite.

**Step 7:** For every ant:

- Choose an Antlion based on the roulette wheel
- Update the values of *c* and *d* utilizing the Equation (3.19).
- Generate a stochastic walk and normalize it using the Equations (3.15) and (3.17).
- Update the position of ant based on the Equation (3.22).

**Step 8:** (Fitness evaluation): Compute the fitness of all ants.

**Step 9:** Substitute an Antlion with its corresponding ant if it becomes fitter using Equation (3.21).

**Step 10:** Update the elite if an Antlion becomes better.

**Step 11:** If the maximum number of iterations is achieved go to the step 11. Otherwise, loop to the step 6.

**Step 12:** The elite comprised the best fitness value was selected. Therefore, the best location for reactive power support was determined.

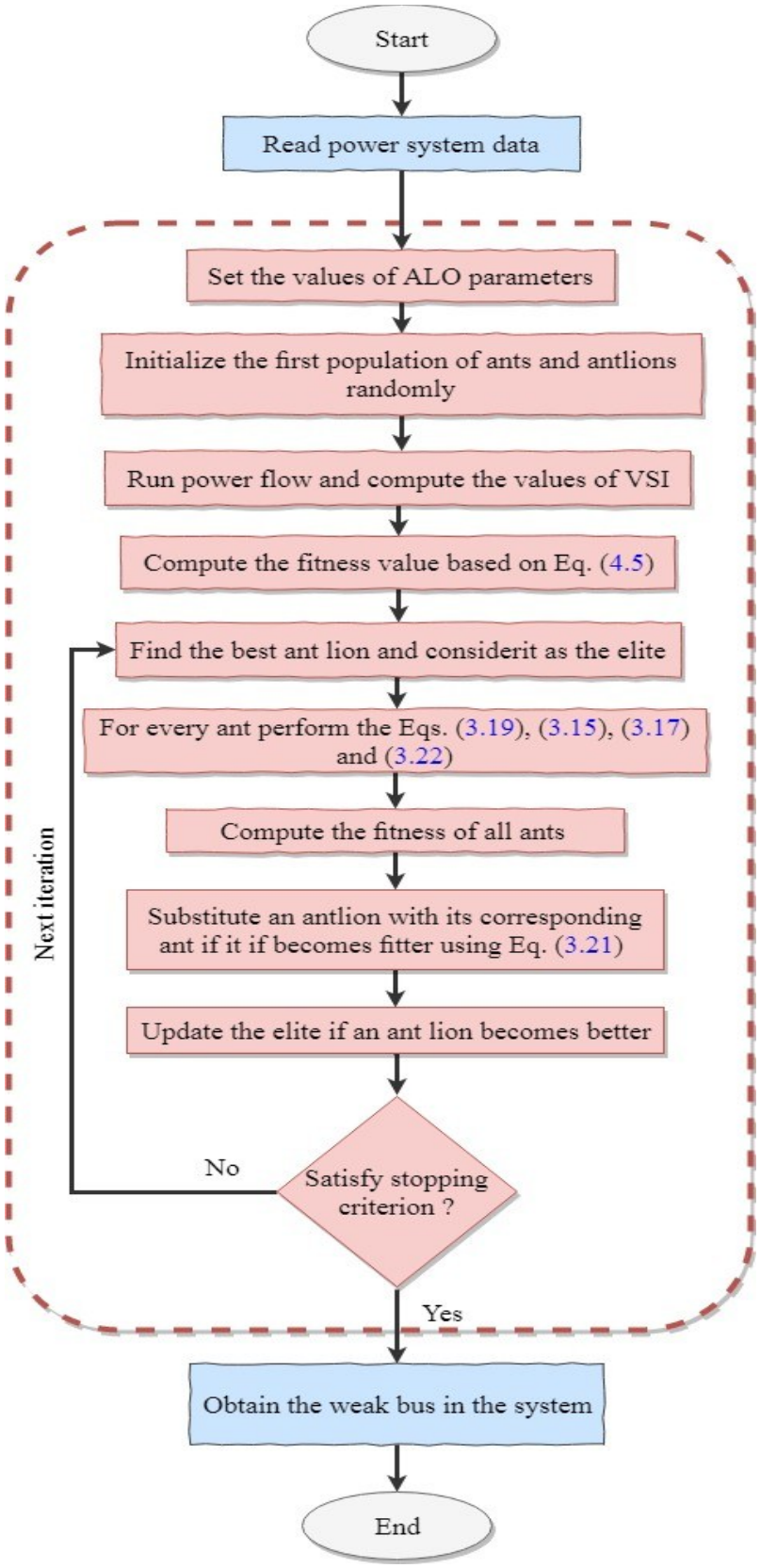


**Figure 4.1** Flowchart of the proposed weak buses identification using ALO algorithm

### 4.3.2 Implementation of DA algorithm

The general process of the implementation of DA optimization algorithm in weak locations identification is presented in Figure 4.2 and described as follows:

**Step 1:** Read power system data i.e., bus data, line data, and generator data;

**Step 2:** Set the values of DA parameters such as:

- The number of dragonflies (candidate solutions);
- The maximum number of iterations;
- The number of variables;
- The upper and the lower bounds of variables (the real power outputs and the locations of reactive power support). The candidate locations are in the range [1 $N_{lb}$], where $N_{lb}$ is the number of load buses in the system.

**Step 3:** Initialize the step vectors $\Delta X_i$ ($i=1, 2, ..., n$), the values of $s$, $a$, $c$, $f$, $e$ and $w$, the values of the real power outputs and the location of reactive power support.

**Step 4:** Run power flow; compute VSI for all branches in the power system and find the minimum value of VSI ($VSI_{min}$).

**Step 5:** Compute the fitness value of each dragonfly according to the objective function in Equation (4.5).

**Step 6:** Update the food source the enemy and the values of $s$, $a$, $c$, $f$, and $e$.

**Step 7:** For all individuals, calculate the values of $S$, $A$, $C$, $F$, and $E$ using Equations (3.24) to (3.28).

**Step 8:** Update the neighbouring radius.

**Step 9:** If the dragonfly has at least one neighbouring dragonfly, the velocity and the position of the dragonfly are updated based on the Equations (3.29) and (3.30). Otherwise, the position vector is updated using Equation (3.31).

**Step 10:** Correct the new positions taking into account the upper and lower values of variables.

**Step 11:** If the stopping criterion is achieved go to the Step 11. Otherwise, repeat steps 4 to the 10.

**Step 12:** The best position of all individuals comprised the best fitness value was selected and the best location for reactive power support was obtained.

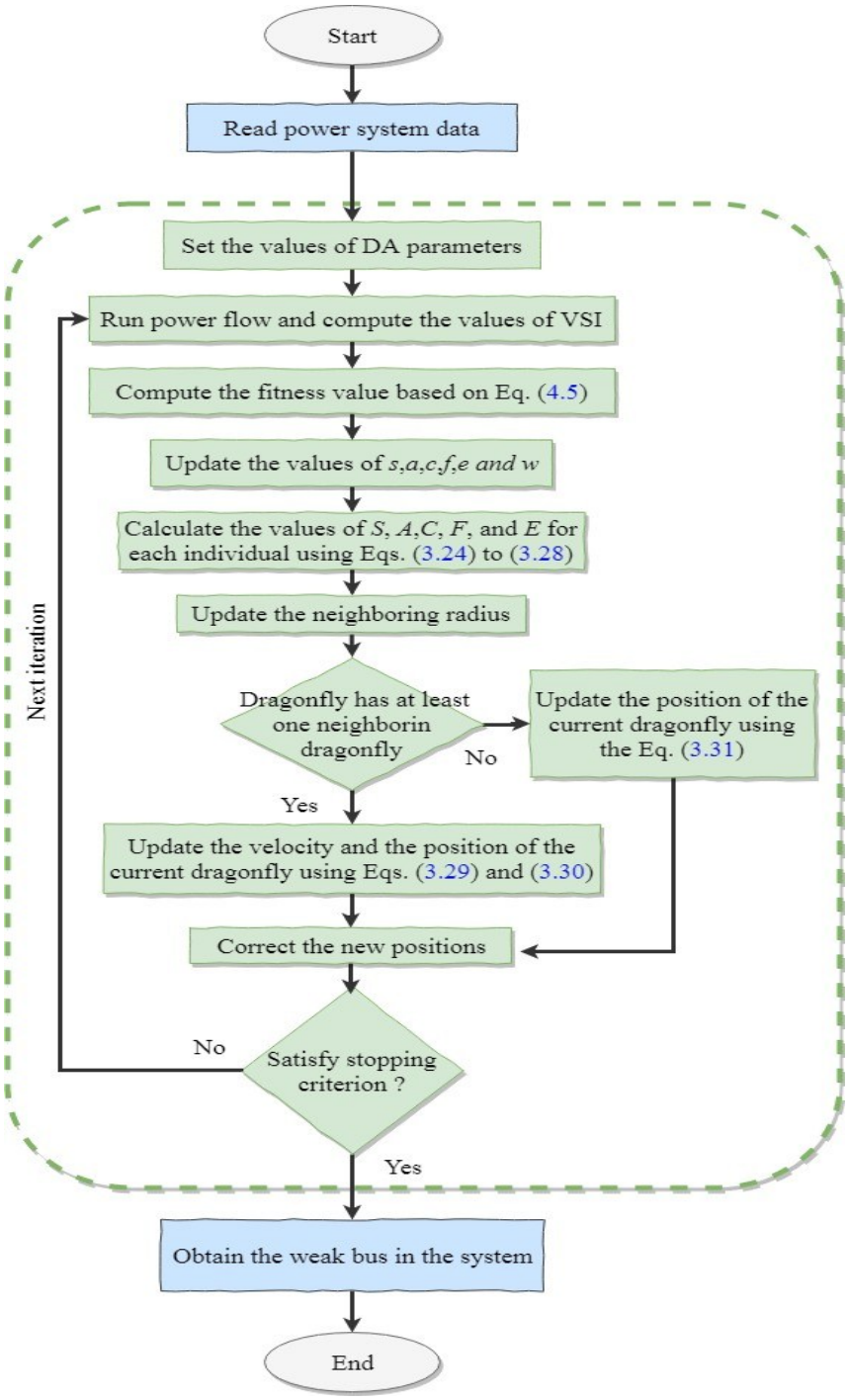


**Figure 4.2** Flowchart of the proposed weak buses identification using DA algorithm

### 4.3.3 Implementation of WOA algorithm

The general process of the application of WOA optimization algorithm in weak buses identification is depicted in Figure 4.3 and the main steps are presented as follows:

**Step 1:** Read power system data (line data, bus data and unit data);

**Step 2:** Set WOA parameters:

- Number of search agents (whales);
- Maximum number of iterations;
- Problem dimensions or variables number;
- Upper bound and lower bound of the real power outputs and the locations for reactive power support. The candidate locations are in the range [1 $N_{lb}$], where $N_{lb}$ is the number of load buses in the system.

**Step 3:** Randomly generate the initial population of $N$ whales within the specified maximum and minimum values.

**Step 4:** Run power flow; compute VSI for all branches in the power system and find the minimum value of VSI ($VSI_{min}$);

**Step 5:** Compute the fitness value of each search agent according to the objective function in Equation (4.5);

**Step 6:** Find out minimum cost function and select the best solution corresponding to the obtained minimum cost function;

**Step 7:** Improve the solutions (search agent positions) based on Equations (3.35), (3.38) and (3.40) taking in the account the specified limits of security constraints and keeping population size constant;

**Step 8:** Update the best solution;

**Step 9:** Check the stopping condition, if the stopping condition reached, show results (the best location for reactive power support); otherwise increase iteration count and go to Step 4.

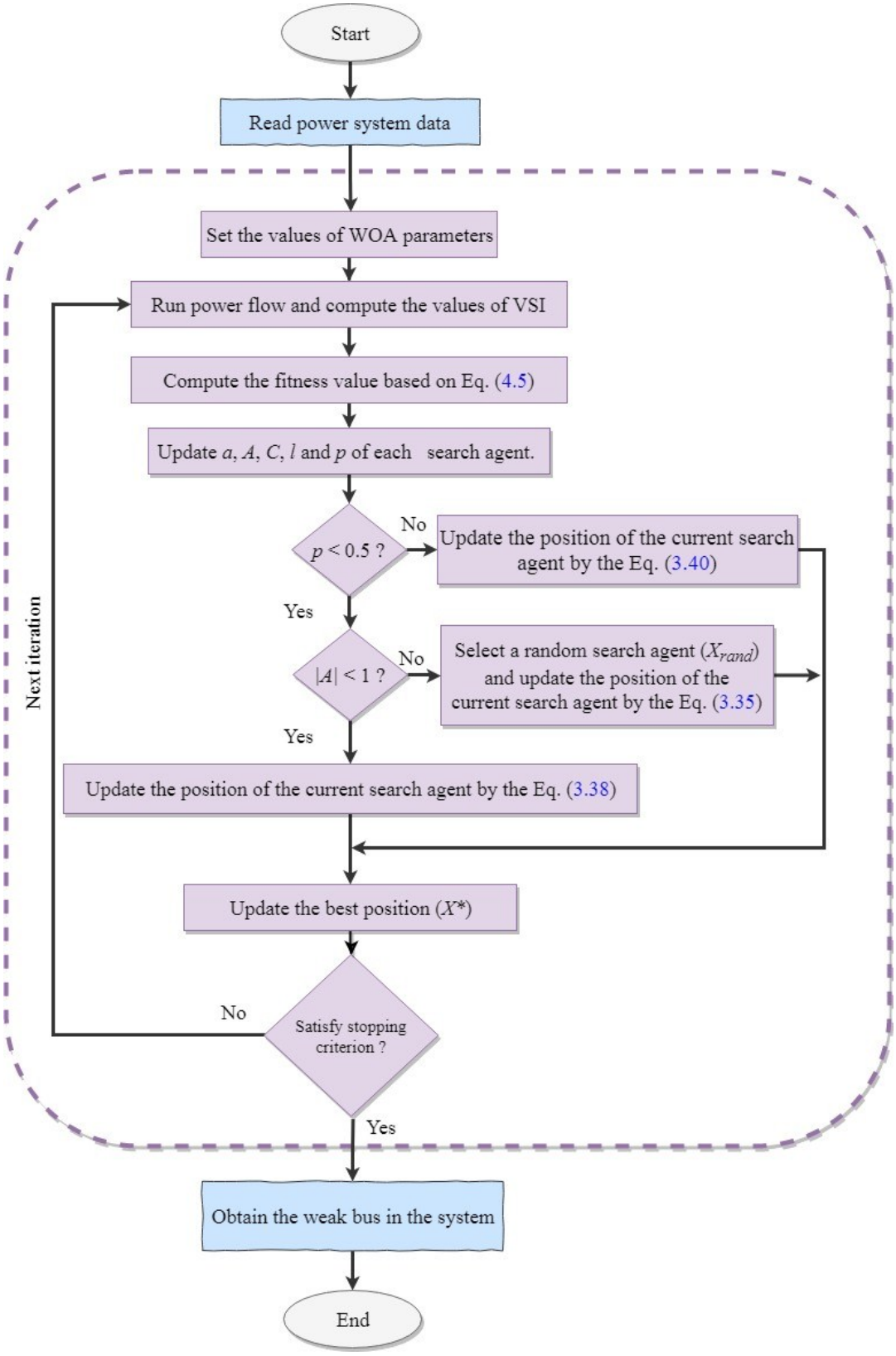


**Figure 4.3** Flowchart of the proposed weak buses identification using WOA algorithm

## 4.4 Simulation and results

In this section, the proposed methods to identify the weak buses in the power system are tested on the IEEE 14-bus and the Algerian 114-bus systems. As mentioned before, the IEEE 14-bus consists of 14 buses, 5 generators (one of which is the slack bus), and 20 lines. The total system load in the base case operating state is 259 MW and the generators cost coefficients are represented in Appendix A. The proposed methods to find the weak buses are based on the determination of the optimal location for reactive power support using ALO, DA and WOA algorithms. For these three optimization algorithms, the population size is set to 30 and the total number of iteration is set to 500. The $4^{th}$ bus is identified as the weakest location in the IEEE 14-bus test system. The identification and the ranking of the first five weak buses in the system are performed using the aforementioned optimization techniques. The obtained results are tabulated in Table 4.1. The buses are ranked based on VSI values starting with the most critical bus. By comparing the obtained results, it indicates that the ALO and WOA algorithms produce similar results in which the weak buses are 4, 5, 7, 14 and 9. The weak buses found using DA algorithm are the buses 4, 5, 7, 10 and 9.

Ultimately these optimization algorithms identify the system's area shown in Figure 4.4, consisting of buses 4, 5, 7, 14, 10 and 9 to be the most prone area to voltage instability. We can observe that these areas have not included any generators and they are remote from the generator buses. Therefore, much attention and priority should be given to these buses among the load buses within the power system for security and stability reasons. Consequently, voltage collapse will be prevented and large blackouts will be mitigated.

**Table 4.1** Comparison of ALO, DA and WOA algorithms in weak buses ranking (IEEE 14-bus)

| Ranking | Method | | |
|---|---|---|---|
| | **ALO** | **DA** | **WOA** |
| $1^{st}$ | 4 | 4 | 4 |
| $2^{nd}$ | 5 | 5 | 5 |
| $3^{rd}$ | 7 | 7 | 7 |
| $4^{th}$ | 14 | 10 | 14 |
| $5^{th}$ | 9 | 9 | 9 |

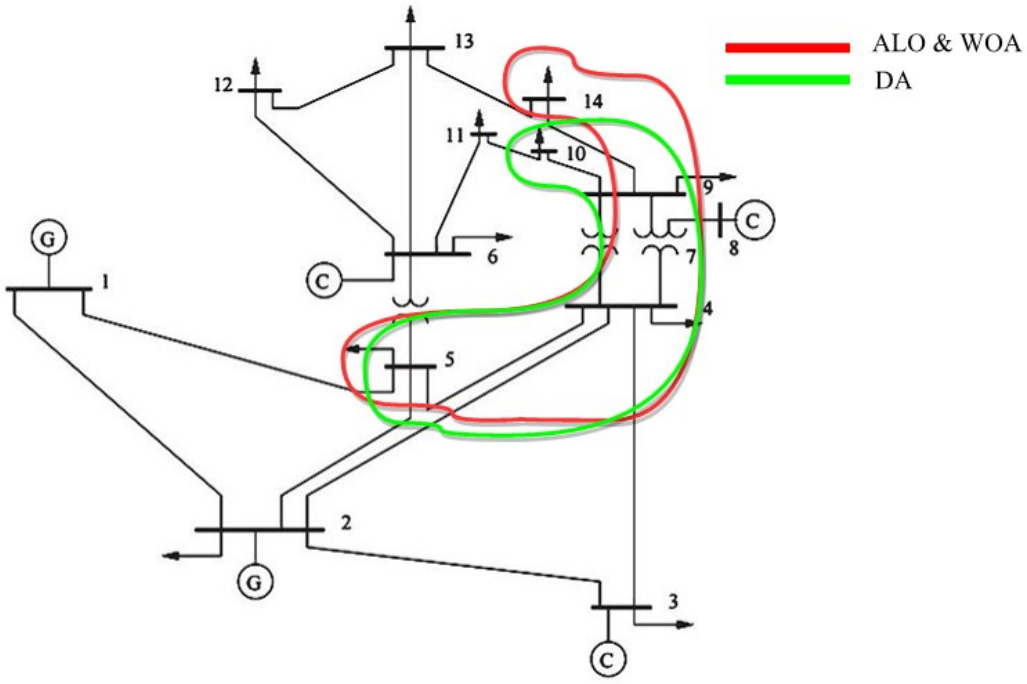


**Figure 4.4** Weak buses of IEEE 14-bus test system based on ALO, DA and WOA algorithms

The results from the proposed methods are compared with those obtained from other existing methods in the literature such as CPF method. In the CPF-based method, the real power at load buses is increased in proportion to their initial base caseload levels, step by step up to the critical loading point with the help of continuation parameter (loading parameter). The generator output is also increased in proportion to their initial base case generations to meet the increased load. In CPF, the bus(s) which first violate or reach their minimum security limit(s) is (are) called weak bus(es). Accordingly, the weak buses from the CPF method are buses 4, 5, 7, 9, 14 and 10 as shown in Figure 4.5. In addition, the detailed voltage profiles of all buses in the IEEE 14-bus system for the heavy load condition (when the system is close to its voltage stability limit), shown in Table 4.2 and Figure 4.6, confirmed that with the increase of load, most of these buses cross their limits of voltage magnitudes.

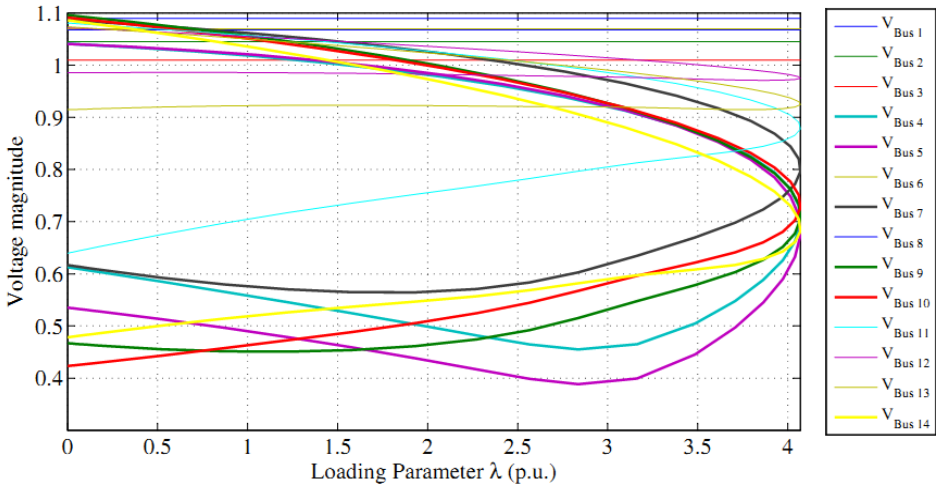


**Figure 4.5** Weak buses of IEEE 14-bus test system based on CPF method

**Table 4.2** Voltage profiles in the base case and heavy load case

| Bus N°. | Voltage magnitude (p.u.) | |
|---|---|---|
| | Base case | Heavy load |
| 1 | 1.0600 | 1.0600 |
| 2 | 1.0450 | 1.0450 |
| 3 | 1.0100 | 1.0100 |
| 4 | 1.0214 | 0.9474 |
| 5 | 1.0235 | 0.9524 |
| 6 | 1.0700 | 1.0700 |
| 7 | 1.0632 | 0.9846 |
| 8 | 1.0900 | 1.0900 |
| 9 | 1.0572 | 0.9374 |
| 10 | 1.0520 | 0.9347 |
| 11 | 1.0574 | 0.9893 |
| 12 | 1.0553 | 1.0136 |
| 13 | 1.0505 | 0.9900 |
| 14 | 1.0363 | 0.8939 |

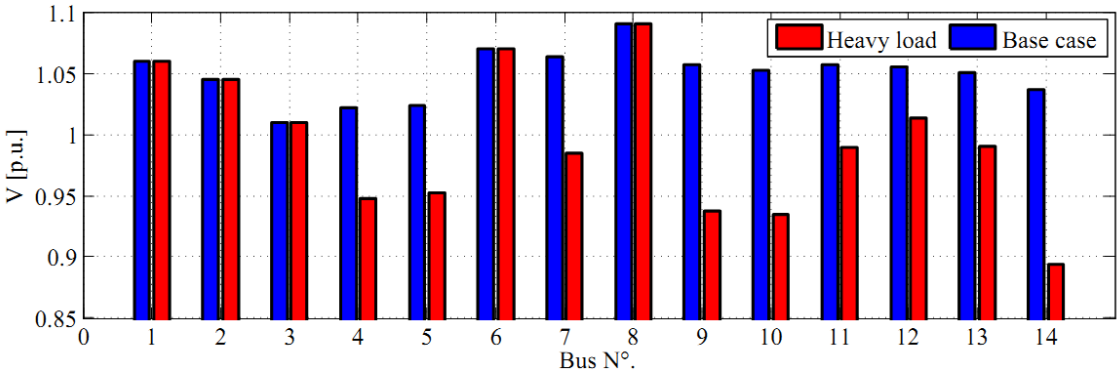


**Figure 4.6** Voltage magnitude profiles

The ALO, DA and WOA optimization algorithms are applied also to determine the weak buses in the Algerian 114-bus system. This power system can be regarded as a realistic transmission level power network in terms of a number of buses and branches. It consists of 114 bus and 175 branches. The ranking of the first ten critical buses that participate in the voltage instability in the Algerian 114-bus system is presented in Table 4.3.

**Table 4.3** Comparison of ALO, DA and WOA algorithms in weak buses ranking (Algerian power system)

| Ranking | Method | | |
|---|---|---|---|
| | **ALO** | **DA** | **WOA** |
| 1st | 89 | 89 | 89 |
| 2nd | 68 | 68 | 68 |
| 3rd | 92 | 66 | 67 |
| 4th | 67 | 67 | 92 |
| 5th | 69 | 92 | 91 |
| 6th | 91 | 88 | 69 |
| 7th | 88 | 93 | 77 |
| 8th | 66 | 77 | 56 |
| 9th | 77 | 55 | 88 |
| 10th | 56 | 70 | 93 |

## 4.5 Conclusion

This chapter presents the application of ALO, DA and WOA optimization techniques in the identification of the weak locations in the large-scale power system. In the proposed methodology the optimization algorithms are adapted to search for the optimal locations of reactive power support which considered as the weak buses in the system in the viewpoint of voltage stability. Simulations have been carried out on the IEEE 14-bus and real Algerian power systems to examine the effectiveness of the proposed methods. The simulation results show that the weak locations in the power system were successfully identified using the proposed methods. In the next chapter, these sensitive locations will be employed to improve the voltage stability of power system.

# Chapter 5: Event-driven emergency demand response based voltage stability margin

## 5.1 Introduction

Emergency Demand Response (EDR) is a type of DR programs that are called upon when power generation is anticipated to experience a shortfall or during the contingency situations [161]. EDR helps the power system to eschew cascading failures by coordinating multiple electricity customers to reduce their consumption during emergency conditions and it is triggered after the occurrence of critical contingencies or depleting of reactive power reserve supplies [162]. In this chapter, an Event-Driven Emergency Demand Response (EEDR) based VSM is proposed to prevent a power system from experiencing voltage collapse. The proposed EEDR approach aims to maintain VSM in an acceptable range and it activates in emergency conditions when the VSM leaves their permitted ranges. As the implementation of Demand Response (DR) programs dictates the determination of the amounts of load reductions, the WOA optimization algorithm is adopted for this purpose. The rest of the chapter is organized as follows: Firstly, the EEDR is described and formulated as an optimization problem in which the goal is to minimize the demand reduction cost and the main constraint is the VSM. Then, the above-mentioned optimization algorithm i.e., WOA algorithm is adopted to solve this optimization problem. Finally, several simulations are carried out on the IEEE 14-bus, and the Algerian 114-bus systems for the validation purposes.

## 5.2 Demand-Side Management (DSM)

In the conventional power systems, the consumer (called also a customer) of electrical energy is considered as a passive actor. In such systems, the generation is dispatched to meet the demand, and it takes the main liability for demand-generation

balance. In the case of inadequate capacity (if consumers requested more power), the problem treated at the supply side and solved by constructing more generation units to ensure that the generation meets the demand and the power system operates in a reliable way. According to [163], this concept is called a *supply-side management*. In recent years, the power systems are moving towards the concept of a Smart Grids (SG) where the major operations (e.g., electricity generation, transmission, distribution, and consumption) are executed in a coordinated and efficient manner. The SG conceptual model adopted by National Institute of Standards and Technology (NIST) [164] is shown in Figure 5.1. NIST has divided the SG into seven domains; each domain is composed of a group of actors which are typically devices (smart meters), systems (control systems) or programs that make decisions and exchange information necessary for performing applications [164], as described in Table 5.1. In such systems, the focus for solving power system problems has moved more from the supply-side to demand-side, with the purpose of making the demand-side an active element of the power system. This concept is also called a Demand-Side Management (DSM) [165]. DSM is expected to play a crucial role in the improvement of grid efficiency and reliability as well as the creation of additional benefits for the consumers. DSM can be classified into two main categories which are: Energy Efficiency (EE) and Demand Response (DR) [166]. EE has the aim of reducing the energy conception while obtaining the same amount of product and services, and the goal of DR is the adjustment of load profile by load shifting and shedding driven by market incentives.

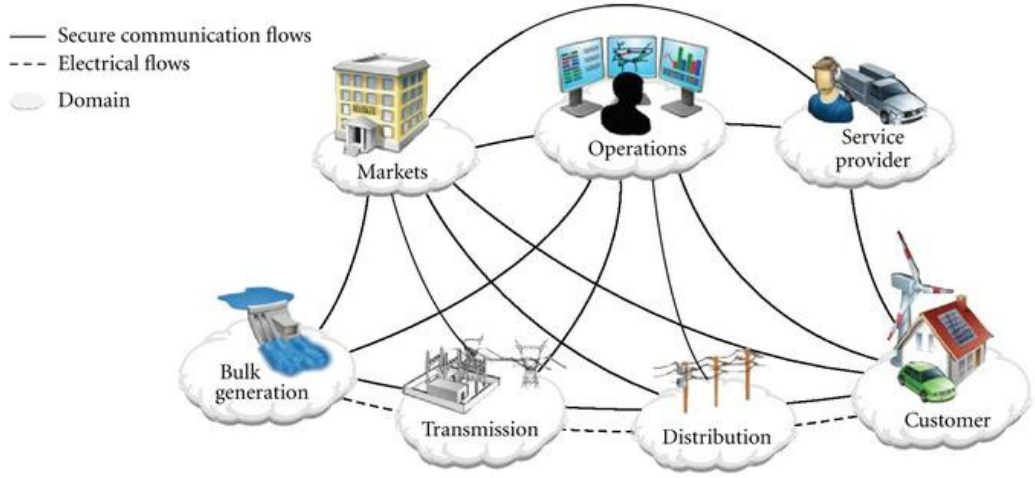


**Figure 5.1** Interaction of actors in different Smart Grid domains [164]

**Table 5.1** Smart Grid domains and Actors

| Domain | Actors |
|---|---|
| Bulk generation | Generators of electricity in bulk quantity |
| Transmission | Carriers of electricity over long distances |
| Distribution | Distributors of electricity to and from customers |
| Customer | End users of electricity |
| Markets | Operators and participants in electricity markets |
| Operators | Managers of the movement of electricity |
| Service providers | Organization providing service to electrical customers and utilities |

## 5.3 Demand Response (DR)

As mentioned in the previous section the SG infrastructure allows consumers to communicate with each other, with operations and with other deferent parties of the power system. By exchanging information, consumers can adjust their load profile by load shifting and shed if this is beneficial. Such operation is commonly known as Demand Response (DR).

According to the definition reported by Department of Energy (DoE), *DR is a changes in electricity usage by end-use customers from their normal consumption patterns in response to changes in the price of electricity over the time, or to incentive payments designed to induce lower electricity usage at times of high wholesale market prices or when reliability problems occur in the power system* [167]. Consequently, the main objective of the DR is to encourage electricity customers to reduce and/or shift electricity usage during peak periods. It should be noted that the DR actions can implement at any time, not only during the peak duration, and their implementation are usually less costly than the construction of more power plants [168].

### 5.3.1 Types of DR programs

Several DR programs have been proposed in the literature. According to the motivations offered to consumers, these programs can be divided into two main groups: *price-based programs* and *incentive-based programs* [169].

#### 5.3.1.1 Price-based demand response programs

Price-based demand response programs refer to manage of energy consumptions in response to changes in the electricity prices. The typical price-based program can be

classified into three categories [170]: Time of Use (ToU) tariffs, Real-Time Pricing (RTP) and critical-peak pricing (CPP) as shown in Figure 5.2.

- **Time of Use (ToU)**

  ToU is the most common example of price-based demand response in which the electricity prices are determined based on the peak and off-peak periods [171]. By running ToU programs, which usually defined for the duration of 24 hours, it is foreseeable that consumers set their consumption by prices so that the peak demand is reduced and loads are transferred to the off-peak period.

- **Real-Time Pricing (RTP)**

  RTP are the programs in which customers are charged based on hourly fluctuating prices reflecting the real cost of electricity in the wholesale market. Contrary to ToU programs, where electricity prices are determined months ahead of time, in RTP programs price of electricity is defined for shorter periods of time, commonly 1 h [172].

- **Critical Peak Pricing (CPP)**

  CPP is a combination of the above-mentioned programs where ToU is the base program and the much higher peak pricing is used during critical power system conditions (e.g., when supply costs are very high) [171]. Participants in CPP programs are foreseeable to shed or shift load in response to the supply costs in the critical periods.

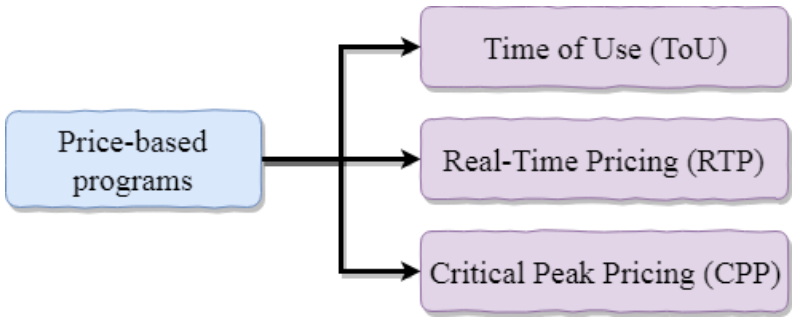


**Figure 5.2** Categories of price-based demand response program

#### 5.3.1.2 Incentive-based demand response programs

Incentive-based demand response programs can be established by utilities, load-serving entities, or by a regional grid operator to provide rebates to customers to reduce

their consumption. These programs include the seven categories shown in Figure 5.3 and defined below [170].

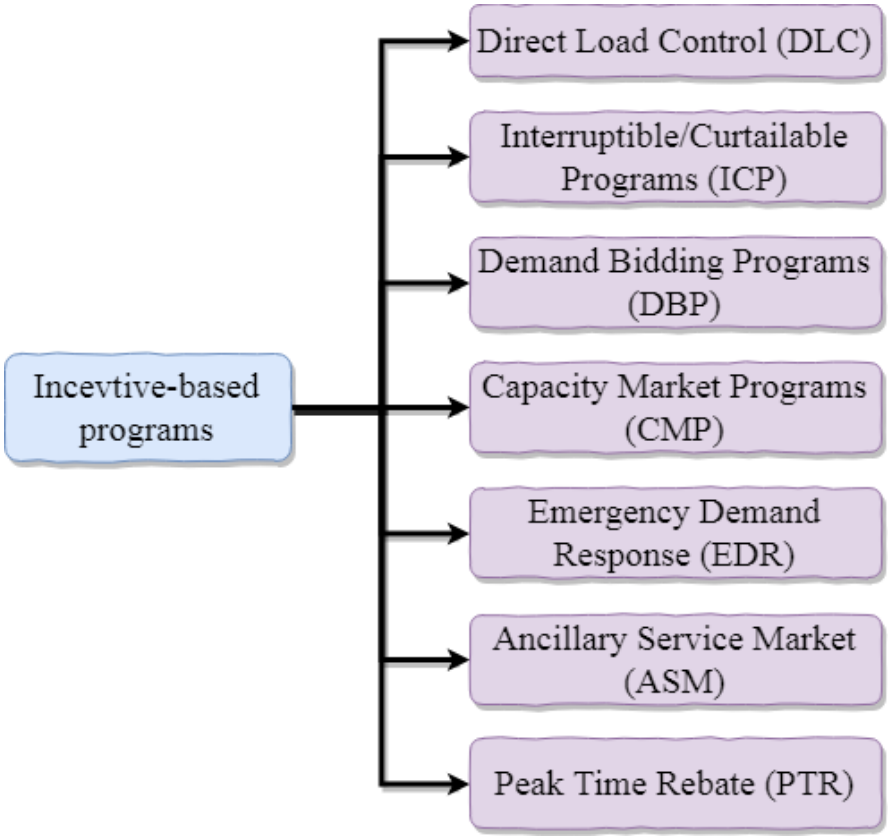


**Figure 5.3** Categories of incentive-based demand response program

- **Direct Load Control (DLC)**

  DLC is a program that allows utilities to shed the end-user customer loads (residential or small commercial customers) in order to curtail the system peak load. Loads such as air-conditioners and water heaters are good candidates for DLC;

- **Interruptible/Curtailable Programs (ICP)**

  In ICP program, consumers receive a rebate or reward in exchange for accepting to reduce their consumption during system contingencies. These programs are traditionally provided to larger industrial consumers;

- **Demand Bidding Programs (DBP)**

  In such programs, consumers offer curtailment capacity bids and large consumers are generally preferred;

- **Capacity Market Programs (CMP)**
  CMP is another commonly used DR program. Customers in CMP offering load curtailment as system capacity to replace conventional energy production and delivery resources;
- **Emergency Demand Response (EDR)**
  EDR offered incentive payments to consumers for load reduction attained during an emergency event. Large consumers, who are able to curtail a portion/all of their loads, participate in this program;
- **Ancillary Service Market (ASM)**
  ASM is basically similar to DBP programs; however, in the ASM programs the offer is only applied to the ancillary services market;
- **Peak Time Rebate (PTR)**
  PTR rewards electricity consumers for using less electricity during peak hours. Peak-time rebate is different from ToU programs which change prices more for electricity use during peak times.

It should be noted that the DR participants require the controlled devices to be able to shift/reschedule their operation, and the energy storage systems should be installed at the end-user level in order to facilitate the implementation of DR programs.

### 5.3.2 Benefits of DR programs

The most important benefits of DR programs are listed below [173]:

- DR programs can reduce system peak load in the long term and therefore postpone the need for building new power plants, leading to considerable environmental impacts;
- Transmission System Operator (TSO) can benefit from DR programs by being able to enhance the reliability of the power system. By reducing electricity demand at critical times (e.g. when a generator or a transmission line is unexpectedly lost), DR dispatched by the TSO can help to return system reserves to pre-contingency levels. Moreover, DR can be dispatched in less than 5 minutes,

whereas a peaking power plant can take up to 30 minutes to ramp up to full capacity;

- Demand system operators can use DR programs for managing power system constraints at the distribution level by relieving the voltage constrained power transfer problem, relieving congestion in the distribution substations or by simplifying outage management and enhancing the quality of supply;
- Retailers buy electricity from the wholesale market and sell it to their consumers at a flat rate. So they are exposed to the financial risks involved with the spot price volatility in the real-time horizons. In order to cover most of these risks they can ask their consumers to reduce their consumption during the times when spot prices are most volatile and reach their peaks, provided the customers can receive financial reward for such decrease in consumption;
- The short-term impacts of DR on electricity markets lead to financial benefits for both the utility and the consumers.

Deployment of new technologies like, distributed generation (solar, small wind, geothermal) and storage (standalone, Plug-in Hybrid Electric Vehicles (PHEV)) also motivate the inclusion of DR as a key component of the smart grid. For example, during times of high wind speeds, the generation is quite in excess. A curtailment in wind generation proves to be inefficient for the wind farm, making its payback period quite high. So DR can be used to increase the demand during such periods.

## 5.4 Proposed Event-driven Emergency Demand Response (EEDR)

The previously designed strategy to assess voltage stability in an on-line manner, without the need to perform voltage stability analysis every time an event occurs, can help system operators in choosing the most convenient remedial actions to arrest voltage instability at its onset. EDR program is one of the recently introduced methods that improve the power system security. It meant to motivate consumers to reduce their electricity consumption during the emergency situations in exchange for incentive payments. In this section, an EEDR based VSM has been proposed to protect power system in the emergency conditions. The proposed EEDR has the objective to maintain

the VSM in an acceptable range and it activates when VSM leaves their permitted ranges during the emergency period.

Further to the on-line prediction of VSI, which is described in Section 3.5, the EEDR process consists of two others main steps that are explained below.

### 5.4.1 Selection of loads for EEDR

The selection of loads for EEDR, which considered as an important step in the implementation of DR programs, involves the determination of the best locations for load reduction. In EEDR based VSM, an effective way to find the suitable locations for load reduction is to identify the load buses having a higher impact on voltage stability. As it is known, the main reason for the voltage collapse is the sag in reactive power at various locations in power system. In this context, the problem of identification of the best locations for EEDR can be formulated and resolved as represented in the previous chapter.

### 5.4.2 Determination of demand reduction amount

EDR program permits system operators, in emergency conditions, to reduce or cut a portion of a customers' load in reciprocation for incentive payments. During emergency situations, EDR coordinates many large energy consumers (e.g., large commercial and industrial sectors) for demand reduction. For each event, it must minimize the amount of demand reduction to achieve the desired VSI with the minimum cost of demand reduction. These requirements lead to a nonlinear optimization problem in which the optimization goal is to minimize the demand reduction cost and the constraint is that the VSM after the demand reduction must be larger or equal to the desired one. Other constraints, such as power flow equations and safety operation constraints are also considered. Combining the objective function and all these constraints, the nonlinear optimization problem can be defined as presented below.

$$\text{minimize} \sum_{i=1}^{m} C_{di} \tag{5.1}$$

Subjected to the following constraints:

- The system constraints indicated in Equations (4.6) – (4.12);
- The available amounts of demand participants;
- The voltage stability constraint represented by the following equation:

$$VSI_{\min} \geq VSI_{req} \tag{5.2}$$

where $C_{di}$ is the cost for reducing demand at load bus $i$; $m$ is the number of available response providers; $VSI_{min}$ is the minimum value of voltage stability index; $VSI_{req}$ is the required value of voltage stability index.

The cost of reducing demand is described as follows [9]:

$$C_{di} = 50 + 5\left(\frac{\Delta S_i}{S_i}\right)^2, \qquad i = 1, 2, 3, \ldots, m \tag{5.3}$$

where $S_i$ and $\Delta S_i$ are, respectively, the load and the total load reduction at the selected location $i$. The unit-price for each load is assumed to be 50$/hr at the base case and changes with a second-order polynomial function as shown in Equation (5.3).

As represented in Equations (5.1)-(5.3), the main purpose is to obtain the optimal amount of load reduction with respect to the minimum cost and the required voltage stability index ($VSI_{req}$), which forms a complex optimization problem. To solve this problem, the WOA algorithm has been used. The flowchart describing the process of demand reduction amount optimization using this optimization algorithm is shown in Figure 5.4.

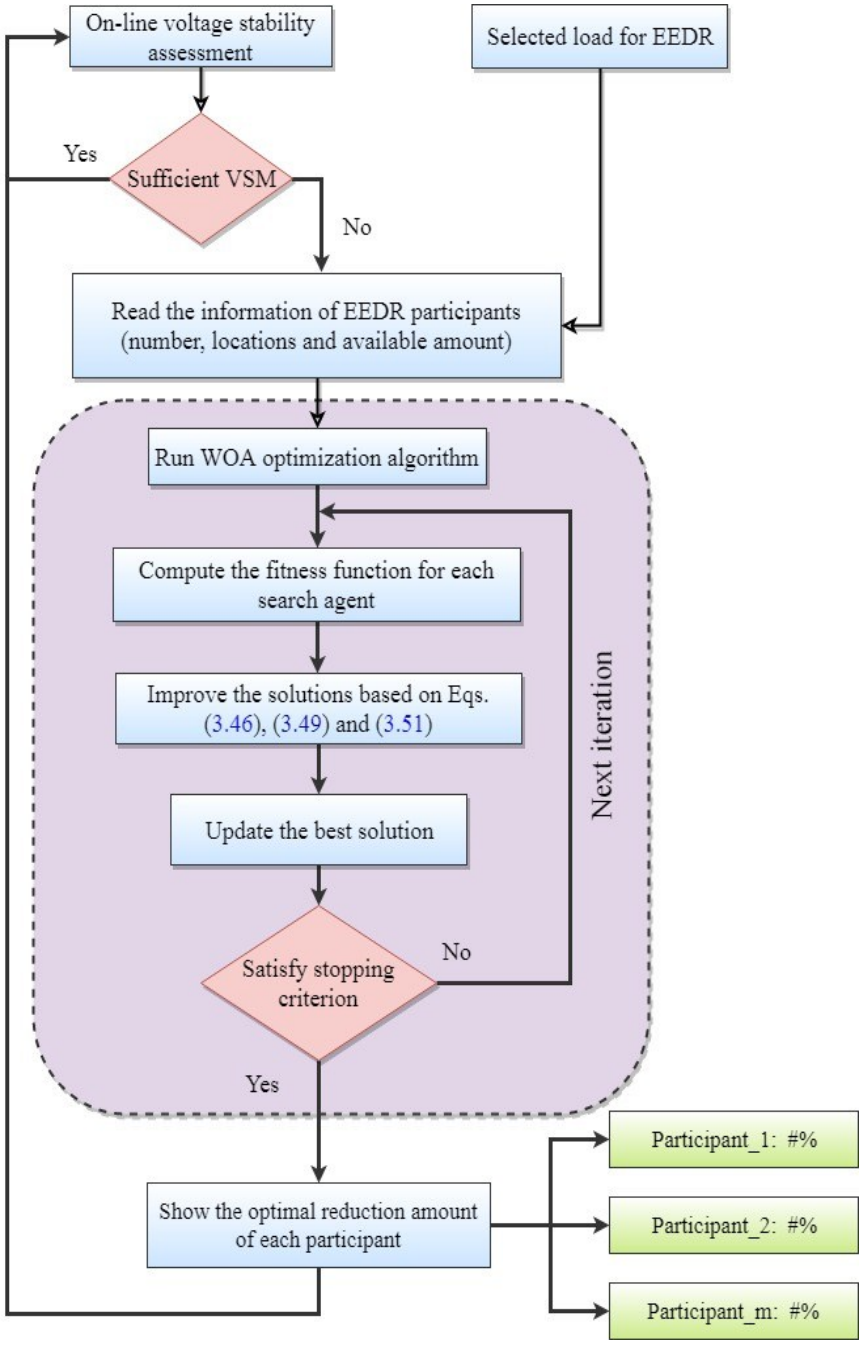


**Figure 5.4** Flowchart illustrating the process of demand reduction amount optimization using WOA

## 5.5 Numerical results

In this section, the effectiveness of the proposed EEDR strategy has been validated on the IEEE 14-bus and real Algerian 114-bus power systems. Two scenarios have been simulated:

### 5.5.1 Examples of line tripping

Firstly, in order to validate the proposed EEDR, the same scenario with that of Ref. [9] has been simulated. In this operating scenario, the load demand of the IEEE 14-bus system is increased by 85% from its base case operating state. After the occurrence of two lines outages (lines from bus 2 to bus 4 and from bus 2 to bus 5) as shown in Figure 5.5, insufficient VSM is detected. So the proposed EEDR act to ensure that the VSI is no less than 0.3 which is corresponding to 5% of operation reserve in this case. It is noteworthy to mention that the value of VSI can be further adjusted according to the VSM needs and the determination of the number of EEDR participants is based on the most severe contingency. As aforementioned in the previous Chapter, the buses 4, 5, 7, 14 and 9 are identified to be the most sensitive buses in the case of IEEE 14-bus system. In this section, these buses are taken as the appropriate locations for EEDR. The second stage interested in the determination of the optimal amount of load reduction for each participant. The convergence curve of WOA algorithm searching for the optimal load reduction at the selected buses is shown in Figure 5.6.

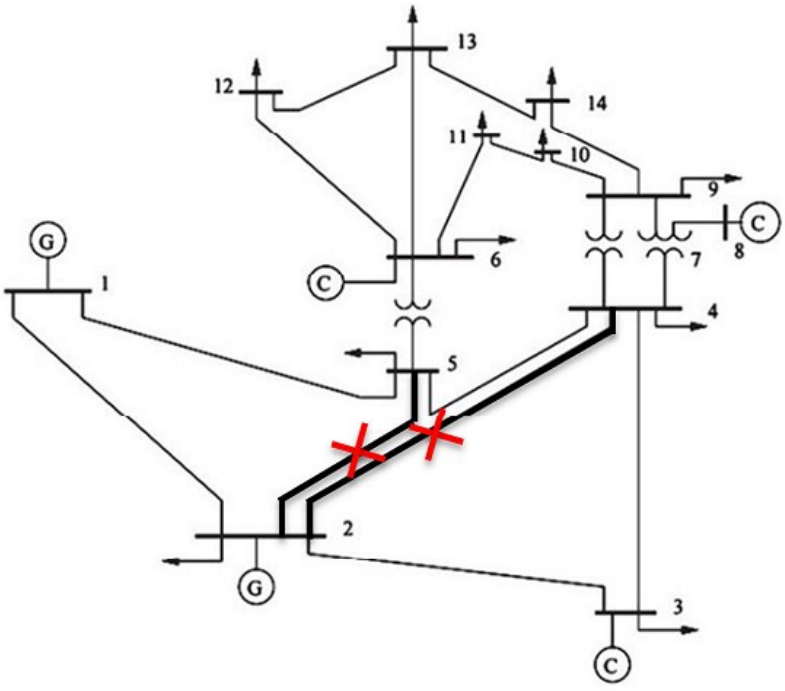


**Figure 5.5** Modified IEEE 14-bus system

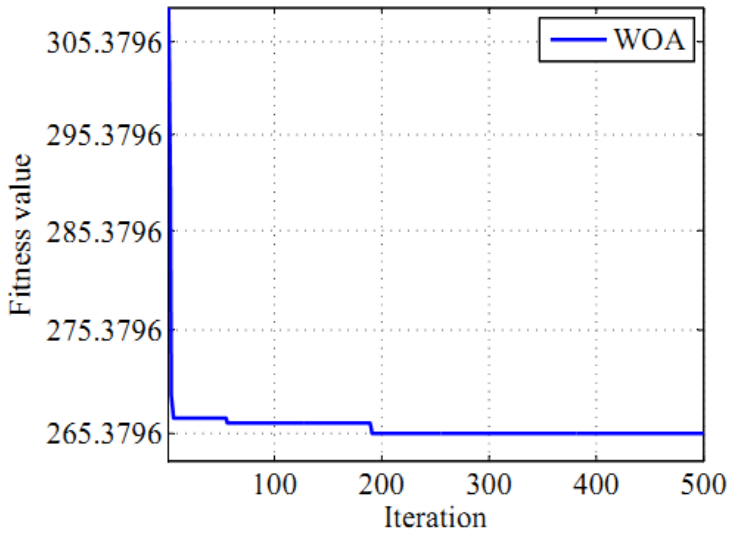


**Figure 5.6** Convergence characteristic of the proposed WOA with EEDR in the case of IEEE 14-bus

Table 5.2 shows the EEDR results obtained using the proposed method and those obtained by using the multi-stage optimization strategy [9]. As shown in this Table, the real and reactive powers of loads located at buses 4, 5, 7, 14 and 9 are reduced by 11%, 0%, 0%, 6%, and 9%, respectively. With performing the proposed EEDR to maintain the required VSM, better results are obtained in the aspect of total demand reduction cost.

**Table 5.2** Comparison of two approaches of EEDR (IEEE 14-bus)

| Method | Location | Amount (%) | Total amount | Total cost [$/hr] |
|---|---|---|---|---|
| Multistage method [9] | 14<br>9<br>10 | 30<br>30<br>10 | 14.22 MW,<br>7.06 MVAr | 822.0 |
| WOA algorithm | 4<br>5<br>7<br>14<br>9 | 11<br>0<br>0<br>6<br>9 | 14.6817 MW,<br>2.3305 MVAr | 265.2326 |

In order to confirm the effectiveness of the proposed EEDR strategy employment in voltage stability improvement, some further events have been simulated. Firstly, the line connecting the buses 1 and 2 in the IEEE 14-bus system was tripped when the system is in its normal operating state. During this contingency, the voltage magnitudes at all buses are within the predetermined voltage limits as shown in Figure 5.7. However, the lowest value of VSI ($VSI_{min}$) drops below the constraint of 0.3. This would indicate that the

corresponding line is closed to its voltage stability limit and the control strategy will be activated accordingly as shown in Figure 5.8. The WOA algorithm is employed to determine the optimal load reduction for each participant to improve the VSM. Figure 5.9 shows the convergence curve of WOA algorithm searching for optimal load reduction cost. The amount of load reduction for each participant and the values of VSI after the application of EEDR are shown in Figures 5.10 and 5.11. It is clearly seen that the values of VSI are enhanced. The obtained EEDR results are displayed in Table 5.3. It can be seen that at the total reduction cost when the line 1-2 is tripped is 446.8791 [$/hr], the total real and reactive powers required to avoid a risk of voltage collapse are, respectively, 21.433 MW and 3.6351 MVAr.

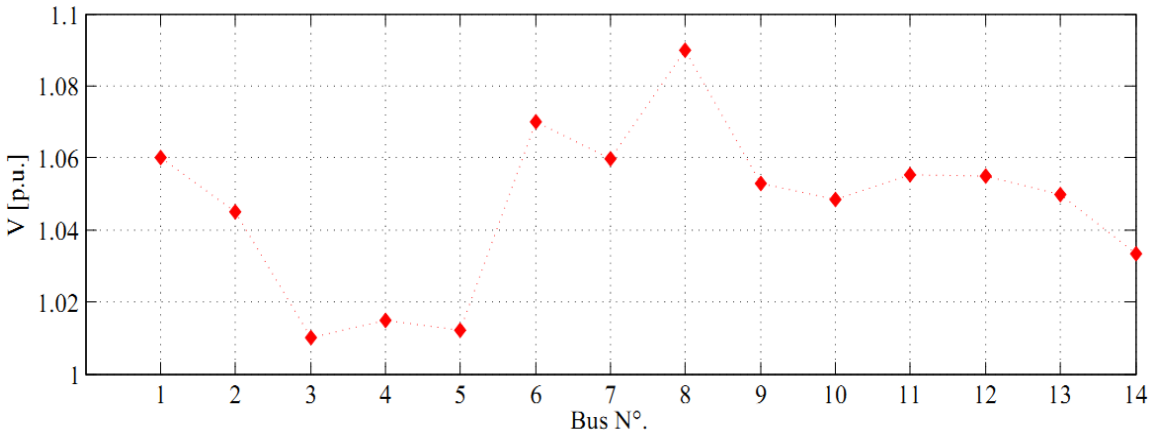


**Figure 5.7** Voltage profiles in the case of loss of line (1−2) in the IEEE 14-bus system

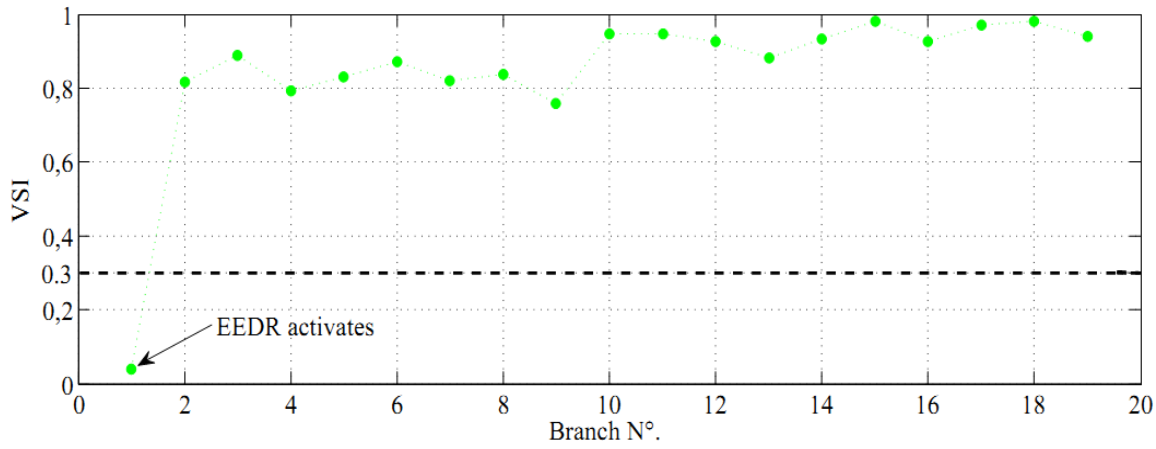


**Figure 5.8** VSI in the case of loss of line (1−2) in the IEEE 14-bus system

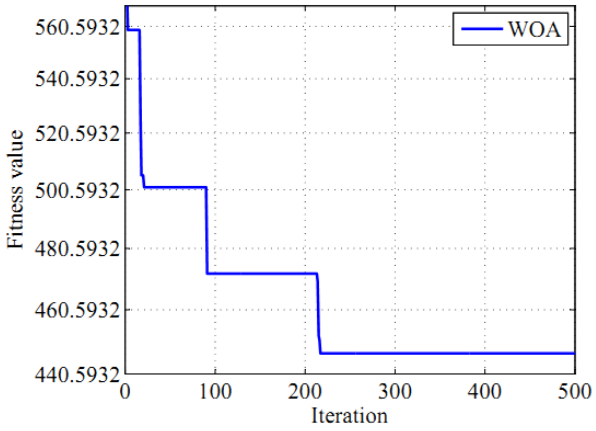


**Figure 5.9** Convergence characteristic of WOA in the case of loss of line (1−2) in the IEEE 14-bus system

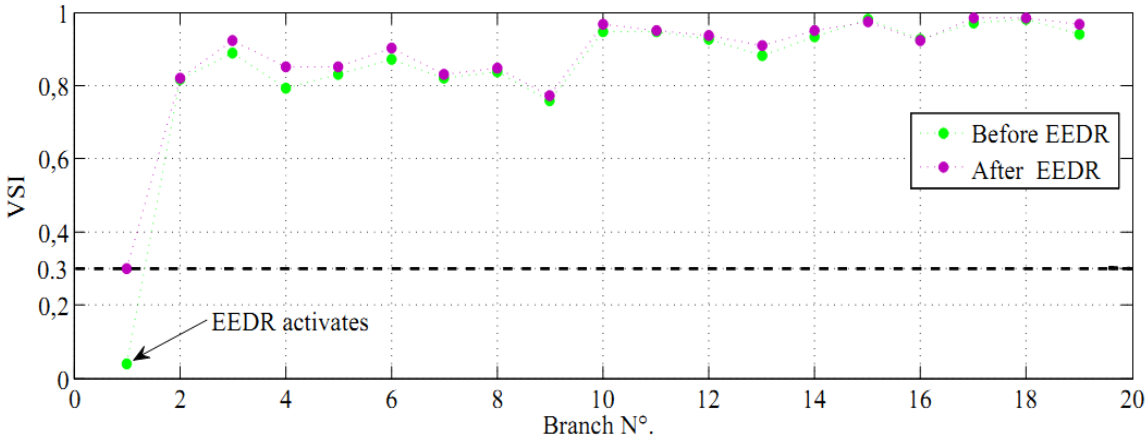


**Figure 5.10** VSI before and after EEDR in the case of loss of line (1−2) in the IEEE 14-bus system

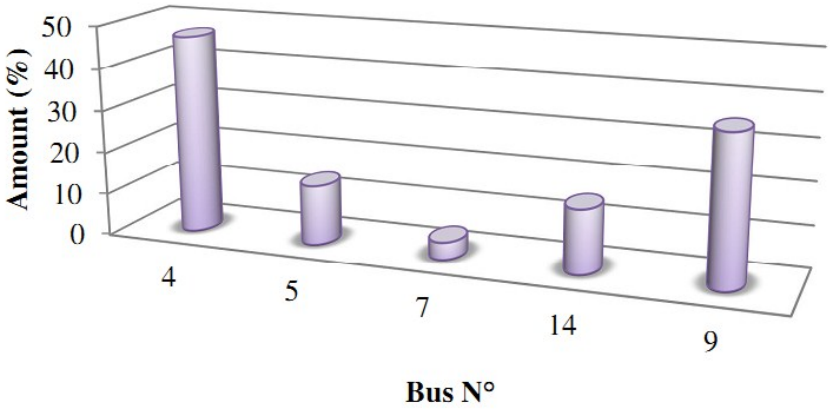


**Figure 5.11** Amount of load reduction for each participant in the case of loss of line (1−2) in the IEEE 14-bus system

The breadth of the study was expanded by performing another test on the Algerian power system. The selected load buses for the EEDR were buses 89, 68, 92 and 67. Two

different branch outage contingencies were chosen randomly to perform the tests. The first one is the loss of the line between buses 63 and 66 where the minimum value of VSI was 0.1261. The second contingency is the outage of the branch between buses 81 and 90 where the minimum value of VSI was 0.1720. This low VSIs violation activates the proposed EEDR.

Figure 5.12(a) and (b) shows the convergence curves of WOA algorithm searching for the optimal load reduction in both branch outage contingencies.

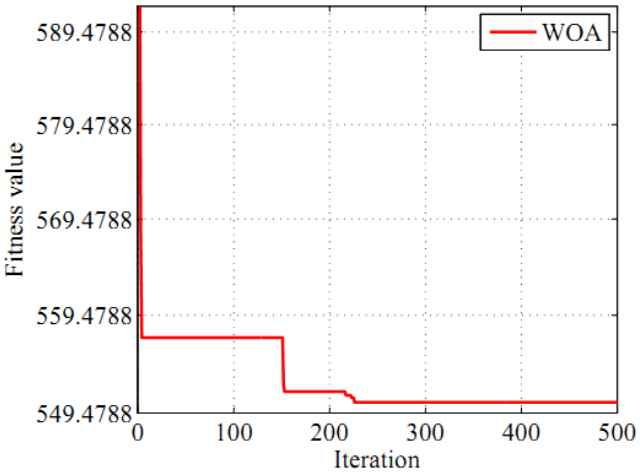


**(a)**

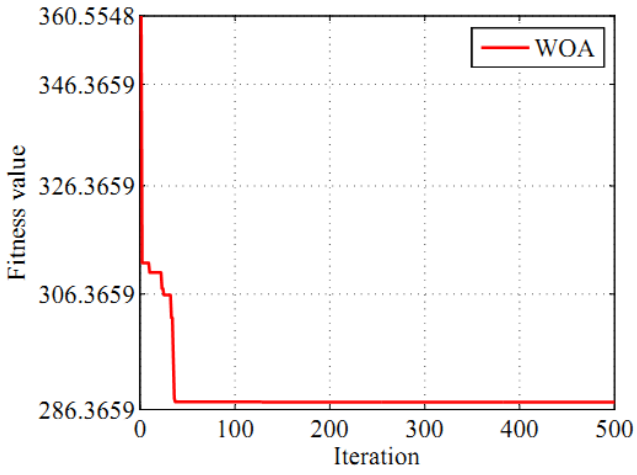


**(b)**

**Figure 5.12** Convergence characteristic of WOA for the Algerian 114-bus system in the case of **(a)** loss of line (63−66), **(b)** loss of line (81−90)

The reduction in the load power demand is distributed among the participants as shown in Figure 5.13. Figures 5.14 and 5.15 represent the power system voltage profiles

and VSIs, with respect to each event, before and after the application of the proposed EEDR method. As can be expected, before the application of EEDR the system has poor voltage profile, as shown in Figure 5.14, and insecure voltage stability margin due to the line outage contingencies. However, after the application of EEDR, the voltage magnitudes and the VSIs are improved. We can observe also from the Figure 5.15 that the VSI is successfully increased from 0.1251 to 0.3 when the line 63-66 is tripped and from 0.1720 to 0.3 in the case of the loss of line 81-90.

The detailed EEDR results for the above two cases are also summarized in Table 5.3. The 4$^{th}$ column of Table 5.3 indicates the obtained amount of load reduction for each participant. The 5$^{th}$ and 6$^{th}$ columns show the total amount and the cost of load reduction, respectively. Columns 7 and 8 of Table 5.3 show the minimum value of VSI for different line outages, before and after the application of EEDR, respectively. It appears from these results that the proposed EEDR strategy works satisfactorily in the case of line outage contingencies.

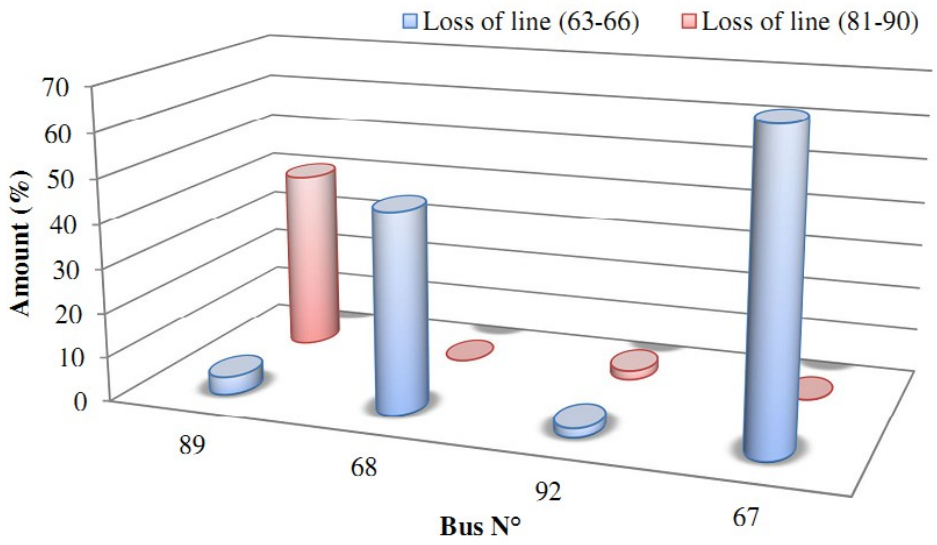


**Figure 5.13** Amount of load reduction for each participant in the case of line outage contingencies in the Algerian 114-bus system

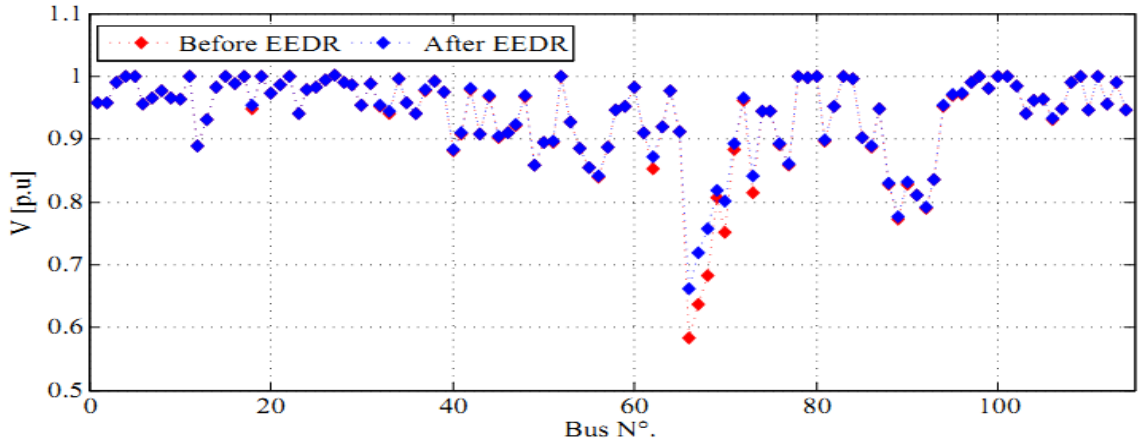


**(a)**

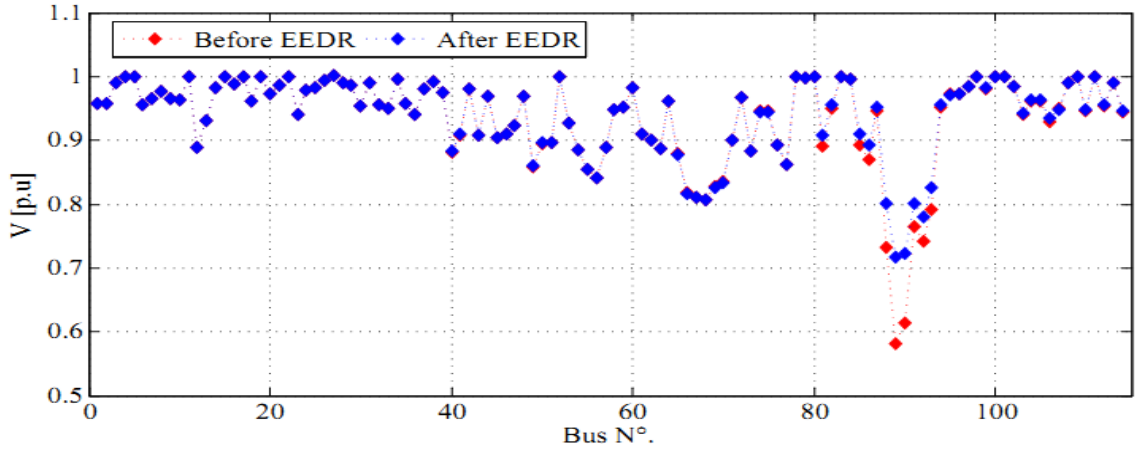


**(b)**

**Figure 5.14** Voltage profiles of the Algerian 114-bus system in the case of **(a)** loss of line (63−66), **(b)** loss of line (81−90)

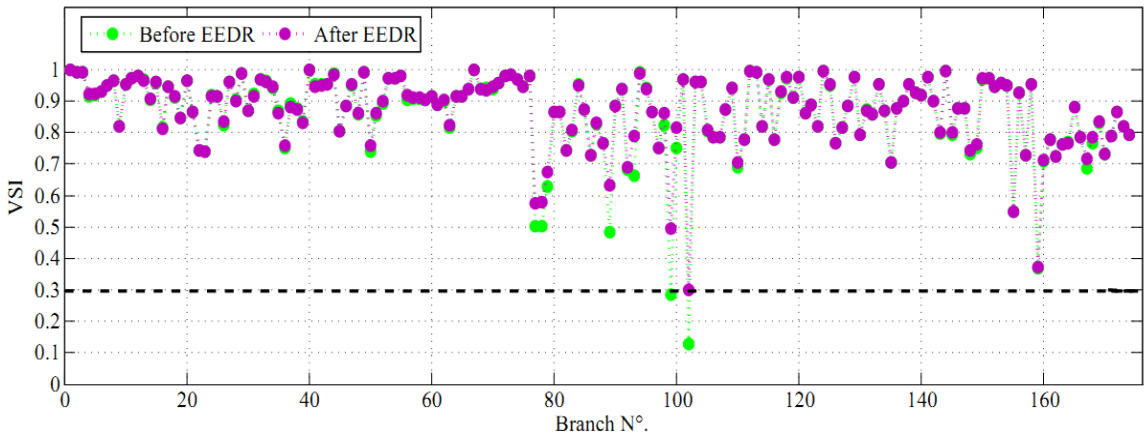


**(a)**

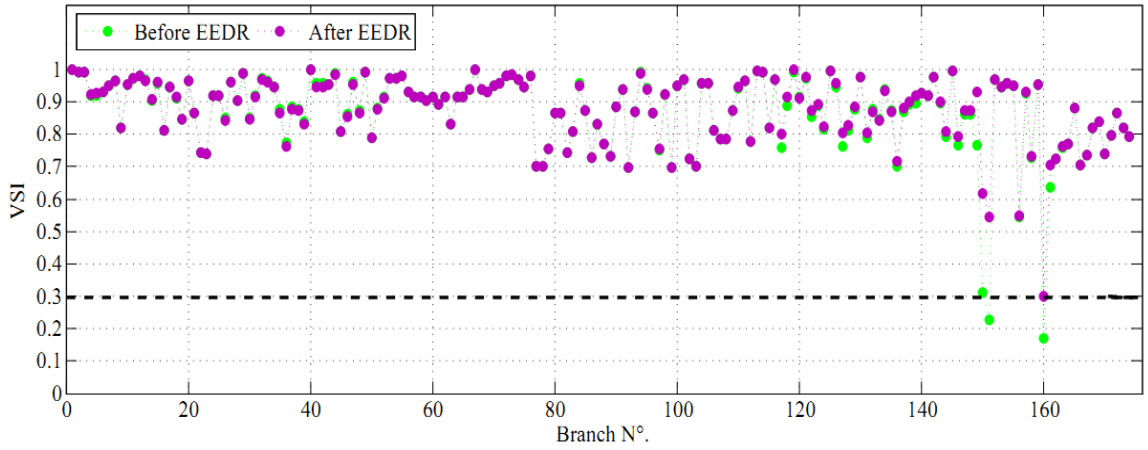


**(b)**

**Figure 5.15** VSI of the Algerian 114-bus system in the case of **(a)** loss of line (63−66), **(b)** loss of line (81−90)

**Table 5.3** EEDR results in IEEE 14-bus and Algerian 114-bus systems in the case of line tripping

| System | Events | Location | Amount (%) | Total amount | Total cost [$/hr] | VSI | |
|---|---|---|---|---|---|---|---|
| | | | | | | Before EEDR | After EEDR |
| IEEE 14-bus | Loss of the line (1−2) | 4<br>5<br>7<br>14<br>9 | 47<br>14<br>4<br>15<br>35 | 21.4330 MW, 3.6351 MVAr | 446.8791 | 0.0381 | 0.3004 |
| Algerian 114-bus | Loss of the line (63−66) | 89<br>68<br>92<br>67 | 4<br>45<br>2<br>69 | 6.3631 MW, 3.0578 MVAr | 550.5759 | 0.1261 | 0.3 |
| | Loss of the line (81−90) | 89<br>68<br>92<br>67 | 41<br>0<br>2<br>0 | 8.4208 MW, 4.2103 MVAr | 287.5827 | 0.1720 | 0.3001 |

### 5.5.2 Examples of load increase

The second scenario demonstrates the performance of the proposed scheme with respect to the load increase. Thus, all loads in the IEEE 14-bus system are increased by 170% and 190% from its initial load level. In a similar way, all loads in the Algerian 114-bus power system are increased by 20% and 35%. In these cases, the predicted values of VSI for both test systems are less than the threshold level of 0.3. This means that the systems have a great possibility of voltage collapse without any remedial actions. Since

insufficient VSM (VSI<0.3) is detected, the EEDR strategy will be activated accordingly. Figures 5.16 and 5.17 show the convergence curves of WOA algorithm seeking for the optimal load reduction at the selected buses in both test systems.

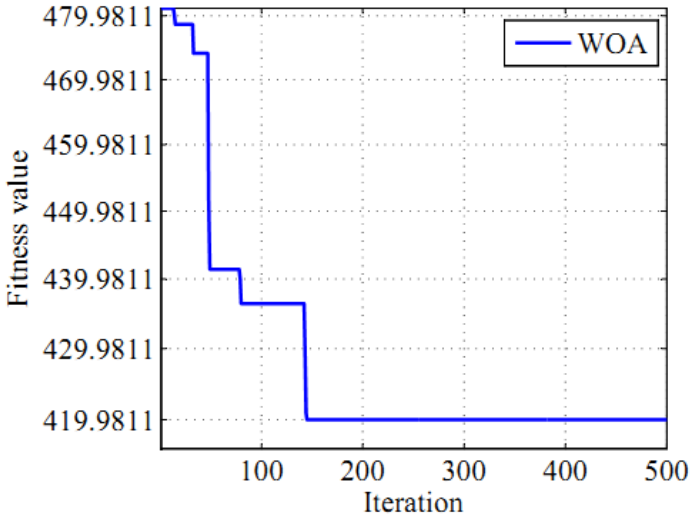


**(a)**

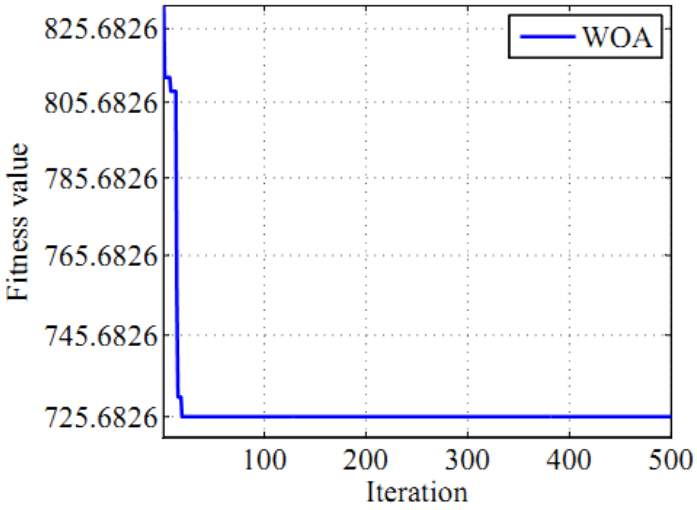


**(b)**

**Figure 5.16** Convergence characteristic of the proposed WOA with EEDR in the IEEE 14-bus system: **(a)** increasing of load by 170%, **(b)** increasing of load by 190%

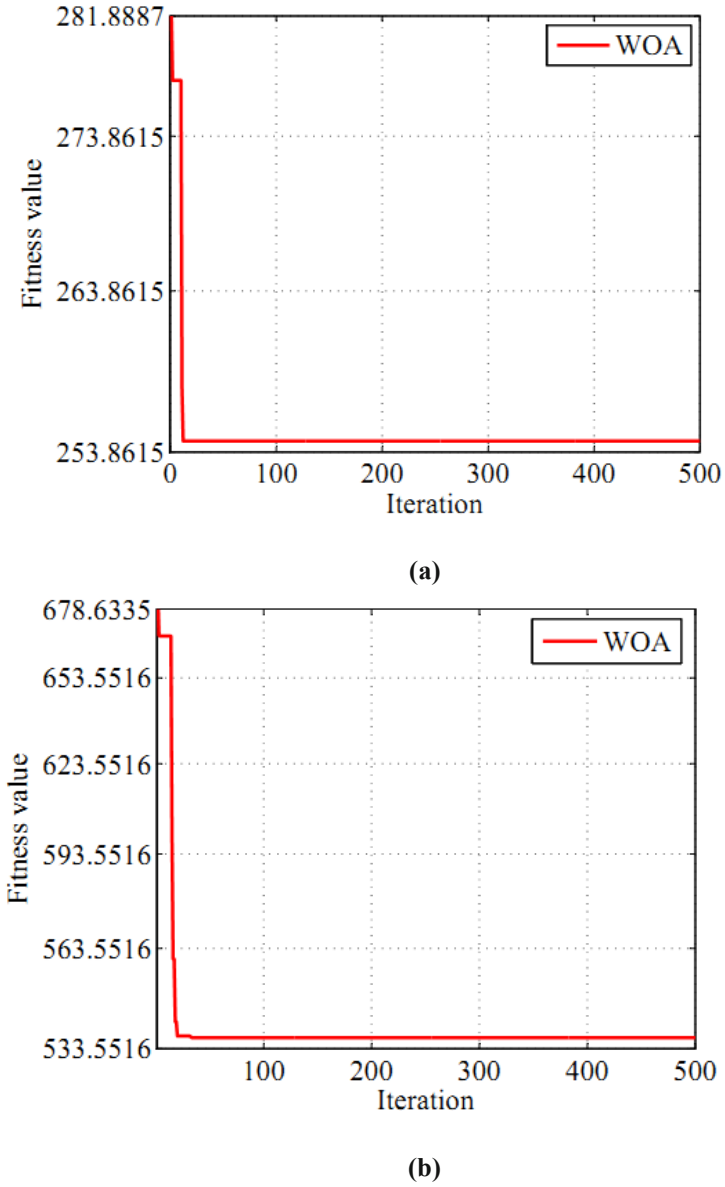


**Figure 5.17** Convergence characteristic of the proposed WOA with EEDR in the Algerian 114-bus system: **(a)** increasing of load by 20%, **(b)** increasing of load by 35%

After the implementation of the proposed EEDR, the VSI violations have been eliminated effectively as shown in Figures 5.18 and 5.19. In addition, the voltage profiles of the overall load buses at both test systems have been improved simultaneously as shown in Figures 5.20 and 5.21. In all the above-mentioned cases, the reduction in the load power demand is distributed among the participants as shown in Figures 5.22 and 5.23.

Table 5.4 summarized the obtained results for the above four cases. Columns 5 and 6 of this Table show, respectively, the total load reduction that results in a minimum total cost per hour, satisfying the minimum VSM requirement. Columns 7 and 8 of Table 5.4 show the minimum value of VSI for different load increasing levels, before and after EEDR application, respectively. The obtained results demonstrate the effectiveness of the proposed event-driven emergency demand response method in the enhancement of the VSM.

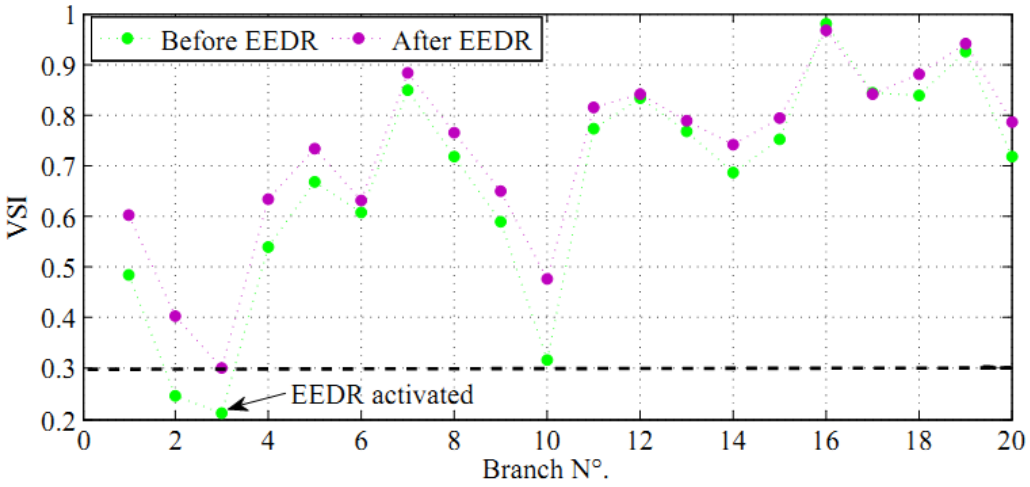


**(a)**

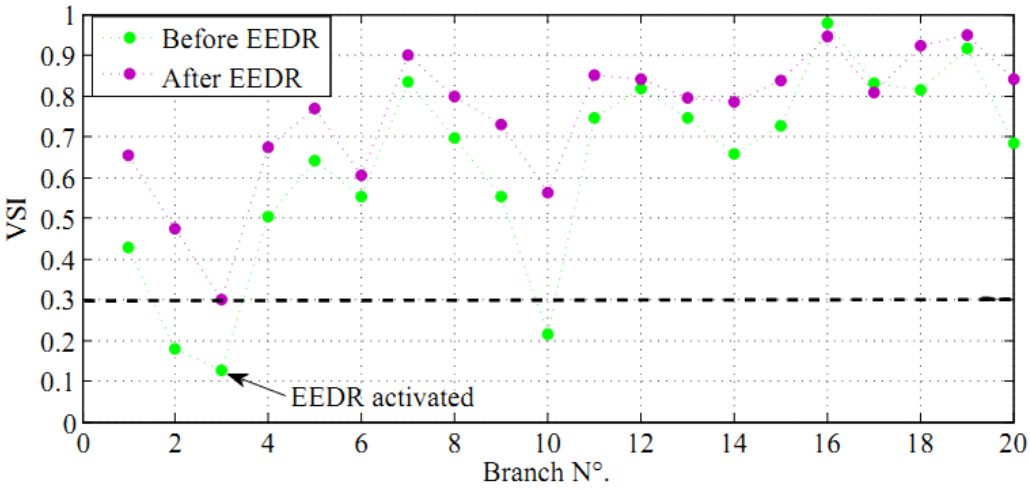


**(b)**

**Figure 5.18** VSI of the IEEE 14-bus system in the case of: **(a)** increasing of load by 170%, **(b)** increasing of load by 190%

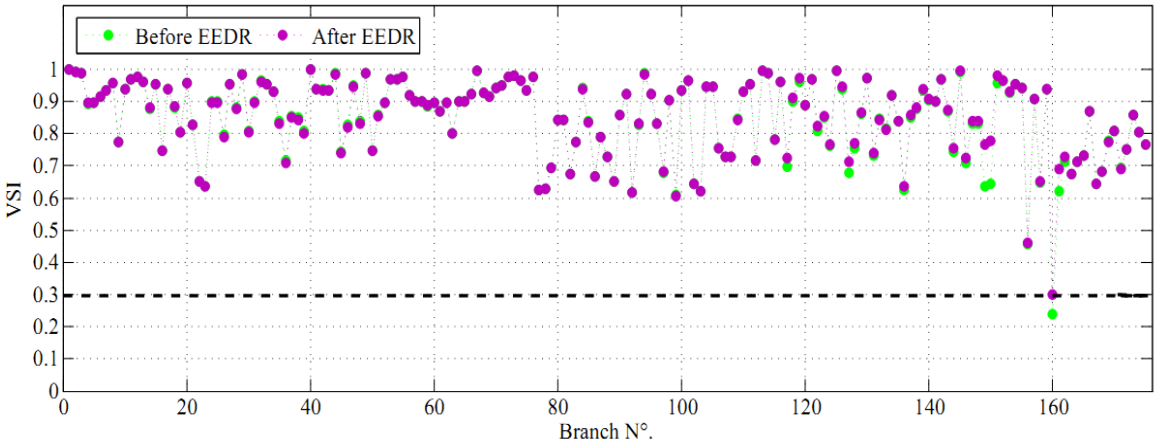


**(a)**

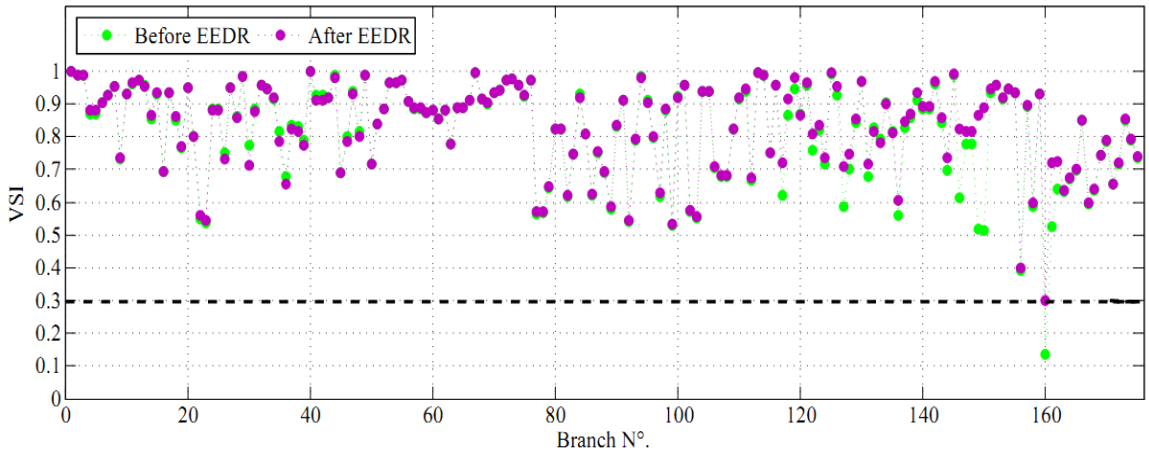


**(b)**

**Figure 5.19** VSI of the Algerian 114-bus system in the case of: **(a)** increasing of load by 20%, **(b)** increasing of load by 35%

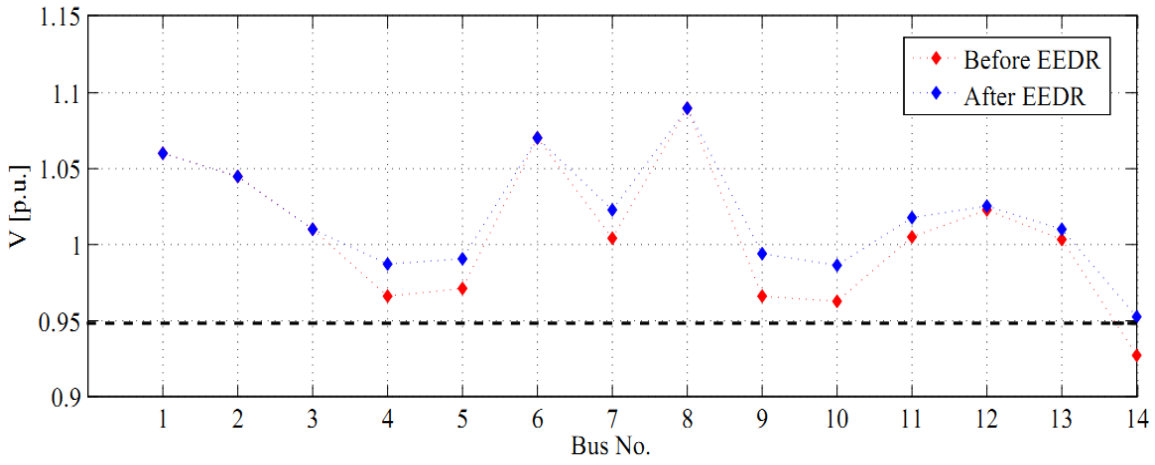


**(a)**

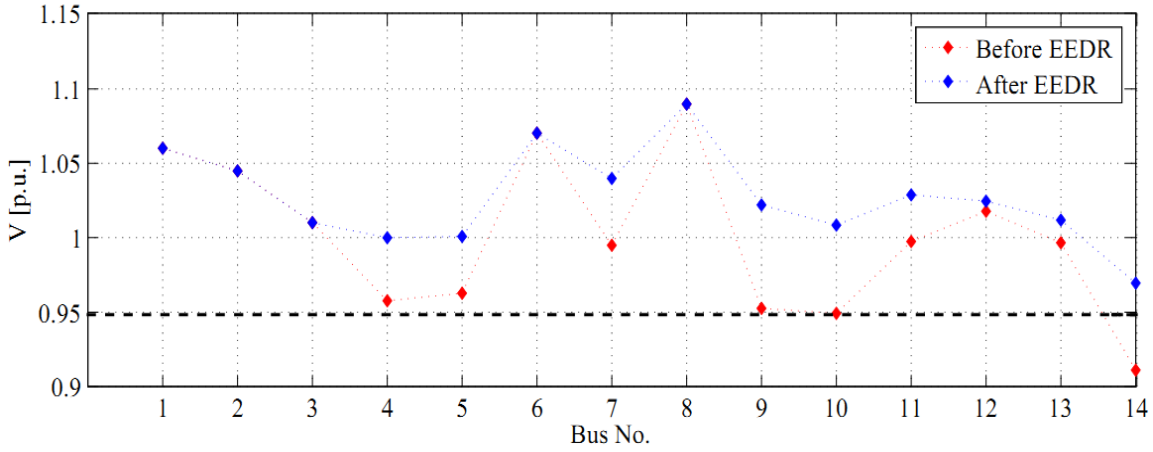


**(b)**

**Figure 5.20** Voltage profiles of the IEEE 14-bus system in the case of: **(a)** increasing of load by 170%, **(b)** increasing of load by 190%

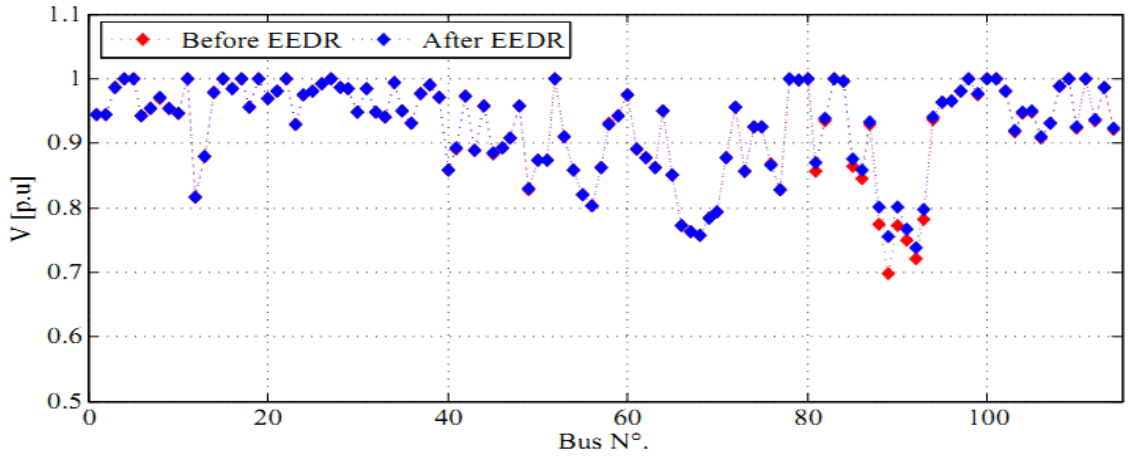


**(a)**

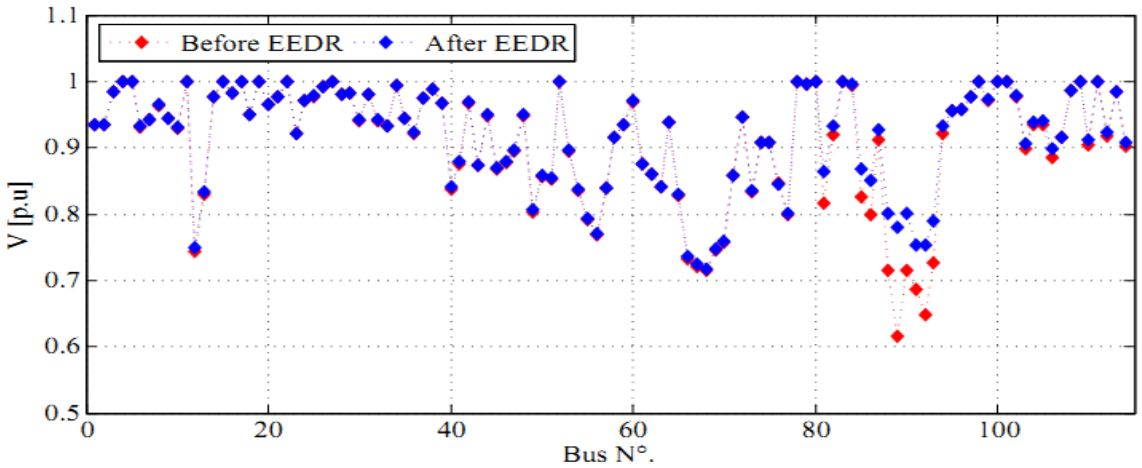


**(b)**

**Figure 5.21** Voltage profiles of the Algerian 114-bus system in the case of: **(a)** increasing of load by 20%, **(b)** increasing of load by 35%

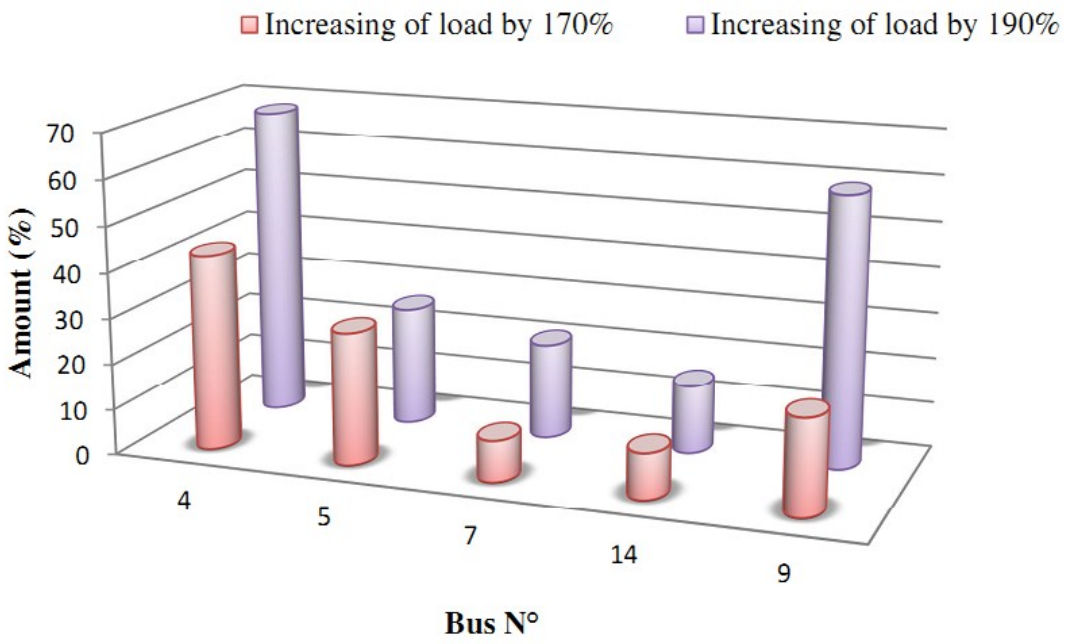


**Figure 5.22** Amount of load reduction for each participant in the case of load increasing in the IEEE 14-bus system

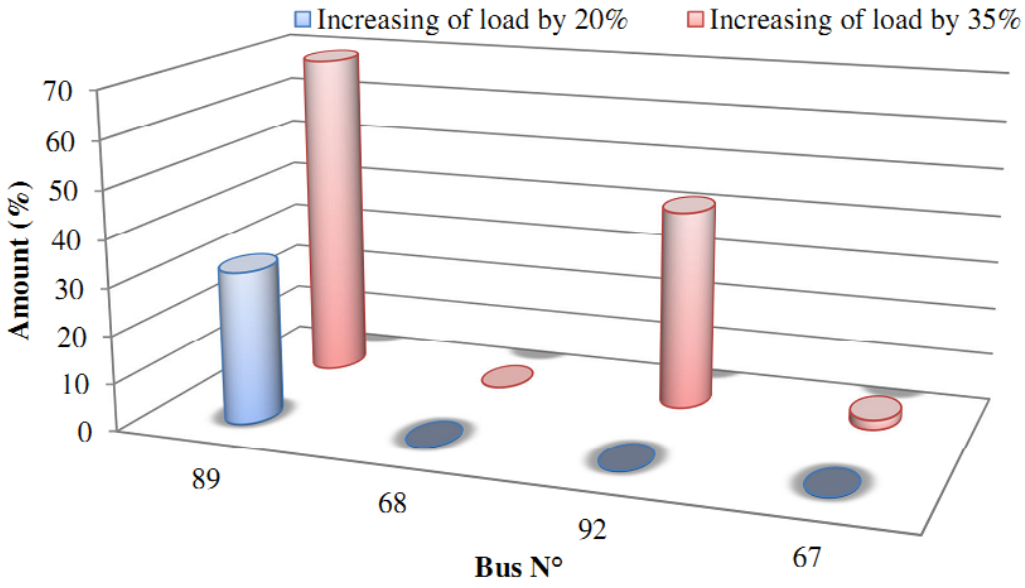


**Figure 5.23** Amount of load reduction for each participant in the case of load increasing in the Algerian 114-bus system

**Table 5.4** EEDR results in IEEE 14-bus and Algerian 114-bus systems in the case of load increasing

| System | Events | Location | Amount (%) | Total amount | Total cost [$/hr] | VSI | |
|---|---|---|---|---|---|---|---|
| | | | | | | Before EEDR | After EEDR |
| IEEE 14-bus | Increasing of load by 170% | 4<br>5<br>7<br>14<br>9 | 43<br>29<br>9<br>10<br>21 | 52.6923 MW, 6.9592 MVAr | 419.9811 | 0.2109 | 0.3 |
| | Increasing of load by 190% | 4<br>5<br>7<br>14<br>9 | 68<br>26<br>21<br>15<br>59 | 60.6080 MW, 11.9255 MVAr | 725.6826 | 0.1261 | 0.3001 |
| Algerian 114-bus | Increasing of load by 20% | 89<br>68<br>92<br>67 | 32<br>0<br>0<br>0 | 8.8781 MW, 4.4390 MVAr | 254.5213 | 0.2390 | 0.3011 |
| | Increasing of load by 35% | 89<br>68<br>92<br>67 | 69<br>0<br>42<br>2 | 13.2722 MW, 6.6361 MVAr | 536.7319 | 0.1376 | 0.3 |

## 5.6 Conclusion

In this chapter, an Event-driven Emergency Demand Response (EEDR) based Voltage Stability Margin (VSM) is proposed to improve the voltage stability of power system as well to avoid a risk of voltage collapse. In the proposed approach, the Whale Optimization Algorithm (WOA) is adapted to seek for the optimal amounts of load reductions. The main objective of the proposed EEDR approach is to maintain the VSM in an acceptable range during emergency conditions by driving the operating condition of a power system away from the insecure points. The simulation results carried out using the IEEE 14-bus and the Algerian power system proved the potential of the proposed EEDR scheme in the restoration of the power system from the emergency operating conditions. On the other hand, the use of the proposed strategy, to reach the desired VSM, results in lower demand reduction costs compared to the other methods in the literature.

# Chapter 6 : Conclusions and future work

## 6.1 Conclusions

Motivated by the increasing concern of power system operators in voltage instability phenomenon after several serious blackouts occurred around the world, this research work presented the efforts performed to assess and to improve the power system voltage stability.

In the first part of this thesis, three nature-inspired optimization algorithms-namely, Antlion optimizer (ALO), Dragonfly Algorithm (DA) and Whale Optimization Algorithm (WOA) were presented and adopted for the Support Vector Regression (SVR) parameter optimization. Thereafter, three hybrid models namely ALO-SVR, DA-SVR and WOA-SVR have been developed and applied to assess the voltage stability of power system in an on-line manner. The input features of the hybrid models were the voltage magnitudes and voltage phase angles provided by the Phasor Measurement Units (PMUs) which ensure the appropriateness of the proposed approach for on-line applications. This is very useful for the power system utility with a view to assisting the operators in taking the required measures to avoid large blackouts. The models were successfully applied to predict the Voltage Stability Margin (VSM) of the IEEE 14-bus and Algerian 114-bus systems. The obtained results proved that the presented methodologies are a viable and effective in assessing voltage stability. A comparison between the proposed hybrid models and the other existing techniques in the literature such as GA-SVR and ANFIS model is performed. The comparison results showed that the proposed models significantly outperformed these methods.

The second part of this thesis has been focused on the presentation of a simplified technique to identify the weak buses in the power system for voltage stability improvement purposes. The weak buses identification is formulated as a nonlinear optimization problem considering the voltage stability constraint. The control variables consist of real power outputs and Var sources positions in power system. The ALO, DA

and WOA algorithms have been adopted to solve this optimization problem. The proposed algorithms proved their efficiencies, as was shown in the simulations in the IEEE 14-bus and Algerian 114-bus systems.

In the last part of this thesis, an Event-driven Emergency Demand Response (EEDR) based Voltage Stability Margin (VSM) using WOA algorithm has been proposed for voltage stability improvement. The main objective of the proposed approach is to maintain VSM in an acceptable range during emergency conditions by driving the operating condition of a power system away from the insecure points. Thus, the WOA was employed to determine the optimal load reduction for each participant and to minimize the total cost of load reduction. As the branch outage contingencies and the increase in the loading level are the most reasons that cause voltage instability, these two scenarios have been simulated. The simulation results carried out using the IEEE 14-bus and the Algerian 114-bus power system show the ability of the proposed EEDR strategy to restore the voltage system from the emergency operating conditions to a stable point. A comparison with the other existing methods in the literature shows the superiority of the proposed technique.

## 6.2 Suggestions for future work

There are a number of issues that can be addressed in the future works for on-line voltage stability assessment using machine learning techniques, weak buses identification and for emergency demand response based voltage stability improvement. The addressed issues can be listed as below:

- The on-line voltage stability assessment approach presented in this work can certainly be improved, especially with regard to the SVR computational complexity which increases proportionally with the number of inputs. The integration of extraction methods to reduce the input variables may reduce, to a certain extent, the computational complexity, thus, the computational time.
- The real-time measurements should be used to completely validate the voltage stability monitoring approach. Dynamic modelling of power system is suggested;

- The recently developed optimization techniques can be incorporated into other machine learning methods to develop powerful tools that can be exploited in the on-line voltage stability monitoring as well as in other power system problems;
- The extension of the application of weak buses ranking based meta-heuristic optimization techniques to identify the weakest buses of smart grids over 24 hours considering the impacts of demand response and Plug-In Electric Vehicle (PEV) charging stations;
- Event-driving Emergency Demand Response (EEDR) programs based voltage stability improvement can be performed using other advanced optimization techniques;
- The integration of the presented EEDR in a complete defense plan should be studied;
- The extension of our EEDR formulation to take into account the effect of renewable energy sources and PEV charging stations would be of great interest.

# References


[1] B. Zeng, S. Ouyang, J. Zhang, H. Shi, G. Wu, M. Zeng, 'An analysis of previous blackouts in the world: Lessons for China's power industry', Renewable and Sustainable Energy Reviews, vol. 42, pp. 1151–1163, 2015.

[2] Fethi Boussaadia, Saad Belkhiat, 'Analysis of February 3, 2003, Blackout In Algerian power system', International conference on processing information and electrical Engineering, Tebessa, 2014.

[3] C. Hsu, C. Chang, C. Lin, 'A practical guide to support vector classification', 2016, (available at): https://www.csie.ntu.edu.tw/~cjlin/papers/guide/guide.pdf

[4] K. Chung, W. Kao, C. Sun, L. Wang, C. Lin, 'Radius margin bounds for support vector machines with the RBF kernel', Neural Comput, vol. 15, pp. 2643–2681, 2003.

[5] K. Sajan, V. Kumar, B. Tyagi, 'Genetic algorithm based support vector machine for on-line voltage stability monitoring', Electrical Power and Energy Systems, vol. 73, pp. 200–208, 2015.

[6] Tukaram Moger, Thukaram Dhadbanjan, 'A novel index for identification of weak nodes for reactive compensation to improve voltage stability', IET Generation, Transmission & Distribution, vol. 9, no. 14, pp. 1826-1834, 2015.

[7] J. Modarresi, E. Gholipour, A. Khodabakhshian, 'comprehensive review of the voltage stability indices, Renew. Sustain. Energy Rev. vol. 63, pp. 1–12, 2016.

[8] Jamshid Aghaei, Mohammad-Iman Alizadeh, Pierluigi Siano, Alireza Heidari, 'Contribution of emergency demand response programs in power system reliability', Energy, vol. 103, pp. 688-696, 2016.

[9] Yunfei Wang, Iraj Rahimi Pordanjani, Wilsun Xu, 'An Event-Driven Demand Response Scheme for Power System Security Enhancement', IEEE Transactions on Smart Grid, vol. 2, no. 1, pp. 23-29, 2011.

[10] IEEE/CIGRE 'Joint Task Force on Stability Terms and Definitions, Definition and classification of power system stability', IEEE Tran. Power Sys. vol. 19, no. 2, 2004.

[11] C. Taylor, 'Power System Voltage Stability', McGraw-Hill, 1994.

[12] CIGRÉ TF 38-02-08, 'Long-Term Dynamics Phase II', 1995.

[13] T. Ohno, S. Imai, 'The 1987 Tokyo blackout'. In Power Systems Conference and Exposition, 2006. PSCE '06. 2006 IEEE PES, pp. 314–318, Oct 2006.

[14] A. Kurita, T. Sakurai, 'The power system failure on July 23, 1987, in Tokyo', Proc. 27th conf. on Decision and Control, Austin, Texas, December 1988, pp 2093-2097.

[15] CIGRÉ Task Force 38-02-10, 'Modelling of Voltage collapse Including Dynamic Phenomena', 1993.

[16] Benjamin Genet, 'Online monitoring methods and load modelling to improve voltage stability assessment', PhD thesis, Universié Libre de Bruxelles, 2009.

[17] B. Gao, G.Morison, P. Kundur, 'Voltage Stability Evaluation Using Modal Analysis', IEEE Trans. On Power Systems, vol.7, no.4, pp. 1423-1543, 1992.

[18] C. Sharma, M.G. Ganness, 'Determination of the applicability of using modal analysis for the prediction of voltage stability', In Proceedings of the 2008 IEEE/PES Transmission and Distribution Conference and Exposition, Chicago, IL, USA, 21–24 April 2008; pp. 1–7.

[19] Farbod Larki, Mahmood Joorabian, 'Voltage Stability Evaluation of The Khouzestan Power System in Iran Using CPF Method and Modal Analysis', Power and Energy Engineering Conference (APPEEC), 2010 Asia-Pacific, China.

[20] Z. Eifadil, R. Kamal, E. Dalia, 'Identification of Voltage Collapse Vulnerable Buses Using Modal Analysis', International Conference on Computing, Control, Networking, Electronics and Embedded Systems Engineering, 2015.

[21] A. Isaiah, S. Yanxia, New Performance Indices for Voltage Stability Analysis in a Power System, Energies 2017, 10, 2042.

[22] A. Abdelaziz, M. Abu-Elnaga, M. Elsharkawy, K. Elbahrawy, 'Voltage Stability Assessment of Multi-Machine Power Systems Using Energy Function and Neural Networks Techniques', Electric Power Components and Systems, vol. 34, pp; 1313–1330, 2006.

[23] C. DeMarco, T. Overbye, 'An energy based security measure for assessing vulnerability to voltage collapse', IEEE trans on Power Systems, vol. 5, no. 2, pp. 419-425, 1990.

[24] T. Overbye, C. DeMarco, 'Improved techniques for power system voltage stability assessment using energy methods', IEEE trans on Power Systems, vol. 6, no. 4, pp. 1446-1452, 1991.

[25] A. Zambroni, W. Fritz, F. Isabella, R. Tito, 'Using PV and QV curves with the meaning of static contingency screening and planning', Electric Power Systems Research, vol. 81, pp. 1491-1498, 2011.

[26] Yves Tchokont, 'Real-time identification and monitoring of the voltage stability margin in electric power transmission systems using synchronized phasor measurements', PhD thesis, Kessel University, Germany, 2009.

[27] D. Zimmerman, E. Murillo-Sanchez, Matpower 6.0 User's Manual, December 16, 2016, http://www.pserc.cornell.edu/matpower/manual.pdf

[28] Venkataramana Ajjarapu, 'Computational Techniques for Voltage Stability Assessment and Control', Springer US, 2007.

[29] A . Mohamed, G. Jasmon, S.Yusoff, 'A Static Voltage Indicator Using Line Stability Factors', Journal of industrial Technology. vol. 7, pp. 73-85, 1989.

[30] M. Moghavvemi, F. Omar, 'Technique for contingency monitoring and voltage collapse prediction', IEE. Proc Generat. Trans. Distrib. vol. 14, no. 5, pp. 634–640, 1998.

[31] I. Musirin, T. Rahman, 'Novel Fast Voltage Stability Index (FVSI) for Voltage Stability Analysis in Power Transmission System', 2002 Student Conference on Research and Development Proceedings, Shah Alam, Malaysia, July 2002.

[32] Yanfeng Gong, Noel Schulz, Armando Guzmán, 'Synchrophasor-Based Real-Time Voltage Stability Index', Power Systems Conference and Exposition, USA, 2006.

[33] Hebb DO, 'The organization of behaviour', New York: Wiley, 1949.

[34] B. Farley, W. Clark, 'Simulation of Self-Organizing Systems by Digital Computer, IRE Transactions on Information Theory', vol. 4, no. 4, pp. 76–84, 1958.

[35] F. Rosenblatt, 'The Perceptron: A Probabilistic Model For Information Storage And Organization In The Brain', Psychological Review, vol. 65, no. 6, pp. 386–408, 1958.

[36] P. Werbos, R. Beyond, 'New Tools for Prediction and Analysis in the Behavioral Sciences', PhD thesis, Harvard University, 1974.

[37] J. Hopfield, 'Neural networks and to physical systems with emergent collective computational abilities', Proc Natl Acad Sci, vol. 79, pp. 2554–8, 1982.

[38] T. Kohonen, 'Self-organization and associative memory', New York, Springer; 1984.

[39] D. Rumelhart, J. McClelland, 'The PDP research group, parallel distributed processing: explorations in the microstructure of cognition'. Cambridge, MA: MIT Press/Bradford Books; 1986.

[40] F. Robert, 'Neural fuzzy systems'. Abo Akademi University, 1995.

[41] Jürgen Schmidhuber, 'Deep learning in neural networks', 'An overview Neural Networks', vol. 61, pp. 85–117, 2015.

[42] B. Jeyasurya, 'Artificial neural networks for power system steady-state voltage instability evaluation', Electric Power Systems Research, vol. 29, pp. 85-90, 1994.

[43] A. El-Keib, X. Ma, 'Application of artificial neural networks in voltage stability assessment', IEEE Transactions on Power Systems, vol. 10, no. 4, pp. 1890-1896, 1995.

[44] D. Salatino, R. Sibrizzai, M. Trovato, M. La Scala, 'Online voltage stability assessment of load centres by using neural networks', Electric Power Systems Research, vol. 32, no. 3, pp. 165–173, 1995.

[45] M. La Scala, M. Trovato, F. Torelli, 'A neural network-based method for voltage security monitoring', IEEE Transactions on Power Systems, vol. 11, no. 3, pp. 1332-1341, 1996.

[46] D. Popovic, D. Kukolj, F. Kulic, 'Monitoring and assessment of voltage stability margins using artificial neural networks with a reduced input set', IEE Proc-Gener. Transm. Distrib, vol. 145, no. 4, 1998.

[47] F. Ying, T. Fu, S. Chung, 'A hybrid artificial neural network (ANN) and Ward equivalent approach for on-line power system voltage security assessment', Electric Power Systems Research, vol. 53, pp. 165 – 171, 2000.

[48] Sami Repo, IEEE Midnight-Sun Workshop on Soft Computing Methods in Industrial Applications, June 16-18, 1999.

[49] C. Vallabhan B. Jeyasurya, 'Application of artificial neural networks for prediction of voltage instability', Electric Machines & Power Systems, vol. 25, no. 2, pp. 215-226, 2006.

[50] C. Saikat, B. Jeyasurya, 'On-line Voltage Stability Monitoring Using Artificial Neural Network', Large Engineering Systems Conference on Power Engineering, 2004.

[51] D. Devaraj, J. Preetha Roselyn, R. Uma Rani, 'Artificial neural network model for voltage security based contingency ranking', Applied Soft Computing, vol. 7, pp. 722–727, 2007.

[52] G. Joya, F. García-Lagos, F. Sandoval, 'Contingency evaluation and monitorization using artificial neural networks', Neural Comput Appl, vol. 19, no. 1, pp. 139–50, 2007.

[53] S. Chakrabarti, B. Jeyasurya, 'Generation rescheduling using ANN-based computation of parameter sensitivities of the voltage stability margin', Engineering Applications of Artificial Intelligence, vol. 21, pp. 1164– 1169, 2008.

[54] M. Venkatesan, B. Jolad, 'Artificial Neural Network Based Contingency Ranking', Computer Networks and Information Technologies, vol. 1, no. 142, pp. 33-38, 2011.

[55] P. Duraipandy, D. Devaraj, 'Extreme Learning Machine Approach for On-Line Voltage Stability Assessment', Swarm, Evolutionary and Emotic Computing, vol. 8298, pp. 397-405, 2013.

[56] P. Aravindhababu, G. Balamurugan, 'ANN-based voltage estimation', Applied Soft Computing, vol. 12, pp. 313-319, 2012.

[57] A. Bahmanyar, A. Karami, 'Power system voltage stability monitoring using artificial neural networks with a reduced set of inputs', Electrical Power and Energy Systems, vol. 58, pp. 246–256, 2014.

[58] Syed Mohammad Ashraf, Ankur Gupta, Dinesh Kumar Choudhary, Saikat Chakrabarti, 'Voltage stability monitoring of power systems using reduced network and artificial neural network', Electrical Power and Energy Systems. vol. 87, pp. 43–51, 2017.

[59] T. Jain, L. Srivastava, S. Singh, 'Fast Voltage Contingency Screening using Radial Basis Function Neural Network', IEEE Trans. Power Syst., vol. 18, no. 4, pp. 705-715, 2003.

[60] S. Sahari, A. Abidin, T. Abdulrahman, 'Development of Artificial Neural Network for Voltage Stability Monitoring', National Power and Energy Conference (PECon) 2003 Proceedings, Bangi, Malaysia.

[61] M. Rashidi, F. Rashidi, 'Design of adaptive artificial neural network for online voltage stability assessment', Innovations in Applied Artificial Intelligence, vol. 3029, pp. 1053-1061, 2008.

[62] L. Arya, L. Titare, D. Kothari, 'Determination of probabilistic risk of voltage collapse using radial basis function (RBF) network', Electric Power Systems Research, vol. 76, pp. 426–434, 2006.

[63] B. Moradzadeh, S. Hosseinian, M. Toosi et al., 'Online Voltage Stability Monitoring and Contingency Ranking using RBF Neural Network, IEEE PES PowerAfrica 2007 Conference and Exposition Johannesburg, South Africa, 16-20 July 2007.

[64] D. Devaraj, J. Preetha, 'On-line voltage stability assessment using radial basis function network model with reduced input features', Electrical Power and Energy Systems, vol. 33, pp. 1550–1555, 2011.

[65] M. Moghavvemi, S. Yang, 'ANN Application Techniques for Power System Stability Estimation', Electric Machines & Power Systems, vol. 28, no. 2, pp. 167-178, 2011.

[66] S. Hashemi, M. Aghamohammadi, 'Wavelet based feature extraction of voltage profile for online voltage stability assessment using RBF neural network', Electrical Power and Energy Systems, vol. 49, pp. 86–94, 2013.

[67] E. Handschin, D. Kuhlmann, C. Rehtazn, 'Visualisation and analysis of voltage stability using Self-Organizing neural network', Artificial Neural Network ICANN-97, Switzerland, October 8-10, 1997.

[68] P. Modi, S. Singh, G. Sharma, 'Loadability margin calculation of power system with SVC using artificial neural network', Engineering Application of Artificial Intelligence, vol. 18, pp. 695-703, 2005.

[69] W. Chen, Q. Jiang, Y. Cao, 'Low voltage risk assessment in power system using neural network ensemble', Advances in Neural Networks, vol. 3972, pp. 1416-1421, 2006.

[70] K. Chakraborty, A. De, A. Chakrabarti, 'Voltage stability assessment in power network using self-organizing feature map and radial basis function', Computers and Electrical Engineering, vol. 38, pp. 819–826, 2012.

[71] Bedoya, D. Castro, C. Silva,'A method for computing minimum voltage stability margins of power systems', IET Gener. Transm. Distrib., vol. 2 pp. 5, pp. 676-689, 2008.

[72] Jang, 'Adaptive-network-based fuzzy inference system', IEEE Trans Syst Man Cybern vol. 23, no. 3, pp. 665–685, 1993.

[73] K. Yabe, J. Koda, K. Yoshida, K. Chiang, P. Khedkar, D. Leonard, N. Miller, 'Conceptual designs of AI-based Systems for local prediction of voltage collapse', IEEE Trans. Power Syst., vol. 11, no. 1, pp. 137–145, 1997.

[74] P. Modi, S. Singh and J. Sharma, 'Voltage stability evaluation of power system with FACTS devices using fuzzy neural network', Engineering Applications of Artificial Intelligence, vol. 20, pp. 481–491, 2007.

[75] A. Berizzi, C. Bovo, M. Delfanti, M. Merlo, M. Pozzi, 'A Neuro-Fuzzy Inference System for the Evaluation of Voltage Collapse Risk Indices', Bulk Power System Dynamics and Control - VI, August 22-27, 2004, Cortina d'Ampezzo, Italy.

[76] P. Torres, H. Peralta, A. Castro, 'Power System Loading Margin Estimation Using a Neuro-Fuzzy Approach', IEEE transactions on power systems, vol. 22, no. 4, pp. 1955-1964, 2007.

[77] A. Berizzi, C.Bovo, D. Cirio, M. Delfanti, M. Merlo, M. Pozzi, 'Online fuzzy voltage collapse risk quantification', Electric Power Systems Research, vol. 79, pp. 740–749, 2009.

[78] B. Boser, I. Guyon, N. Vapnik, 'A training algorithm for optimal margin classifiers', in D. Haussler, editor, 5th Annual ACM Workshop on COLT, pp. 144–152, Pittsburgh, PA. ACM Press, 1992.

[79] M. Cortés-Carmona, G. Jiménez-Estévez, J. Guevara-Cedeño,'Support Vector Machines for on-line Security Analysis of Power Systems', Transmission and Distribution Conference and Exposition IEEE/PES, Latin America, 2008.

[80] M. Mohammadi, G. Gharehpetian, 'Power System on-line Static Security Assessment by using Multi-Class Support Vector Machines', Journal of Applied Sciences, vol. 8, no. 12, pp. 2226-2233, 2008.

[81] S. Kalyani, K. Swarup, 'Classification of Static Security Status Using Multi-Class Support Vector Machines', TJER, vol. 9, no. 1, pp. 21-30, 2012.

[82] M. Suganyadevi, C. Babulal, 'Fast Assessment of Voltage Stability Margin of a Power System', J. Electrical Systems, vol. 10, no. 3, pp. 305-316, 2014.

[83] M. Suganyadevi, C. Babulal, 'Support Vector Regression Model for the prediction of Loadability Margin of a Power System', Applied Soft Computing, vol. 24, pp. 304–315, 2014.

[84] K. Sajan, K. Vishal, T. Barjeev, 'Genetic algorithm based support vector machine for on-line voltage stability monitoring', Electrical Power and Energy Systems, vol. 73, pp. 200–208, 2015.

[85] Han Li, Y. H. Song, 'Identification of Weak Busbars in Large Scale Power System, International Conference on Power System Technology', China, 2002.

[86] Peng Gao, Libao Shi, Liangzhong Yao, Yixin Ni, Masoud Bazargan, 'Multi-criteria Integrated Voltage Stability Index for Weak Buses Identification', Transmission & Distribution Conference & Exposition: Asia and Pacific, 2009.

[87] T. He, S. Kolluri, S. Mandal, F. Galvan, P. Rasigoufard, 'Identification of weak locations in bulk transmission systems using voltage stability margin index', IEEE Power Engineering Society General Meeting, Denver, CO, USA, 2004.

[88] Wenping Qin, Wei zhang, Peng Wang, 'Power System Reliability Based on Voltage Weakest Bus Identification', Power and Energy Society General Meeting, 2011.

[89] P. Juanuwattanakul, A. Mohammad, A. Masoum, 'Identification of the Weakest Buses in Unbalanced Multiphase Smart Grids with Plug-In Electric Vehicle Charging Stations', Innovative Smart Grid Technologies Asia (ISGT), 2011.

[90] T. Moger, A. Dhadbanjan, 'novel index for identification of weak nodes for reactive compensation to improve voltage stability', IET Generation, Transmission & Distribution, vol. 9, no. 14, pp. 1826-1834, 2015.

[91] R. Alammari, 'fuzzy system applications for identification of weak buses in power systems', Arabian Journal for Science and Engineering, vol. 27, 2002.

[92] Rajesh Kumar, Uday Kumar, Sushil Chauhan, 'A CPF based neural approach for critical contingency evaluation and weak bus identification', International Conference on Energy-Efficient Technologies for Sustainability (ICEETS), India, 2013.

[93] Isaac Guevara, Marco Gutierrez, Pavel Zuniga, 'Identification of Weak Buses for Proper Placement of Reactive Compensation Through Sensitivity Analysis Using a Neural Network Surrogate model', IEEE International Autumn Meeting on Power, Electronics and Computing (ROPEC), Ixtapa, Mexico, 2015.

[94] P. Acharjee, 'Identification of maximum loadability limit and weak buses using security constraint genetic algorithm', Electrical Power and Energy Systems, vol. 36, pp. 40–50, 2012.

[95] P. Acharjee, S. Mallick, S.S. Thakur, S.P. Ghoshal, 'Detection of maximum loadability limits and weak buses using Chaotic PSO considering security constraints', Chaos, Solitons & Fractals, vol. 44, pp. 600–612, 2011.

[96] M. Amroune, B. Arif, T. Bouktir, 'Weak Buses Identification and Ranking in Large Power Transmission Network by Optimal Location of Reactive Power Supports', Telkominika, vol. 12, no. 10, pp. 7123-7130, 2014.

[97] D. Vournas, A. Manos, "Emergency tap-blocking to prevent voltage collapse", IEEE Porto Power Tech Conference, Porto, Portugal, 2001.

[98] Benjamin Genet, 'On monitoring methods and load modeling to improve voltage stability assessment', PhD thesis, Université Libre de Bruxelles, 2009.

[99] B. Otomega, V. Sermanson, T. Van Cutsem, 'Reverse-logic control of load tap changers in emergency voltage conditions', In IEEE PowerTech Conference Proceedings, Bologna, Jun. 2003.

[100] C. Vournas, M. Karystianos, 'Load tap changers in emergency and preventive voltage stability control', IEEE Trans. on Power Systems, vol. 19, no. 1, pp. 492-498, 2004.

[101] L. Barboza, A. Lerm, R. Salgado, 'Load shedding – an efficient use of LTC transformers', In 15th Power System Computation Conference (PSCC), Liège, Belgium, Aug. 2005.

[102] S. Ashwani Kumar, S. Srivastava, A. Singh, 'Zonal Congestion Management Approach Using Real and Reactive Power Rescheduling', IEEE Transactions on Power Systems, vol. 19, no. 1, 2004.

[103] B.Talukdar, A. Sinha, S. Mukhopadhyay, 'A computationally simple method for cost-efficient generation rescheduling and load shedding for congestion management', Int. J. Electr. Power Energy Syst., vol. 77, pp. 379–388, 2005.

[104] G. Yesuratnam, D. Thukaram, 'Congestion management in open access based on relative electrical distances using voltage stability criteria', Elect. Power Syst. Res., vol. 77, pp. 1608–1618, 2007.

[105] S. Dutta, S. Singh, 'Optimal rescheduling of generator for congestion management based on particle swarm optimization', IEEE Trans. Power Syst., vol. 23, no. 4, pp. 1560–1569, 2008.

[106] Habibollah Raoufi, Mohsen Kalantar, 'Reactive power rescheduling with generator ranking for voltage stability improvement', Energy Conversion and Management, vol. 50, no. 4, pp. 1129-1135, 2009.

[107] Rajalakshmy Sa, Jasmy Paul, 'Voltage stability by reactive power rescheduling using PSO Algorithm', Procedia Computer Science, vol. 46, pp. 1377–1384, 2015.

[108] Sumit Verma, Vivekananda Mukherjee, Optimal real power rescheduling of generators for congestion management using a novel ant lion optimiser, IET Generation, Transmission & Distribution, vol. 10, no. 10, pp. 2548-2561, 2016.

[109] Sadhan Gope, Arup Kumar Goswami, Prashant Kumar Tiwari, Subhasish Deb, 'Rescheduling of real power for congestion management with integration of pumped storage hydro unit using firefly algorithm', Electrical Power and Energy Systems, vol. 83, pp. 434–442, 2016.

[110] J. Jeslin Drusila Nesamalar, P. Venkatesh, S. Charles Raja, 'Energy management by generator rescheduling in congestive deregulated power system', Applied Energy, vol. 171, pp. 357–371, 2016.

[111] J. Laghari, H. Mokhlis, A. Bakar, Hasmaini Mohamad, 'Application of computational intelligence techniques for load shedding in power systems, A review', Energy Conversion and Management, vol. 75, pp. 130–140, 2013.

[112] H. Lokay, V. Burtnyk, 'Application of under-frequency relays for automatic load shedding'. IEEE Transactions on Power Apparatus and Systems, vol. 3, pp. 776–783, 1968.

[113] E. Thalassinakis, E. Dialynas, 'A Monte-Carlo simulation method for setting the under-frequency load shedding relays and selecting the spinning reserve policy in

autonomous power systems', IEEE Transactions on Power Systems, vol. 19, no. 4, 2044–2052, 1968.

[114] D. Aik, 'A general-order system frequency response model incorporating load shedding: Analytic modeling and applications', IEEE Transactions on Power Systems, vol. 21, no. 2, 709–717, 2006.

[115] Stefan Arnborg, Goran Anderson, J. David Hill, A. Ian Hiskens, 'On Influence of Load Modelling for Undervoltage Load Shedding Studies', IEEE Transactions on Power Systems, vol. 13, no. 2, 1998.

[116] J . Tang, J. Liu, F. Ponci, A. Monti, 'Adaptive load shedding based on combined frequency and voltage stability assessment using synchrophasor measurements', IEEE T Power Syst, vol. 28, pp. 2035–47, 2013.

[117] J. Ford, H. Bevrani, G. Ledwich, 'Adaptive load shedding and regional protection', Electrical Power and Energy Systems, vol. 31, pp. 611–618, 2009.

[118] M. Mitchell, Lopes JAP, J. Fidalgo, JD. McCalley, 'Using a neural network to predict the dynamic frequency response of a power system to an under-frequency load shedding scenario', IEEE Power Eng Soc, pp. 346–51, 2000.

[119] M. Purnomo, C. Patria, E. Purwanto, 'Adaptive load shedding of the power system based on neural network', TENCON Proc Comput, Commun, Control Power Eng, pp. 1778–81, 2002.

[120] C. Hsu, M. Kang, C. Chen, 'Design of adaptive load shedding by artificial neural networks', IET Gener Transm Dis, vol. 15, no. 2, pp. 415–21, 2005.

[121] C.Hsu, H.Chuang, C.Chen, 'Adaptive load shedding for an industrial petroleum cogeneration system', Exp Syst Appl, vol. 38, no. 13, pp. 967–74, 2001.

[122] A. Haidar, A. Mohamed, M. Al-Dabbagh, A. Hussain, 'Vulnerability assessment and control of large-scale interconnected power systems using neural networks and neuro-fuzzy techniques', Power Eng Conf 2008, pp. 1–6.

[123] A. Haidar, A. Mohamed, A, Hussain, 'Vulnerability control of large scale interconnected power system using neuro-fuzzy load shedding approach', Exp Syst Appl, vol. 37, no. 3, pp. 171–6, 2010.

[124] A. Bikas, E. Voumvoulakis, N. Hatziargyriou, 'Neuro-fuzzy decision trees for dynamic security control of power systems', Int Conf Intell Syst Appl Power Syst 2009, pp. 1–6.

[125] W. Luan, M. Irving, J. Daniel, 'Genetic algorithm for supply restoration and optimal load shedding in power system distribution networks', IET Gener Transm Dis, vol. 149, pp. 145–51, 2002.

[126] Abbas Ketabi, Masoud Hajiakbari, 'Adaptive under-frequency load shedding using particle swarm optimization algorithm', Journal of Applied Research and Technology, vol. 15, pp. 54–60, 2017.

[127] N. Sadati, T. Amraee, A. Ranjbar, 'A global particle swarm-based-simulated annealing optimization technique for under-voltage load shedding problem', Appl Soft Comput, vol. 9, pp. 652–7, 2017.

[128] L. Arya, P. Singh, L. Titar, 'Optimum load shedding based on sensitivity to enhance static voltage stability using DE', Swarm and Evolutionary Computation, vol. 6, pp. 25–38, 2012.

[129] R. Mageshvaran, T. Jayabarathi, 'GSO based optimization of steady-state load shedding in power systems to mitigate blackout during generation contingencies', Ain Shams Engineering Journal, vol. 6, pp. 145–160, 2015.

[130] R. Mageshvaran, T. Jayabarathi, 'Steady-state load shedding to mitigate blackout in power systems using an improved harmony search algorithm', Ain Shams Engineering Journal, vol. 6, pp. 819–834, 2015.

[131] G. Nikolaos, Paterakis, Ozan Erdinç, P. João Catalão, 'An overview of Demand Response', Key-elements and international experience, Renewable and Sustainable Energy Reviews, vol. 69, pp. 871–891, 2017.

[132] H. Aalami, M. Moghaddam, G.Yousefi, 'Demand response modeling considering Interruptible/Curtailable loads and capacity market programs', Applied Energy, vol. 87, no. 1, pp. 243–250, 2010.

[133] A. Yousefi, E.Shayesteh, K. Zare, S. Jalal Kazempour, M. Moghaddam, M. Haghifam, 'Risk-based spinning reserve allocation considering emergency demand response program', 43rd International Universities Power Engineering Conference, UPEC 2008., pp. 1– 5.

[134] A. Azami, A. Abbasi, J.Shakeri, A. Faraji Fard, 'Impact of EDRP on the composite reliability of restructured power systems', IEEE 2009 Bucharest Power Tech Conf., 28 June – 2 July.

[135] E. Shayesteh, A. Yousefi, Parsa Moghaddam, M. K. Sheikh-EL-Eslami, 'ATC Enhancement Using Emergency Demand Response Program', IEEE/PES Power System Conference and Exposition, 2009.

[136] Rajesh Tyagi, W. Jason Black, 'Emergency Demand Response for Distribution System Contingencies', IEEE PES Transmission and Distribution Conference, and Exposition, New Orleans, LA, USA, 2010.

[137] M. Sahebi, E. Duki, M. Kia, A. Soroudi, M. Ehsan, 'Simultaneous emergency demand response programming and unit commitment programming in comparison with interruptible load contracts', IET Gener. Transm. Distrib., vol. 6, no. 7, pp. 605 – 611, 2012.

[138] M. Rahmani-Andebili, A. Abdollahi, M. Parsa Moghaddam, 'An Investigation of Implementing Emergency Demand Response Program (EDRP) in Unit Commitment Problem', Power and Energy General Meeting, 2011.

[139] Dong-Min Kim, Jin-O. Kim, 'Design of Emergency Demand Response Program Using Analytic Hierarchy Process', IEEE Transactions on Smart Grid, vol. 3, no. 2, pp. 635-644, 2012.

[140] Habib Allah Aalami, Ahmadali Khatibzadeh, 'Regulation of market clearing price based on nonlinear models of demand bidding and emergency demand response programs', Int. Trans. Electr. Energy. Syst. 2016.

[141] Real-Time Application of Synchrophasors for Improving Reliability, North American Electric Relaibility Corporation, 2010.

[142] G. Phadke, 'Synchronized phasor measurements a historical overview', IEEE/PED Transmission and Distribution Conference and Exhibition 2002: the Asia Pacific, vol. 1, pp. 476 – 479.

[143] B. Singh, N. Sharma, A. Tiwari, K. Verma, S. Singh, 'Applications of phasor measurement units (PMUs) in electric power system networks incorporated with FACTS controllers', International Journal of Engineering, Science, and Technology, vol. 3, pp. 64–82, 2012.

[144] C. Taylor, 'Wide Area Measurement, Monitoring and Control in Power Systems, Presented at Workshop on Wide Area Measurement, Monitoring and Control in Power Systems', Imperial College, London, 16–17 Mar. 2006.

[145] Xinran Zhang, Chao Lu, Shichao Liu, Xiaoyu Wang, 'A review on wide-area damping control to restrain interarea low-frequency oscillation for large-scale power systems with increasing renewable generation', Renewable and Sustainable Energy Reviews, vol. 57, pp. 45–58, 2016.

[146] Y. Wang, L. Wenyuan, L. Jiping, 'Reliability Analysis of Wide-Area Measurement System'. IEEE Trans. on power delivery', vol. 25, no. 3, pp. 1483-1491, 2010.

[147] V. Vapnik, 'The Nature of Statistical Learning Theory', Springer, New York, 1995.

[148] A. Smola, B. Scholkopf, 'A tutorial on support vector regression', Statistics and Computing, vol. 14, pp. 199–222, 2004.

[149] L. Xiao-li, L. Li-hong, Z. Bao-lin, G. Qian-jin, 'Hybrid self-adaptive learning based particle swarm optimization and support vector regression model for grade estimation', Neurocomputing, vol. 118, pp. 179-190, 2013.

[150] F. Glover, 'Future paths for integer programming and links to artificial intelligence', Computers & Operations Research, vol. 13, no. 5, pp. 533–549, 1986.

[151] Seyedali Mirjalili, Andrew Lewis, 'The Whale Optimization Algorithm', Advances in Engineering Software, vol. 95, pp. 51–67, 2016.

[152] Mirjalili, S. 'The antlion optimizer', Adv. Eng. Softw., vol. 83, pp. 80–98, 2015.

[153] Seyedali Mirjalili, 'Dragonfly algorithm: a new meta-heuristic optimization technique for solving single-objective, discrete, and multi-objective problems', Neural Comput & Applic., vol. 27, no. 4, pp. 1053-1073, 2015.

[154] V. Salehi, O. Mohammed, 'Real-time voltage stability monitoring and evaluation using synchrophasor', IEEE North American Power Symposium (NAPS), 2011.

[155] C. Ertekin, O. Yaldiz, 'Comparison of some existing models for estimating global solar radiation for Antalya (Turkey)'. Energy Convers Manage, vol. 41, pp. 311–30, 2000.

[156] F. Milano, Power system analysis toolbox (PSAT) (Available at:) http://faraday1.ucd.ie/psat.html.

[157] L. Slimani, T. Bouktir, 'Optimal power flow solution of the Algerian electrical network using differential evolution algorithm,' Telkomnika, vol. 10, no. 2, pp. 199-210, 2012.

[158] D. Zimmerman, E. Carlos. Murillo-Sánchez et al., Matpower, A MATLAB Power System Simulation Package, (Available at:) http://www.pserc.cornell.edu/matpower/

[159] S. Chiu, 'Fuzzy model identification based on clustere stimation', J. Intell. Fuzzy Syst. vol. 2, no. 3, pp. 267–278, 1998.

[160] M. Amroune, T. Bouktir, I. Musirin, 'Power System Voltage Stability Assessment Using a Hybrid Approach Combining Dragonfly Optimization Algorithm and Support Vector Regression', Arabian Journal for Science and Engineering, DOI: 10.1007/s13369-017-3046-5

[161] Huaguang yan, et al., 'Future evolution of automated demand response system in smart grid for low-carbon economy', Journal of Modern Power Systems and Clean Energy, vol. 3, no. 1, pp. 72-81, 2015.

[162] B. Hoseinzadeh, F.M. Faria Da Silva, and C.L. Bak, 'Adaptive tuning of frequency thresholds using voltage drop data in decentralized load shedding', IEEE Trans. Power Syst., vol. 30, no. 4, pp. 2055-2062, 2015.

[163] K. Karunanithi et al., 'Integration of Demand and Supply Side Management strategies in Generation Expansion Planning', Renewable and Sustainable Energy Reviews, vol. 73, pp. 966-982, 2017.

[164] NIST Framework and Roadmap for Smart Grid Interoperability Standards, Release 1.0, 2010.

[165] Nikolaos G. Paterakis, Ozan Erdinç, João P.S. Catalão, 'An overview of Demand Response: Key-elements and international experience', Renewable and Sustainable Energy Reviews, vol. 69, pp. 871–891, 2017.

[166] Q. Zhang, E. Ignacio, 'Planning and Scheduling for Industrial Demand Side Management: Advances and Challenges, Alternative Energy Sources and Technologies, pp. 383-414.

[167] US Department of Energy, Energy Policy Act of 2005, Industry Applications Magazine, IEEE, 2007, pp. 14–20.

[168] Manuel Alcázar Ortega, 'Evaluation and Assessment of New Demand Response Products Based on the Use of Flexibility in Industrial Processes: Application to the Food Industry', Dual PhD. The program between the Universidad Politécnica de Valencia and the University of South Florida, 2011.

[169] US Department of Energy. Benefits of Demand Response in Electricity Markets and Recommendations for Achieving Them, A Report to the United States Congress Pursuant to Section 1252 of the Energy Policy Act of 2005:122. doi:CiteULike-article-id:10043893; 2006.

[170] Zhaoyu Wang, Implementation and assessment of demand response and voltage/Var control with distributed generators', PhD thesis, Georgia Institute of Technology, 2015.

[171] P. Faria, Z. Vale, 'Demand response in electrical energy supply: An optimal real-time pricing approach', Energy, vol. 36, pp. 5374-5384, 2011.

[172] Sioshansi R, Short W. 'Evaluating the impacts of real-time pricing on the usage of wind generation'. IEEE Transactions on Power Systems, vol. 24, no. 2, 2009.

[173] Murthy Balijepalli, Vedanta Pradhan, S. Khaparde, R. Shereef, 'Review of Demand Response under Smart Grid Paradigm', 2011 IEEE PES Innovative Smart Grid Technologies – India.

# Appendix

## A.1. IEEE 14-bus test system data

The IEEE 14-bus system is shown in Figure 3.24. The system data is taken from [156]. The minimum and maximum of voltage magnitude are considered to be [0.95 1.05] p.u for load buses, and [0.90 1.1] p.u for generator buses.

**Table A.1.1** Line data of the IEEE 14-bus test system

| Line number | From bus | To bus | Resistance | Reactance | Susceptance |
|---|---|---|---|---|---|
| 1 | 1 | 2 | 0.01938 | 0.05917 | 0.02640 |
| 2 | 1 | 5 | 0.05403 | 0.22304 | 0.02190 |
| 3 | 2 | 3 | 0.04699 | 0.19797 | 0.01870 |
| 4 | 2 | 4 | 0.05811 | 0.17632 | 0.02460 |
| 5 | 2 | 5 | 0.05695 | 0.17388 | 0.01700 |
| 6 | 3 | 4 | 0.06701 | 0.17103 | 0.01730 |
| 7 | 4 | 5 | 0.01335 | 0.04211 | 0.00640 |
| 8 | 4 | 7 | 0 | 0.20912 | 0 |
| 9 | 4 | 9 | 0 | 0.55618 | 0 |
| 10 | 5 | 6 | 0 | 0.25202 | 0 |
| 11 | 6 | 11 | 0.09498 | 0.1989 | 0 |
| 12 | 6 | 12 | 0.12291 | 0.25581 | 0 |
| 13 | 6 | 13 | 0.06615 | 0.13027 | 0 |
| 14 | 7 | 8 | 0 | 0.17615 | 0 |
| 15 | 7 | 9 | 0 | 0.11001 | 0 |
| 16 | 9 | 10 | 0.03181 | 0.0845 | 0 |
| 17 | 9 | 14 | 0.12711 | 0.27038 | 0 |
| 18 | 10 | 11 | 0.08205 | 0.19207 | 0 |
| 19 | 12 | 13 | 0.22092 | 0.19988 | 0 |
| 20 | 13 | 14 | 0.17093 | 0.34802 | 0 |

**Table A.1.2** Generator data of the IEEE 14-bus test system

| Generator N° | $P_i^{min}$ | $P_i^{max}$ | $a_i$ | $b_i$ | $c_i$ |
|---|---|---|---|---|---|
| 1 | 0 | 332.4 | 0.0430293 | 20 | 0 |
| 2 | 0 | 140 | 0.25 | 20 | 0 |
| 3 | 0 | 100 | 0.1 | 40 | 0 |
| 6 | 0 | 100 | 0.1 | 40 | 0 |
| 8 | 0 | 100 | 0.1 | 40 | 0 |

**Table A.1.3** Transformers tap setting data of the IEEE 14-bus test system

| From bus | To bus | Tap setting value (*p.u*) |
|---|---|---|
| 4 | 7 | 0.978 |
| 4 | 9 | 0.969 |
| 5 | 6 | 0.932 |

**Table A.1.4** Bus data of the IEEE 14-bus test system

| Bus N° | Bus type | Bus voltage | | Generation | | load | |
|---|---|---|---|---|---|---|---|
| | | Magnitude (*p.u*) | Phase angle (degree) | Real power (MW) | Reactive power (MVAR) | Real power (MW) | Reactive power (MVAR) |
| 1 | 3 | 1.060 | 0 | 114.17 | -16.9 | 0 | 0 |
| 2 | 2 | 1.045 | 0 | 40.00 | 0 | 21.7 | 12.7 |
| 3 | 2 | 1.010 | 0 | 0 | 0 | 94.2 | 19.1 |
| 4 | 1 | 0 | 0 | 0 | 0 | 47.8 | -3.9 |
| 5 | 2 | 0 | 0 | 0 | 0 | 7.6 | 1.6 |
| 6 | 1 | 0 | 0 | 0 | 0 | 11.2 | 7.5 |
| 7 | 1 | 0 | 0 | 0 | 0 | 0 | 0 |
| 8 | 2 | 0 | 0 | 0 | 0 | 0 | 0 |
| 9 | 1 | 0 | 0 | 0 | 0 | 29.5 | 16.6 |
| 10 | 1 | 0 | 0 | 0 | 0 | 9.0 | 5.8 |
| 11 | 1 | 0 | 0 | 0 | 0 | 3.5 | 1.8 |
| 12 | 1 | 0 | 0 | 0 | 0 | 6.1 | 1.6 |
| 13 | 1 | 0 | 0 | 0 | 0 | 13.8 | 5.8 |
| 14 | 1 | 0 | 0 | 0 | 0 | 14.9 | 5.0 |

## A.2 Algerian 114-bus power system

The Algerian power system shown in Figure 3.25 is sub-divided into the transmission (High voltage) grids and distribution (Medium and low voltage) grids. The voltage levels of the Algerian power system are shown in Table A.2.1. Figure A.2.1 shows the main structure of the sub-transmission and distribution systems. The 220kV transmission system is interconnecting five regional power systems: Alger, Oran, Annaba, Sétif Hassi Massoud and Hassi Berkine. The national load dispatch centre has the jurisdiction to control 220 Kv substations, transmission lines and all the power plants while five regional load dispatch centres (Alger, Oran, Annaba, Sétif, Hassi Massoud and Hassi Berkine) monitor and control the 60-90 kV transmission lines, substations in their respective regions [2].

The bus data of the Algerian 114-bus system is represented in detail in Table A.2.2.

**Table A.2.1** Voltage levels of the Algerian power system

| | **Voltage Level** |
|---|---|
| Transmission Grid | 400kV |
| Transmission Grid | 150 to 220 kV |
| Transmission Grid | 60 kV to 90kV |
| Medium Voltage | 10 kV to 30 kV |
| Low Voltage | 220V to 380 V |

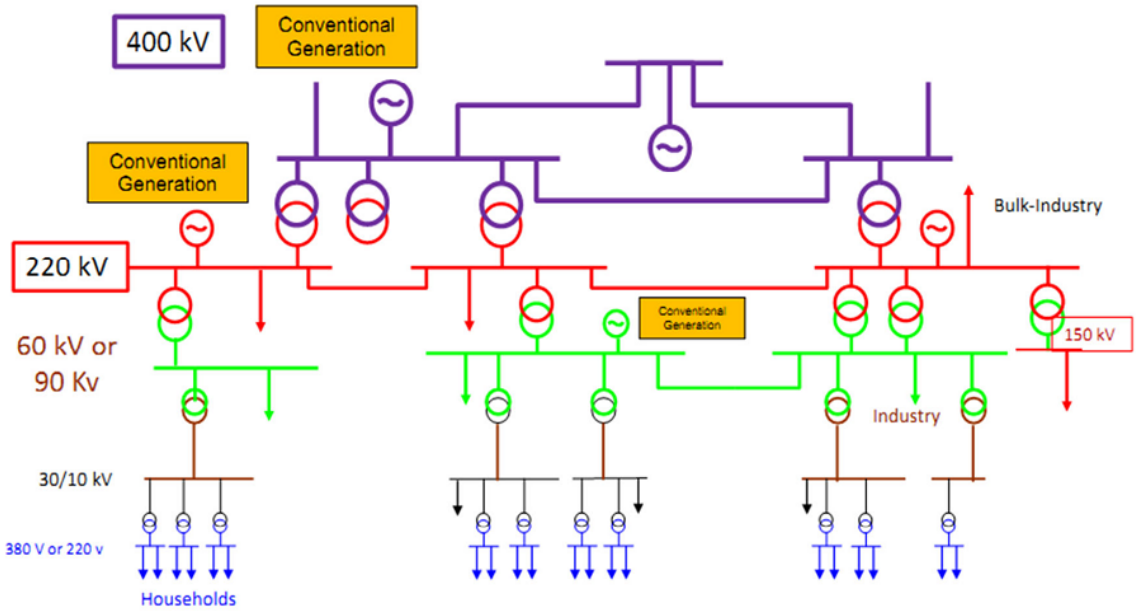


**Figure A.2.1** Structure of the Algerian electrical power system

**Table A.2.2** Bus data of the Algerian 114-bus power system

| **Bus name** | **Bus N°** | **Bus voltage** | | **load** | | **Generation** | |
|---|---|---|---|---|---|---|---|
| | | **Magnitude (*p.u*)** | **Phase angle (degree)** | **Real power (MW)** | **Reactive power (MVAR)** | **Real power (MW)** | **Reactive power (MVAR)** |
| 1OUJDA6 | 1 | 1 | 0.0 | 0 | 0 | 0 | 0 |
| 1GHAZA6 | 2 | 1 | 0.0 | 36 | 17 | 0 | 0 |
| 1ZAHAN6 | 3 | 1 | 0.0 | 64 | 31 | 0 | 0 |
| 1MEHA16 | 4 | 1 | 0.0 | 125 | 94 | 750 | 400 |
| 1MEHA26 | 5 | 1 | 0.0 | 335 | 250 | 300 | 160 |
| 1TLEMC6 | 6 | 1 | 0.0 | 78 | 37 | 0 | 0 |
| 1SBABE6 | 7 | 1 | 0.0 | 55 | 26 | 0 | 0 |
| 1RELIZ6 | 8 | 1 | 0.0 | 50 | 24 | 0 | 0 |
| 1BESAF6 | 9 | 1 | 0.0 | 40 | 19 | 0 | 0 |
| 1SAIDA6 | 10 | 1 | 0.0 | 42 | 21 | 0 | 0 |
| 1TIARE6 | 11 | 1 | 0.0 | 96 | 47 | 160 | 30 |
| 1BECHA6 | 12 | 1 | 0.0 | 31 | 15 | 0 | 0 |

| | | | | | | | |
|---|---|---|---|---|---|---|---|
| 1AISEF6 | 13 | 1 | 0.0 | 13 | 6 | 0 | 0 |
| 1PELAC6 | 14 | 1 | 0.0 | 136 | 65 | 0 | 0 |
| 1RABLA6 | 15 | 1 | 0.0 | 0 | 0 | 60 | 30 |
| 1RABLA6 | 16 | 1 | 0.0 | 0 | 0 | 0 | 0 |
| 2ALEST6 | 17 | 1.0682 | 0.0 | 0 | 0 | 640 | 400 |
| 2ALEST3 | 18 | 1 | 0.0 | 0 | 0 | 0 | 0 |
| 2APORT3 | 19 | 1 | 0.0 | 11 | 5 | 100 | 60 |
| 2ARBAA3 | 20 | 1 | 0.0 | 14 | 9 | 0 | 0 |
| 2ARBAA6 | 21 | 1 | 0.0 | 70 | 52 | 0 | 0 |
| 2BAEZO3 | 22 | 1 | 0.0 | 42 | 25 | 60 | 40 |
| 2BEAKN3 | 23 | 1 | 0.0 | 23 | 11 | 0 | 0 |
| 2HARA3 | 24 | 1 | 0.0 | 60 | 36 | 0 | 0 |
| 2GLAC3 | 25 | 1 | 0.0 | 17 | 8 | 0 | 0 |
| 2HAMMA3 | 26 | 1 | 0.0 | 55 | 26 | 0 | 0 |
| k2HAMM16 | 27 | 1 | 0.0 | 0 | 0 | 0 | 0 |
| 2HAMM26 | 28 | 1 | 0.0 | 0 | 0 | 0 | 0 |
| 2KOUBA3 | 29 | 1 | 0.0 | 37 | 18 | 0 | 0 |
| 2OFATaYE3 | 30 | 1 | 0.0 | 30 | 15 | 0 | 0 |
| 2OFAYE6 | 31 | 1 | 0.0 | 0 | 0 | 0 | 0 |
| 2ROUIB3 | 32 | 1 | 0.0 | 40 | 24 | 0 | 0 |
| 2ROUI13 | 33 | 1 | 0.0 | 29 | 14 | 0 | 0 |
| 2TAFOU3 | 34 | 1 | 0.0 | 29 | 14 | 0 | 0 |
| 2BARAK3 | 35 | 1 | 0.0 | 33 | 16 | 0 | 0 |
| 2ABENI3 | 36 | 1 | 0.0 | 17 | 8 | 0 | 0 |
| 2A.TAY3 | 37 | 1 | 0.0 | 11 | 5 | 0 | 0 |
| 2AURAS3 | 38 | 1 | 0.0 | 20 | 10 | 0 | 0 |
| 2GOLF.3 | 39 | 1 | 0.0 | 20 | 10 | 0 | 0 |
| 2CHLEF3 | 40 | 1 | 0.0 | 21 | 10 | 0 | 0 |
| 2OUSLY | 41 | 1 | 0.0 | 53 | 32 | 0 | 0 |
| 2OUSLY6 | 42 | 1 | 0.0 | 0 | 0 | 0 | 0 |
| 2KHEMI3 | 43 | 1 | 0.0 | 31 | 18 | 0 | 0 |
| 2KHEMI6 | 44 | 1 | 0.0 | 0 | 0 | 0 | 0 |
| 2ADEFL3 | 45 | 1 | 0.0 | 12 | 6 | 0 | 0 |
| 2ADEF13 | 46 | 1 | 0.0 | 0 | 0 | 0 | 0 |
| 2KHERB3 | 47 | 1 | 0.0 | 21 | 10 | 0 | 0 |
| 2KHERB6 | 48 | 1 | 0.0 | 0 | 0 | 0 | 0 |
| 2TENES3 | 49 | 1 | 0.0 | 13 | 6 | 0 | 0 |
| 2OFODA3 | 50 | 1 | 0.0 | 4 | 2 | 0 | 0 |
| 2GHRIB3 | 51 | 1 | 0.0 | 1 | 1 | 0 | 0 |
| 2BOUFA3 | 52 | 1 | 0.0 | 56 | 27 | 80 | 50 |
| 2BLIDA3 | 53 | 1 | 0.0 | 16 | 8 | 0 | 0 |
| 2EAFFR3 | 54 | 1 | 0.0 | 21 | 10 | 0 | 0 |
| 2CHERC3 | 55 | 1 | 0.0 | 18 | 9 | 0 | 0 |
| 2MEDEA3 | 56 | 1 | 0.0 | 33 | 20 | 0 | 0 |
| 2BERRO3 | 57 | 1 | 0.0 | 35 | 21 | 0 | 0 |
| 2BERRO6 | 58 | 1 | 0.0 | 0 | 0 | 0 | 0 |
| 2BEMER3 | 59 | 1 | 0.0 | 36 | 17 | 0 | 0 |
| 2BEMER6 | 60 | 1 | 0.0 | 0 | 0 | 0 | 0 |
| 2KOLEA3 | 61 | 1 | 0.0 | 27 | 14 | 0 | 0 |

| | | | | | | | |
|---|---|---|---|---|---|---|---|
| 2KOLEA3 | 62 | 1 | 0.0 | 22 | 11 | 0 | 0 |
| 2TIOUZ3 | 63 | 1 | 0.0 | 49 | 29 | 0 | 0 |
| 2TIOUZ6 | 64 | 1 | 0.0 | 0 | 0 | 0 | 0 |
| 2FREHA3 | 65 | 1 | 0.0 | 11 | 5 | 0 | 0 |
| 2DBKHE3 | 66 | 1 | 0.0 | 35 | 21 | 0 | 0 |
| 2TIMED3 | 67 | 1 | 0.0 | 10 | 5 | 0 | 0 |
| 2SEDJE3 | 68 | 1 | 0.0 | 11 | 5 | 0 | 0 |
| 2SGHOZ3 | 69 | 1 | 0.0 | 20 | 10 | 0 | 0 |
| 2ILLIT3 | 70 | 1 | 0.0 | 7 | 3 | 0 | 0 |
| 2BOUIR3 | 71 | 1 | 0.0 | 36 | 22 | 0 | 0 |
| 2BOUIR6 | 72 | 1 | 0.0 | 0 | 0 | 0 | 0 |
| 2SIMUS3 | 73 | 1 | 0.0 | 36 | 22 | 0 | 0 |
| 2AOUSS6 | 74 | 1 | 0.0 | 0 | 0 | 0 | 0 |
| 2AOUS16 | 75 | 1 | 0.0 | 0 | 0 | 0 | 0 |
| 2AOUSS2 | 76 | 1 | 0.0 | 12 | 6 | 0 | 0 |
| 2K.BOU3 | 77 | 1 | 0.0 | 7 | 3 | 0 | 0 |
| 2MUSTA3 | 78 | 1 | 0.0 | 13 | 7 | 0 | 0 |
| 2AMIRA3 | 79 | 1 | 0.0 | 14 | 7 | 0 | 0 |
| 3EHADJ6 | 80 | 1 | 0.0 | 157 | 107 | 100 | 56 |
| 3EAOUI6 | 81 | 1 | 0.0 | 0 | 0 | 0 | 0 |
| 3KHROU6 | 82 | 1 | 0.0 | 75 | 36 | 0 | 0 |
| 3SKIKD6 | 83 | 1 | 0.0 | 70 | 51 | 230 | 120 |
| 3RADJA6 | 84 | 1 | 0.0 | 46 | 34 | 0 | 0 |
| 3ABEID6 | 85 | 1 | 0.0 | 45 | 22 | 0 | 0 |
| 3TEBE16 | 86 | 1 | 0.0 | 0 | 0 | 0 | 0 |
| 3AMLIL6 | 87 | 1 | 0.0 | 32 | 15 | 0 | 0 |
| 3EHADJ | 88 | 1 | 0.0 | 46 | 22 | 0 | 0 |
| 3SOAHR4 | 89 | 1 | 0.0 | 34 | 17 | 0 | 0 |
| 3EAOUI4 | 90 | 1 | 0.0 | 18 | 9 | 0 | 0 |
| 3TEBES4 | 91 | 1 | 0.0 | 44 | 21 | 0 | 0 |
| 3DJONK4 | 92 | 1 | 0.0 | 10 | 5 | 0 | 0 |
| 3TEBE14 | 93 | 1 | 0.0 | 0 | 0 | 0 | 0 |
| 4OATHM6 | 94 | 1 | 0.0 | 48 | 23 | 0 | 0 |
| 4AKBOU6 | 95 | 1 | 0.0 | 35 | 17 | 0 | 0 |
| 4AKBO16 | 96 | 1 | 0.0 | 0 | 0 | 0 | 0 |
| 4EKSEU6 | 97 | 1 | 0.0 | 42 | 20 | 0 | 0 |
| 4DARGU6 | 98 | 1 | 0.0 | 13 | 6 | 100 | 30 |
| 4EHASI6 | 99 | 1 | 0.0 | 105 | 50 | 0 | 0 |
| 4JIJEL6 | 100 | 1.0773 | 0.0 | 33 | 16 | 550 | 50 |
| 4MSILA6 | 101 | 1.0818 | 0.0 | 50 | 24 | 360 | 50 |
| 4BBARE6 | 102 | 1 | 0.0 | 34 | 16 | 0 | 0 |
| 4BISKR6 | 103 | 1 | 0.0 | 66 | 32 | 0 | 0 |
| 4BARIK6 | 104 | 1 | 0.0 | 18 | 9 | 0 | 0 |
| 4BARI16 | 105 | 1 | 0.0 | 0 | 0 | 0 | 0 |
| 4BATNA6 | 106 | 1 | 0.0 | 64 | 31 | 0 | 0 |
| 5DJELF6 | 107 | 1 | 0.0 | 65 | 37 | 0 | 0 |
| 5GHARD6 | 108 | 1 | 0.0 | 22 | 11 | 0 | 0 |
| 5TILGH6 | 109 | 1.0818 | 0.0 | 37 | 18 | 180 | 85 |
| 6MGHAI6 | 110 | 1 | 0.0 | 13 | 6 | 0 | 0 |

| | | | | | | | |
|---|---|---|---|---|---|---|---|
| 6HMSNO6 | 111 | 1.0909 | 0.0 | 94 | 56 | 200 | 85 |
| 6TOUGO6 | 112 | 1 | 0.0 | 24 | 12 | 0 | 0 |
| 6OURGL6 | 113 | 1 | 0.0 | 23 | 11 | 0 | 0 |
| 6EOUED6 | 114 | 1 | 0.0 | 24 | 12 | 0 | 0 |

## ملخص

في السنوات الأخيرة، و بسبب القضايا الاقتصادية والبيئية، تظطر نظم الطاقة الحديثة في كثير من الأحيان للاشتغال بالقرب من حدود مجالات استقرارها، مما يزيد من احتمال تعرضها لمخاطر عدم استقرار الجهد. وبالتالي، فإن تطوير أساليب سريعة وفعالة لتقييم وتعزيز استقرار الجهد في نظم الطاقة أصبح ذا أهمية بالغة للخبراء والصناعيين من أجل تجنب خطرالانقطاع الكلي للتيار الكهربائي. في هذه الأطروحة، تم أولا تطوير نماذج هجينة جديدة تقوم على دمج آلة شعاع الدعم (SVR) مع خوارزميات الاستمثال للتنبؤ بهامش استقرار الجهد لنظام الطاقة. وبما أن أداء نموذج SVR يعتمد بشكل كبير على الاختيار الدقيق لمعلماته، فقد تم تكييف خوارزميات حشرة النملة الأسد (AntLion optimization algorithm)، حشرة التنين الطائر (Dragonfly optimization algorithm) و خوارزمية الحوت (Whale optimization algorithm) للبحث عن المعلمات المثلى لنموذج SVR مما يحسن من أدائه بشكل كبير. ومن أجل ضمان ملائمة النماذج المقترحة للتطبيقات على الخط، تم إعداد مدخلات النماذج الهجينة في شكل مقادير للجهد وزوايا طور الجهد التي توفرها وحدات قياس الطور (PMUs). بعد ذلك، تم تطوير تقنية لتحديد العقد الضعيفة في نظام الطاقة، بغية تعزيز استقرار الجهد، و ذلك بالاعتماد على تحديد العقد المثلى لدعم النظام الكهربائي بالطاقة غير الفعالة باستعمال خوارزميات الاستمثال المذكورة آنفا. وأخيرا، تم اقتراح تقنية استجابة لحالات الطوارئ مرتكزة على هامش استقرار الجهد في نظام الطاقة. وتهدف التقنية المقترحة إلى تحسين هامش استقرار الجهد من جهة والحفاظ عليه في نطاق آمن خلال مرور النظام بظروف طارئة من جهة أخرى. من أجل إثبات كفاءة التقنيات المقترحة، تم استخدام النظام القياسي 14 عقدة ونظام الطاقة الجزائري 114 عقدة كأنظمة إختبار لإجراء المحاكاة والمقارنات.



**كلمات مفتاحية** : هامش استقرار الجهد، آلة شعاع الدعم، خوارزمية حشرة النملة الأسد، خوارزمية حشرة التنين الطائر، خوارزمية الحوت، وحدات قياس الطور، تقنية الاستجابة لحالات الطوارئ.



## Abstract

In recent years, due to the economic and environmental issues, modern power systems often operate proximate to the technical restraints enlarging the probable level of voltage instability risks. Hence, fast and efficient methods to assess and enhance power system voltage stability are of great importance to experts and industries in order to avoid a risk of large blackouts. In this thesis, firstly, new hybrid models based on the combination of Support Vector Regression (SVR) with modern meta-heuristic optimization algorithms have been developed and implemented to predict power system Voltage Stability Margin (VSM). As the performance of the SVR model heavily depends on a careful selection of its parameters, the AntLion Optimizer (ALO), Dragonfly Algorithm (DA) and Whale Optimization Algorithm (WOA) are adapted to seek for the SVR's optimal parameters, which significantly improve its performance. In order to ensure the suitability of the proposed approach for on-line applications, the input features of the hybrid models are provided in the form of voltage magnitudes and voltage phase angles, measured by Phasor Measurement Units (PMUs). Consequently, the above-mentioned algorithms i.e., ALO, DA and WOA are used to identify the weak buses in a large-scale power system based on the optimal location of reactive power support. Finally, an Event-driven Emergency Demand Response (EEDR) based VSM is proposed for voltage stability improvement. The main objective of the proposed EEDR approach is to maintain VSM in an acceptable range during emergency conditions. Validation process was conducted on two test systems namely the IEEE 14-bus and the Algerian 114-bus which produced promising results.



**Keywords:** Voltage stability margin, Support vector regression, ALO algorithm, DA algorithm, WOA algorithm, PMUs, Event-driven Emergency Demand Response



## Résumé

Au cours de dernières années et à cause des problèmes économiques et environnementaux, les systèmes de puissance modernes fonctionnent souvent à proximité des contraintes techniques, augmentant le niveau probable des risques d'instabilité de tension. Par conséquent, des méthodes rapides et efficaces pour évaluer et améliorer la stabilité de tension sont d'une grande importance pour les experts et les industriels, et ce, afin d'éviter les blackouts. Dans cette thèse, de nouveaux modèles hybrides basés sur la combinaison de la régression à vecteurs de support (Support Vector Regression : SVR) avec des algorithmes modernes d'optimisation ont été développés et implémentés pour prédire la marge de stabilité de tension du système de puissance. Comme les performances du modèle SVR dépendent fortement d'une sélection précise de ses paramètres, les algorithmes AntLion Optimizer (ALO), Dragonfly Optimizer (DA) et Whale Optimizer (WOA) sont utilisés pour l'optimisation des paramètres du SVR ; ce qui améliore considérablement leurs performances. Afin de garantir l'adéquation de l'approche proposée pour les applications en ligne, les vecteurs d'entrée des modèles hybrides sont fournis sous forme d'amplitudes de tension et d'angles de phase de tension, qui sont supposés être obtenus à partir des unités de mesure de phaseur. De plus, les algorithmes mentionnés ci-dessus, à savoir ALO, DA et WOA, sont utilisés pour identifier les jeux de barres les plus faibles dans un système de puissance. Enfin, une méthode de réponse à une demande d'urgence basée sur la marge de stabilité de tension est proposée pour améliorer cette dernière. L'objectif principal de l'approche proposée est de maintenir la marge de stabilité de tension dans une plage acceptable en cas d'urgence. Afin de démontrer la validité et l'efficacité des méthodes proposées, le réseau IEEE 14 jeux de barres et le réseau algérien 114 jeux de barres sont utilisés comme des réseaux test pour effectuer les simulations et les comparaisons correspondantes.



**Mots clés :** Marge de stabilité de tension, Régression à vecteurs de support, algorithme ALO, algorithme DA, algorithme WOA, PMUs, Réponse à une demande d'urgence.